Some Studies of Transition Metal Chalcogenide Fluorides

John Rook

ABSTRACT

Attempts have been made to synthesise thio-fluoride species of tantalum, osmium and iridium. The reaction of tantalum thiotrichloride and tribromide with an excess of anhydrous HF yields $[SH_3]^+[Ta_2F_{11}]^-$. When anhydrous HF is added to a solution of $TaSX_3$ (X = Cl or Br) in acetonitrile an oil is formed which contains =NH and $\equiv NH^+$. The thermal reactions of the hexafluorides of osmium and iridium with zinc and boron sulphides yield the adducts $SF_4.MF_5$ (M = Os or Ir). Infra-red and X-ray powder diffraction studies indicate that they have contributions to the bonding from the ionic formulations $[SF_3]^+[MF_6]^-$. The reaction of MF_6 with antimony sulphide in anhydrous HF gives only lower oxidation-state fluorides.

The reaction of the alkali metal fluorides with tungsten thiotetrafluoride in anhydrous HF has yielded the first examples of solids containing $[W_2S_2F_9]^-$ and $[WSF_5]^-$, *viz.* $M^+[W_2S_2F_9]^-$ (M = Li, Na, K, Rb or Cs) and $M^+[WSF_5]^-$ (M = Rb or Cs).

Nitrosyl fluoride reacts rapidly with tungsten thiotetrafluoride to yield $[NO]^+[WOF_5]^-$, $[NO]_2^+[WF_8]^{2-}$ and sulphuryl fluoride. However, a low-temperature n.m.r. study has shown that the reaction initially yields $[W_2S_2F_9]^-$ and $[WSF_5]^-$.

Tungsten oxidetetrafluoride reacts with an excess of sulphur tetrafluoride to give $[SF_3]^+[W_2O_2F_9]^-$. X-ray powder diffraction, infra-red and n.m.r. studies have shown that fluorine bridging between $[SF_3]^+$ and $[W_2O_2F_9]^-$ in the solid state or in solution in sulphur dioxide is minimal. The reaction between tungsten thiotetrafluoride and sulphur tetrafluoride yields only tungsten hexafluoride and sulphur.

Xenon difluoride reacts violently with tungsten thiotetrafluoride in the solid state to yield tungsten hexafluoride, xenon and fluorides of sulphur. When the reaction is conducted in sulphuryl chloride fluoride at low-temperature a red-brown solution is formed. This has been shown to consist of tungsten hexafluoride and the radical cation, $S_8^{+\bullet}$ by n.m.r. and e.s.r. spectroscopy.

The standard enthalpy of formation of tungsten thiotetrafluoride has been determined by hydrolysis in alkaline media.

Some Studies of Transition Metal Chalcogenide Fluorides

A Thesis presented for the degree of

Doctor of Philosophy

in the

Faculty of Science

by

John Rook

Department of Chemistry,
The University,
LEICESTER. LE1 7RH

AUGUST 1987

To my Parents

We don't remember the days,
only the moments.

STATEMENT

The experimental work described in this thesis has been carried out by the author in the Department of Chemistry of the University of Leicester between October 1984 and April 1987. The work has not been submitted, and is not currently being submitted, for any other degree at this or any other University.

Signed: John Rodc..... Date: 4/9/87.....

Parts of this work are being submitted for publication as follows:

Attempted preparation of $TaSF_3$; the isolation and characterisation of $[SH_3]^+[Ta_2F_{11}]^-$.

J. H. Holloway and J. Rook. In preparation.

Attempted preparation of $OsSF_4$ and $IrSF_4$; the isolation and characterisation of $SF_4.OsF_5$ and $SF_4.IrF_5$.

J. H. Holloway and J. Rook, submitted to J.C.S. Dalton, September 1986.

Synthesis, Chemistry and Crystal Structures of thio- and seleno-tetrafluorides of tungsten, molybdenum and their derivatives.

R. W. Cockman, W. Dukat, J. H. Holloway, V. Kaučič, D. C. Puddick, J. Rook, D. R. Russell and G. M. Staunton. In preparation.

The reaction of tungsten thiotetrafluoride with the alkali metal fluorides and nitrosyl fluoride; the isolation and characterisation of alkali metal fluorothiotungstates.

W. Dukat, J. H. Holloway and J. Rook. In preparation.

Enthalpy of formation of Tungsten thiotetrafluoride.

J. Burgess, J. H. Holloway and J. Rook. In preparation.

ACKNOWLEDGEMENTS

I would like to thank my supervisor, Dr. J. H. Holloway, for his help and guidance throughout the period of this work.

I would also like to thank:
Dr. W. Dukat for his help with n.m.r. spectroscopy and his continual enthusiasm, interest and sound advice.

Professor M. C. R. Symons and R. Janes for assistance with e.s.r. spectroscopic studies.

Professor E. A. V. Ebsworth and Dr. R. W. Cockman of Edinburgh University for allowing me to use their n.m.r. facilities and for their help.

Dr. D. A. Rice and R. J. Hobson of Reading University for providing samples of tantalum thio-halides.

The members of the inorganic teaching staff, the technical staff of the Chemistry Department and my colleagues in the laboratory for their assistance.

Miss Vicki Wright and Mrs. Ann Crane for preparing the typescript and drawings respectively.

My family and fiancee, Julie Rogers, for their continual help and support.

Finally, financial support from the Science and Engineering Research Council over the period 1984-1987 is gratefully acknowledged.

ABBREVIATIONS

Kel-F	-	polytrifluorochloroethene
FEP	-	tetrafluoroethene/perfluoropropene copolymer
n.m.r.	-	nuclear magnetic resonance
e.s.r.	-	electron spin resonance
X.P.S.	-	X-ray powder spectrometry
E.X.A.F.S.	-	extended X-ray absorption fine structure
I.R.	-	infra-red
Ra	-	Raman
vs	-	very strong
s	-	strong
ms	-	medium strong
m	-	medium
w	-	weak
vw	-	very weak
br	-	broad
sh	-	shoulder
p.p.m.	-	parts per million
o.d.	-	outside diameter
i.d.	-	inside diameter
dpph	-	diphenylpicrylhydrazyl
Genetron-113	-	1,1,2-trichlorotrifluoroethene
Me	-	methyl

LIST OF CONTENTS

LIST OF CONTENTS (Continued) ....

LIST OF CONTENTS (Continued) ....

CHAPTER 1

Thio-, Seleno- and Telluro-Fluorides
of the Transition Metals: A Review

1.1 INTRODUCTION

The oxide fluorides of the transition metals have been known for many years, and their preparations, properties and structures have been well documented.[1]

However, in recent years an increasing interest has been focused on the preparative methods, isolation and characterisation of the thio-, seleno- and telluro-fluorides of the transition metals. This has been made possible by improvements in the handling of and analytical techniques for highly reactive, moisture-sensitive compounds, together with the development of new reaction pathways.

The aim of this review is to summarise the preparation, chemical and physical properties and structures of the thio-, seleno- and telluro-fluorides of the transition metals presently known. At the time of writing, the only transition metals reported to form isolable compounds of this type were Y, La, Mo, W and Re. The only telluro-fluoride reported so far is that of molybdenum, $MoTeF_3$[21] (Table 1).

In general, the preparative routes for the thio-, seleno- and telluro-fluorides involve interaction of the respective transition metal fluorides with the respective chalcogen or chalcogenide. However, the lower chalcogenide fluorides of molybdenum have only been prepared by the reduction of AF_6, A = Se, Te, using a hot filament of molybdenum. The methods of preparation of the thio-, seleno- and telluro-fluorides of the transition metals are summarised in Table 2.

1.2 GROUP IIIA

1.2.1 Yttrium

Yttrium thiofluoride, YSF, was first prepared by Dagron and Thévet from the reaction of Y_2S_3 with YF_3 at 900-1200°C,[2] while later investi-

TABLE 1

Thio-, seleno- and telluro-fluorides of the transition metals

Oxidation State	Group IIIA	Group IVA	Group VA	Group VIA	Group VIIA	Group VIII	Group IB
3	YSF YSeF LaSF LaSeF						
5				$MoSF_3$ $MoTeF_3$	$ReSF_3$		
6				$MoSF_4$ $MoSeF_4$ WSF_4 $WSeF_4$	$ReSF_4$		
7					$ReSF_5$		

TABLE 2

Preparative methods for thio-, seleno- and telluro-fluorides of the transition metals

Group	Species	Preparative Route	Reference
	YSF	$YF_3 + Y_2S_3$ at 900-1200°C	2
		$YF_3 + H_2S$ at 900-1000°C	4
	YSeF	$YF_3 + Y_2Se_3$ at 800-1115°C	7,8
IIIA	LaSF	$LaF_3 + La_2S_3$ at 450-1200°C	2,12-14
		$LaF_3 + H_2S$ at 900-1000°C	4
		$LaF_3 + La_3S_4 + S$ at 500-600°C	15
	LaSeF	$LaF_3 + La_2Se_3$ at 500°C	16
		$LaF_3 + La_3Se_4 + Se$ at 600-650°C	15
	$MoSF_3$	$SF_6 + Mo$ at 600-800°C	18
	$MoTeF_3$	$TeF_6 + Mo$ at 500-600°C	21
	$MoTeF_3.TeF_4$	$TeF_6 + Mo$ at 200-250°C	21
	$MoSF_4$	$MoF_6 + Sb_2S_3$ at 275°C for 6 hrs	22
	$MoSeF_4$	$MoF_6 + Sb_2Se_3$ at 275°C for 6 hrs	22
	WSF_4	$WF_6 + Sb_2S_3$ at 300°C for 3 hrs	27
		$WF_6 + B_2S_3$ at 200°C for 4 hrs	31
		$WF_6 + Sb_2S_3$ in anhydrous HF	35
VIA		$WF_6 + S$ at 300°C for 20 hrs	31
		$WF_6 + ZnS$ at 300°C for 8 hrs	35
		$SF_6 + W$ at 500-700°C	36
	$WSF_4.CH_3CN$	$WF_6 + H_2S$ in CH_3CN	29
		$WF_6 + Sb_2S_3$ in CH_3CN	31
	$WS_2F_2.CH_3CN$	$WSF_4 + H_2S$ in CH_3CN	29
	$WSeF_4$	$WF_6 + Sb_2Se_3$ at 350°C for 60 hrs	23
		$WF_6 + Sb_2Se_3$ in anhydrous HF	35
		$WF_6 + Se$ at 300°C for 20 hrs	31
	$WSeF_4.CH_3CN$	$WF_6 + Sb_2Se_3$ in CH_3CN	42
	$ReSF_3$	$ReF_5 + Sb_2S_3$ in anhydrous HF	43
	$ReSF_4$	$ReF_6 + Sb_2S_3$ at 300°C for 10 hrs	43
		$ReF_6 + Sb_2S_3$ in anhydrous HF	43
VIIA		$ReF_6 + B_2S_3$ at 300°C for 10 hrs	43
		$ReF_6 + S$ at 300°C for 20 hrs	31
	$ReSF_5$	$ReF_7 + Sb_2S_3$ at 300°C for 10 hrs	43
		$ReF_7 + Sb_2S_3$ in anhydrous HF	43
		$ReF_7 + B_2S_3$ at 300°C for 10 hrs	43

gations by Markovskii et al. have lead to the preparation of YSF by the action of other fluorinating agents on Y_2S_3.[3] A more recent study by Brixner and Hyatt has shown that YSF can also be conveniently prepared from the high temperature reaction of H_2S with YF_3.[4]

The compound has both α and β forms which are tetragonal and hexagonal respectively.[2,5,6] The β form, which has been studied by three-dimensional X-ray diffraction, is shown to consist of layers of (YS_2) and (YF_2) units parallel to the (001) plane.[6]

Dagron has reported the preparation of yttrium seleno fluoride, YSeF, from the interaction of YF_3 with Y_2Se_3.[7,8] It is known to exist in at least three forms: orthorhombic,[9] monoclinic[10] and one that is either hexagonal or rhombohedral.[8] Van Dyck et al. have studied structures of other polytypes via lattice imaging using electron microscopy.[11]

1.2.2 Lanthanum

Lanthanum thiofluoride, LaSF, can be prepared by the high-temperature reaction of LaF_3 with La_2S_3,[2,12,13,14] H_2S or La_3S_4 and sulphur.[15] It is a grey-white solid which melts at 1810°C.[14] It possesses a tetragonal structure of the PbClF[4,5,13,15] type and contains layers of $(LaF)_n$ and sulphur.[16] The infra-red spectrum has been recorded and is compared with those of CeSF, PrSF and NdSF.[12]

Lanthanum selenofluoride, LaSeF, can be prepared by analogous methods used to prepare LaSF.[15,16] It is a light grey solid which has been identified in three forms, hexagonal,[17] orthorhombic[15] and tetragonal.[16] The latter form is analogous to that of LaSF[16] whilst the hexagonal form consists of layers of selenium anions and planes of lanthanum and fluoride ions. Each lanthanum and fluorine occupies the centre of an equilateral triangle formed by the other ions. The selenium and

fluorine anions together form a rhombohedral stacking sequence.[17]

Telluro-fluorides of yttrium and lanthanum, to date, have not been reported.

1.3 GROUP VIA

1.3.1 Molybdenum

Chalcogenide fluorides of molybdenum have been isolated in which the metal is in an oxidation state of V or VI. The first reported example of this type of compound was the thiotrifluoride, $MoSF_3$. This was synthesised by the reduction of SF_6 by a hot molybdenum filament in a quartz reactor.[18] Optimum conditions for this synthesis were achieved using a filament temperature of 600-800°C, an initial SF_6 pressure of $(5-8)\times 10^{-1}$ atmospheres and a reactor temperature of 40-60°C. Solid $MoSF_3$ is a bright orange hygroscopic material with a melting point of 86.5°C. It has been characterised by chemical analysis, X-ray powder diffraction, magnetic measurements and infra-red spectroscopy. The infra-red spectrum of the solid shows bands at 690-660 and 635 cm^{-1} $\nu(Mo-F)_{Terminal}$, 584 cm^{-1} $\nu(Mo=S)$ and 525-490 cm^{-1} $\nu(Mo-F-Mo)_{Bridging}$.

Mass spectroscopic investigation[19,20] of the gas phase over $MoSF_3$, in the temperature range 20-62°C, has shown that the vapour consists of mainly the polymeric molecules $(MoSF_3)_2$ and $(MoSF_3)_3$. This investigation also shows that partial disproportionation of $MoSF_3$ occurs during volatilisation. This was evidenced by the presence of the ions $[MoF_5]^+$, $[MoSF_4]^+$ and S_8^+ in the mass spectra. Further mass spectrometric analysis of the vapour phase of $MoSF_3$ has also been used to calculate the heats of sublimation and formation of the thiofluoride species present. These data are summarised in Table 3.

The preparation of molybdenum tellurotrifluoride, $MoTeF_3$, has been

TABLE 3

Thermodynamic data for some thio-fluorides of molybdenum[19,20]

Compound	$\Delta H^{\ominus}$ Sublimation/298 K (kJ mol^{-1})	$\Delta H^{\ominus}$ Formation/298 K (-kJ mol^{-1})	Reference
$MoSF_3$ solid	100.73 ± 12.54	784.16 ± 27.17	20,19
$MoSF_3$ gas	-	694.30 ± 27.17	20
$(MoSF_3)_2$ solid	98.23 ± 8.36	-	19
$(MoSF_3)_3$ solid	98.23 ± 8.36	-	19
$MoSF_4$ gas	-	969.76 ± 29.68	20

TABLE 4

Heats of formation and bond dissociation energies of some thio-fluorides of tungsten[25]

Gaseous Species	$\Delta H^{\ominus}$ Formation/298 K (-kJ mol^{-1})	Bond dissociation energies (kJ mol^{-1})	
		SF_2W-F	W-S
WSF_2	335.3 ± 16.3	-	527
WSF_3	712.5 ± 13.4	456	481
WS_2F_2	496.8 ± 17.6	-	440

recently reported by Ryabov et al.[21] Synthesis of $MoTeF_3$ was achieved via the reduction of TeF_6 by an incandescent molybdenum filament in a Pyrex reaction vessel. With a filament temperature of 500-600°C and an initial TeF_6 pressure of $(4-5) \times 10^{-2}$ atmospheres, the red-brown $MoTeF_3$ condensed onto the walls of the reaction vessel, which were maintained at -78°C. An infra-red spectrum was recorded in the region of 1000-200 cm^{-1} and the observed bands tentatively assigned [717, 675, 610 cm^{-1} $\nu(Mo-F)_{Terminal}$, 560, 540, 525 cm^{-1} $\nu(Mo-F-Mo)_{Bridging}$, 392 $\nu(Mo=Te)$ and 373, 292 cm^{-1} $\delta(F-Mo-F)$]. A mass spectroscopic investigation of the saturated vapour above $MoTeF_3$, at 103°C, has shown TeF_4 to be the major constituent. The presence of ions of the type $[MoTeF_x]^+$ (x = 1 to 4), in the mass spectrum was not reported.

When the conditions of synthesis were varied (filament temperature 200-250°C; initial TeF_6 pressure 4×10^{-1} atmospheres; reaction vessel temperature 0°C), a different compound with the formula $MoTeF_3.TeF_4$ was isolated. Data from thermogravimetric experiments and differential thermal analysis have shown the adduct to break down according to Schemes 1 and 2.

$$MoTeF_3.TeF_{4(s)} \xrightarrow{107°C} MoTeF_{3(s)} + TeF_{4(g)}$$

SCHEME 1

$$4\ MoTeF_{4(s)} \xrightarrow{207°C} 3\ TeF_{4(g)} + 0.5\ MoTe_{2(s)} + 3.5\ Mo_{(s)}$$

SCHEME 2

Analysis of the gas above $MoTeF_3.TeF_4$ by mass spectroscopy reveals the presence of only TeF_4; once again the presence of ions of the type, $[MoTeF_x]^+$ (x = 1 to 4) was not reported.

The thio- and seleno- fluorides of molybdenum, $MoSF_4$ and $MoSeF_4$, have been isolated as amber solids from the reaction of MoF_6 with the

respective antimony chalcogenide, Sb_2X_3 (X = S, Se), in an autoclave at 300°C.[22] Both solids are extremely sensitive to traces of moisture and when exposed to the atmosphere rapidly evolve HF and H_2S or H_2Se respectively. The X-ray powder diffraction patterns of $MoSF_4$ and $MoSeF_4$ have shown that the two species are isostructural with each other but that the structures differ from those of WSF_4 and $WSeF_4$.[23] The infra-red spectra of the thio- and seleno-fluorides show that the solids contain both terminal and bridging fluorine atoms. The infra-red spectrum of $MoSF_4$ also exhibited an additional band at 564 cm^{-1} which was assigned to ν(Mo=S). The analogous molybdenum selenide stretch in $MoSeF_4$, ν(Mo=Se), was not observed and it was assumed to occur below the cut-off frequency of the window used.

Preliminary reactions of liquid MoF_6 with Sb_2Te_3 have been investigated, but evidence for the formation of the telluro-fluoride species, $MoTeF_4$, was not obtained.[24]

1.3.2 Tungsten

The existence of tungsten thio-fluoride species was first recognised by Hildenbrand during the reaction of SF_6 and W in an effusion cell at 1600 K.[25] The resultant mixture of compounds was subjected to mass spectrometric analysis and among the species identified were $[WSF_4]^+$, $[WSF_3]^+$, $[WSF_2]^+$ and $[WS_2F_2]^+$. From the same study, heats of formation and some bond dissociation energies for WSF_3, WSF_2 and WS_2F_2 were obtained. These are summarised in Table 4.

The related anionic species $[WSFCl_4]^-$, $[WSF_2Cl_3]^-$, $[WSF_3Cl_2]^-$, $[WSF_4Cl]^-$, $[W_2S_2F_9]^-$ and $[WSF_5]^-$ were first observed by Buslaev et al. during an ^{19}F nmr study of the reaction of $WSCl_4$ with HF in acetonitrile.[26] This observation was later confirmed by Atherton and

Holloway.[27] They found that when the $WSCl_4$:HF ratio was 1:6, the neutral thio-fluoride species, WSF_4, was also formed. The data from this study are recorded in Table 5. The ^{19}F nmr study of the reaction of $WSCl_4$ with XeF_2 in CH_3CN has shown that, in addition to WSF_4, the neutral mixed chloride fluoride species WSF_2Cl_2, WSF_3Cl and $WSFCl_3$ are also formed.[27] The tungsten thiotetrafluoride ^{19}F nmr spectrum has also been observed in the reaction of WF_6 in acetonitrile with various sulphides such as K_2S, Na_2S, Bu_2S, Ph_2S, Me_2S_2 and thiourea.[28] The adducts $WSF_4.CH_3CN$ and $WS_2F_2.CH_3CN$ were first isolated by Kokunov et al. when H_2S was bubbled through a solution of WF_6 in acetonitrile.[29] However, $WSF_4.CH_3CN$ has since been prepared by the reaction of WF_6 with Sb_2S_3 in acetonitrile.[30,31] A recent single crystal structure determination[31] has shown the adduct, $WSF_4.CH_3CN$, to be monomeric with the tungsten octahedrally surrounded by four fluorine atoms in an equatorial plane and the nitrogen atom of the CH_3CN group trans to the sulphur.

Some of the solution-phase reactions of WSF_4 in acetonitrile have been followed by the use of ^{19}F nmr. It has been shown that butylamine will react vigorously with WSF_4 in solution to produce $[WSF_5]^-$ and $[W(NBu)F_5]^-$[32] and that the reaction with water affords the species $WSF_4.H_2O$, $WOF_4.H_2O$, $[W_2O_2F_9]^-$ and $[WOF_5]^-$.[32] The action of water on $WSF_4/WSCl_4$ mixtures in CH_3CN has been studied and it has been shown that $WOF_{4-n}Cl_n.CH_3CN$ is formed in preference to $WSF_{4-n}Cl_n.CH_3CN$.[33] The displacement of the acetonitrile molecule in the adduct $WSF_4.CH_3CN$ by ethanol, phenol, 1,2-ethanediol, acetylacetone, diethylamine and butan-thiol has also been studied by ^{19}F nmr.[34]

Tungsten thiotetrafluoride, WSF_4, has been isolated as an uncomplexed solid via the thermal reaction of WF_6 with Sb_2S_3,[27] B_2S_3,[31] elemental

TABLE 5

^{19}F nmr parameters for WSF_4 and related anions[27]

Sample	Solvent	Temperature (°C)	δ/ppm[a]	Multiplet[b] structure	Coupling constant (Hz)	Assignment
$WSCl_4$:HF (1:6)	CH_3CN/CD_3CN	-28	-159.3	IX[c]	$^2J_{F-F}$ 71 ± 2	$(F_4)WS-\bar{F}-WS(F_4)$
			-141.2	V	$^2J_{F-F}$ 72 ± 2	$WS(F_4)\bar{F}$
			80.0	II	$^2J_{F-F}$ 72 ± 2	$WSF_4(\bar{F})$
			83.5	I		$WSF_4\bar{Cl}$
			83.7	II	$^2J_{F-F}$ 70 ± 2	$F_4WS-(\bar{F})-WSF_4$
			84.8	I	$^1J_{W-F}$ 32 ± 2	WSF_4
			91.1	I		Unassigned
			109.7	II	$^2J_{F-F}$ 70 ± 2; $^1J_{W-F}$ 33 ± 2	$WSF_3Cl_2^-$
			130.5	I		$WSFCl_4^-$

[a] *Spectra run at 94.1 MHz and referenced with respect to external $CFCl_3$;*
[b] *I, singlet; II, doublet; V, quintet; IX, nonet;*
[c] *Central five lines identified by intensity ratio 29:50:65:55:28.*

sulphur[31] or ZnS[35] in an autoclave. It has also been prepared at room temperature from the reaction of WF_6 with Sb_2S_3 in anhydrous HF solvent.[35] A more indirect method for the preparation of WSF_4 has been achieved by the reduction of SF_6 with an incandescent tungsten filament.[36] Tungsten thiotetrafluoride is a yellow solid which melts to an amber liquid at 89-90°C in vacuo.[27] It has been shown to be extremely-moisture sensitive and, on exposure to the atmosphere, HF and H_2S are rapidly evolved.[27] It has been characterised by mass spectrometry, X-ray powder diffraction and ^{19}F nmr.[27] The infra-red spectrum of the solid shows bands at 733, 699 and 643 cm^{-1} $\nu(W\text{-}F)_{Terminal}$, 577 cm^{-1} $\nu(W{=}S)$ and 534 and 514 cm^{-1} $\nu(W\text{-}F\text{-}W)_{Bridging}$. These data, together with the observation of similarities in the X-ray powder diffraction patterns of WOF_4 and WSF_4, initially suggested that the structure of WSF_4 was based upon the cis-fluorine bridged tetramer of WOF_4.[44] However, a recent single crystal structure study[31] has shown this to be only partially correct, the true structure of WSF_4 being one of a cis-fluorine bridged chain in which the two WSF_5 octahedra in the asymmetric unit are linked by cis-bridged fluorine atoms into polymeric chains lying parallel to the c-axis (Figure 1).

Mass spectroscopic investigations by Malkerova et al.[37] of the vapour phase over WSF_4, in the temperature range 17-72°C, have shown that the vapour consists of mainly monomeric WSF_4. Studies by matrix isolation infra-red[38] and electron diffraction[39] of gaseous WSF_4 have further confirmed these observations. The experimental data from these later investigations have also shown that gaseous WSF_4 has the point group symmetry C_{4v} [Figure 2 and Table 6]. The electronic spectrum of matrix isolated WSF_4 has also been recorded.[38] The principle features of the spectrum are absorptions at 47845 and 32680 cm^{-1}; these being assigned

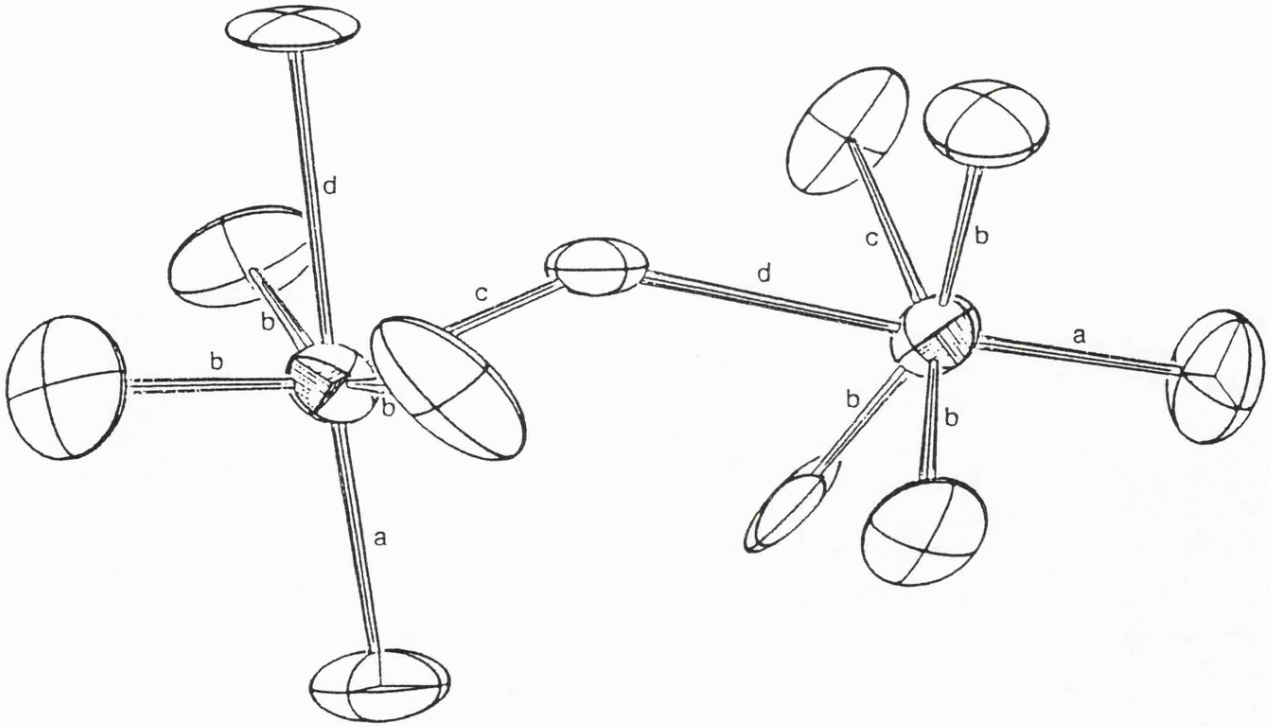

FIGURE 1

Molecular geometry of WSF_4. Average bond lengths (Å) with s.d.s (in parentheses), taken from the two non-equivalent molecular units: a = 2.07(2), b = 1.85(3), c = 1.92(3), d = 2.34(3). The W-F-W bridging angles are 163.7(1.9) and 146.0(1.8)°.

FIGURE 2

Some bond lengths and bond angles of monomeric WSF_4 as deduced from gas-phase electron diffraction [Ref. 39].

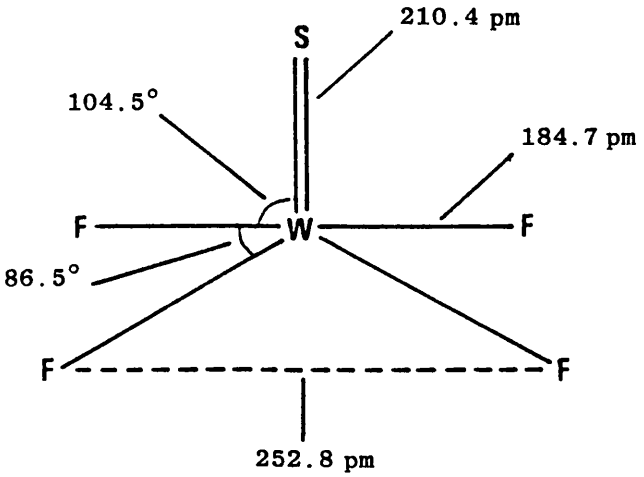

TABLE 6

Vibrational frequencies and assignments of monomeric WSF_4 isolated in a nitrogen matrix[38]

WSF_4	Mode
577	$\nu_{W=S}(A_1)$
707	$\nu_{W-F}(A_1)$
671	$\nu_{W-F}(E)$

to the F→W and S→W charge-transfer bands respectively.

Calculations involving the heat of sublimation of WSF_4 (79.83 ± 5.43 kJ mol^{-1}) and the heat of formation of gaseous WSF_4 (-1136.12 ± 37.6 kJ mol^{-1}) derived via mass spectroscopic investigations[37] have yielded a value of -1215.96 ± 38.03 kJ mol^{-1} for the heat of formation of solid WSF_4. Studies reported in this thesis suggest that this value should be revised to -1150.56 ± 5.39 kJ mol^{-1}. The method of determination and a full discussion of the results is given in Chapter 7.

Preliminary investigations into the reactivity of WSF_4 have shown that, like WOF_4,[40] it forms a 1:1 fluorine-bridged adduct with SbF_5, viz. $WSF_4.SbF_5$.[31] Studies of the fluoride-ion acceptor properties of WSF_4 have been made but, since this is the subject of Chapter 3, no further discussion will be given here.

Tungsten selenotetrafluoride, $WSeF_4$, has been obtained via reactions analogous to those used to isolate WSF_4, by the thermal reactions of WF_6 with Sb_2Se_3[23] or elemental selenium[31] in a stainless steel autoclave. It has also been prepared at room temperature by the reaction of WF_6 with Sb_2Se_3 in anhydrous HF.[35] Tungsten selenotetrafluoride is an amber solid which sublimes at temperatures above 120°C and decomposes at ca. 160°C in vacuo. On exposure to the atmosphere it rapidly hydrolyses to yield HF and H_2Se. It has been characterised by mass spectrometry, ^{19}F nmr and infra-red spectroscopy.[23] The infra-red spectrum has a similar overall band shape to that of WSF_4, with strong bands at 690, 667 and 629 cm^{-1} $\nu(W\text{-}F)_{Terminal}$, 540 and 517 cm^{-1} $\nu(W\text{-}F\text{-}W)_{Bridging}$ and 366 cm^{-1} $\nu(W{=}Se)$. Comparison of the X-ray powder diffraction patterns of $WSeF_4$ and WSF_4 has shown the two solids to be isostructural. Thus, it is likely that solid $WSeF_4$ has a cis-fluorine bridged polymeric structure similar to that of WSF_4 (Figure 1). Studies

by matrix isolation infra-red[38] and electron diffraction[41] have shown that, like gaseous WSF_4, $WSeF_4$ is monomeric in the gas phase. The experimental data also show that gaseous $WSeF_4$ is structurally similar to gaseous WSF_4, and possesses the point group symmetry C_{4v} (Figure 3 and Table 7). The electronic spectrum of matrix-isolated $WSeF_4$[38] has been shown to contain two principle features at 42195 cm^{-1} and 32680 cm^{-1}. These are assigned to the charge-transfer bands, $F \rightarrow W$ and $Se \rightarrow W$ respectively. The complex $WSeF_4.CH_3CN$ has been isolated from the reaction of WF_6 with Sb_2Se_3 in acetonitrile.[42] The yellow-orange solid was characterised by ^{19}F nmr and exhibits a ν(W=Se) stretching frequency at 365 cm^{-1}.

Attempts to prepare telluro-fluorides of tungsten by analogous methods used to isolate WSF_4 and $WSeF_4$ have so far failed.[24,30]

1.4 GROUP VIIA

1.4.1 Rhenium

Thio-fluorides of rhenium have recently been isolated and characterised in which the metal exhibits the oxidation states V, VI and VII, viz. $ReSF_3$, $ReSF_4$ and $ReSF_5$.[43] All of the compounds can be prepared via analogous methods used to isolate the thio-fluorides of tungsten. Thus, $ReSF_5$ and $ReSF_4$ can be prepared by the thermal reactions of the respective fluorides with B_2S_3 or Sb_2S_3 or by the reaction of Sb_2S_3 with the appropriate fluoride in anhydrous HF. The reaction of ReF_6 with elemental sulphur at elevated temperatures has also been shown to afford $ReSF_4$.[31] During attempts to prepare the quintavalent compound, $ReSF_3$, it was found that preparation via thermal means was not possible, since at temperatures in excess of 140°C, ReF_5 disproportionates, and at temperatures below this, reaction with B_2S_3 or Sb_2S_3 does not take

FIGURE 3

Some bond lengths and bond angles of monomeric $WSeF_4$ as deduced from gas-phase electron diffraction [Ref. 41].

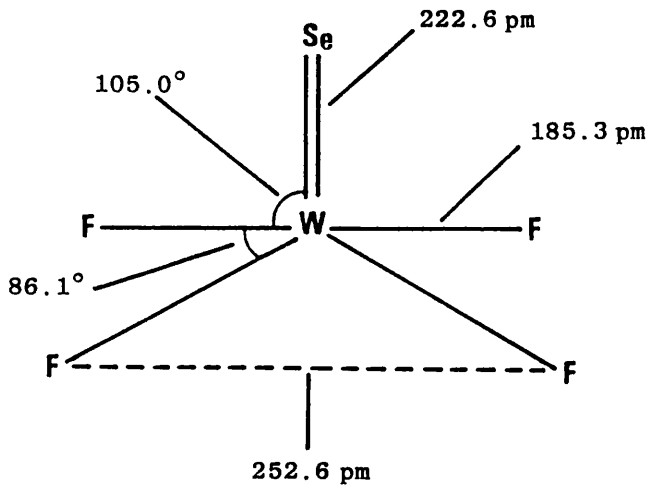

TABLE 7

Vibrational frequencies and assignments of monomeric $WSeF_4$ isolated in a nitrogen matrix[38]

WSeF	Mode
380?	$\nu_{W=Se}$ (A_1)
702	ν_{W-F} (A_1)
669	ν_{W-F} (E)

place. However, the reaction of Sb_2S_3 with ReF_5 in anhydrous HF has been shown to proceed at room temperature.

Freshly prepared $ReSF_5$ is a maroon solid, $ReSF_4$ is red and $ReSF_3$ is yellow. All are extremely sensitive to traces of moisture, and like other thio-fluorides of the transition metals, on exposure to the atmosphere, they rapidly evolve HF and H_2S. The mass spectra of the three species are related. Both $ReSF_5$ and $ReSF_4$ yield the expected splitting pattern. However for $ReSF_3$, the isotopic abundance pattern for the parent ion was not observed, the most abundant rhenium thio-fluoride species being $[ReSF_2]^+$.

The infra-red spectra of solid $ReSF_5$ and $ReSF_4$ showed bands in the regions associated with $\nu(Re\text{-}F)_{\mathbf{Terminal}}$ and $\nu(Re\text{-}F\text{-}Re)_{\mathbf{Bridging}}$ in addition to bands which were tentatively assigned to $\nu(Re{=}S)$. Comparison of the X-ray powder diffraction patterns of $ReSF_5$ and $ReSF_4$ show them not to be isostructural. A recent single crystal structure determination has shown solid $ReSF_4$ to consist of cis-fluorine bridged polymeric chains.[31] The structure is related to that of WSF_4 but the asymmetric unit consists of six $ReSF_5$ cis-linked octahedra and divided equally between two separate chains running parallel to the a-axis (Figure 4).

Because of the extreme reactivity exhibited by $ReSF_3$, satisfactory X-ray diffraction and infra-red data have not been obtained.

Initial attempts to prepare seleno-fluorides of rhenium via the thermal reaction of ReF_6 with Sb_2Se_3 have so far been unsuccessful.[24] Investigations into the preparation of telluro-fluoride species have, to date, not been reported.

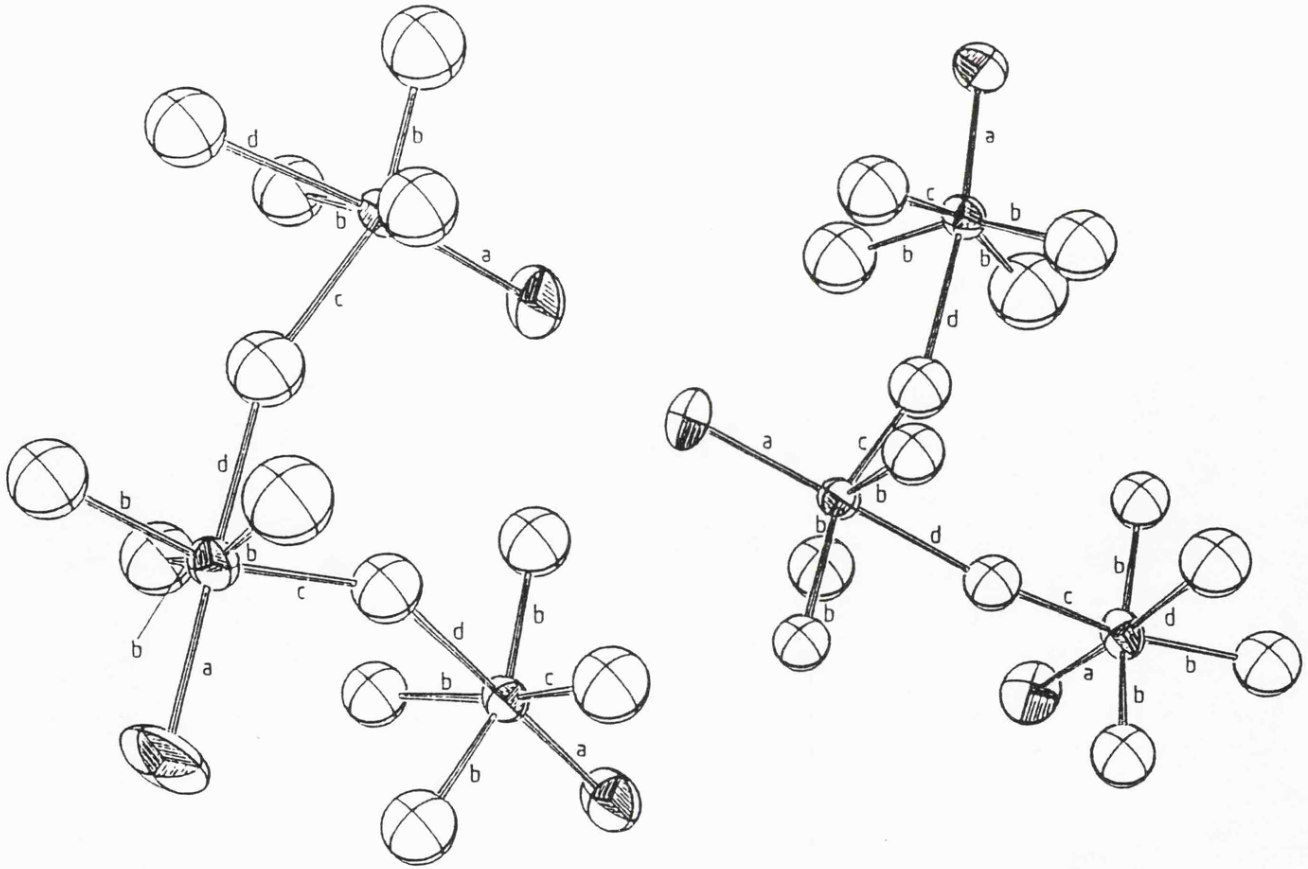

FIGURE 4

Molecular geometry of $ReSF_4$. Average bond lengths (Å) with s.d.s (in parentheses), taken from the six non-equivalent molecular units: a = 2.02(2), b = 1.85(4), c = 1.95(4), d = 2.23(4). The Re-F-Re bridging angles range from 146.8(1.8) to 160.5(1.9)°.

CHAPTER 2

The Attempted Preparation of $TaSF_3$, $OsSF_4$ and $IrSF_4$; the Isolation and Characterisation of $[SH_3]^+[Ta_2F_{11}]^-$, $SF_4.OsF_5$ and $SF_4.IrF_5$

2.1 INTRODUCTION

The preceding Chapter describes the successful preparation, isolation and characterisation of transition metal, thio-, seleno- and telluro-fluorides but, so far, known species occur only in groups IIIA, VIA and VIIA. In attempts to obtain the thiofluorides of tantalum, osmium and iridium, $TaSF_5$, $OsSF_4$ and $IrSF_4$ respectively, reactions analogous to those used to isolate the tungsten and rhenium thio-fluoride species have been investigated.

2.2 THE ATTEMPTED PREPARATION OF $TaSF_3$ FROM THE REACTION OF $TaSX_3$, X = Cl, Br, WITH ANHYDROUS HF

2.2.1 Present Study

Previous investigations into the preparation of $TaSF_3$ have shown that no thermally initiated reaction occurs between TaF_5 and A_2S_3, A = B, Sb.[24,30] However, when TaF_5 was allowed to react with Sb_2S_3 in anhydrous HF solvent, a reaction was observed.[24,30] This reaction was shown to be anomalous when compared to similar reactions of Sb_2S_3 with WF_6 and ReF_x, x = 5, 6, 7, since no evidence for the formation of a tantalum thio-fluoride species was obtained.

The thio-fluoride species of tungsten were first identified in solution via the reaction of anhydrous HF with $WSCl_4$.[26,27] In light of the success of this reaction, the reaction of $TaSX_3$, X = Cl or Br, with an excess of anhydrous HF has been the subject of the present study. It was anticipated that such a reaction would proceed via Scheme 3 to yield $TaSF_3$. However, the isolated product has been shown to be the previously uncharacterised complex of tantalum, $[SH_3]^+[Ta_2F_{11}]^-$, (Scheme 4). The preparation and characterisation of $[SH_3]^+[Ta_2F_{11}]^-$ is fully discussed in section 2.6.

$$TaSX_3 \xrightarrow[\text{Excess}]{HF} TaSF_3 + 3HX, \quad X = Cl \text{ or } Br$$

SCHEME 3

$$TaSX_3 \xrightarrow[\text{Excess}]{HF} [SH_3]^+[Ta_2F_{11}]^- + HX, \quad X = Cl \text{ or } Br$$

SCHEME 4

Investigations of the reaction of a solution of $TaSX_3$ with a stoichiometric amount of anhydrous HF in acetonitrile have also proved unsuccessful. Instead of proceeding via Scheme 5 to yield $TaSF_3(CH_3CN)_2$, oils were isolated which are thought to contain a polymeric species derived from acetonitrile.

$$TaSX_3 + 3HF \xrightarrow{CH_3CN} TaSF_3(CH_3CN)_2 + 3HX, \quad X = Cl \text{ or } Br$$

SCHEME 5

In spite of the lack of success in preparing a thio-fluoride species of tantalum in this study, the reaction procedures and results obtained are discussed here.

2.3 THE REACTION OF $TaSX_3$, X = Cl OR Br, WITH AN EXCESS OF ANHYDROUS HF

2.3.1 General procedure

The reactions were carried out in ¼" Teflon FEP reactor tubes, pre-seasoned with fluorine and fitted with Teflon needle valves. After addition of tantalum sulphide halide (0.3-0.5 mmoles), in a dry box, the FEP reactors were attached to a 'parasite' fluoroplastic vacuum line (Chapter 8) and evacuated to high vacuum. An approximately 15-fold excess of anhydrous HF was then distilled onto the sulphide at liquid nitrogen temperature.

2.3.2 The reaction of $TaSCl_3$ with an excess of HF

The FEP reactor tube containing the $TaSCl_3$ and excess HF was warmed

stepwise (-78, -30 and 0°C) to 25°C. No apparent reaction was evident, only clear, liquid HF above yellow $TaSCl_3$ was observed. After standing at room temperature for several hours it was noticed that diminution of the initial bulk of $TaSCl_3$ had occurred. This had been accompanied by the yellowing of the HF solvent. On cooling to -78°C, an off-white, semi-crystalline material precipitated from the solvent. Examination of the volatile material taken from the FEP tube at -78°C, by gas-phase infra-red, revealed the presence of HCl. This indicated that a fluorine exchange reaction, similar to that expected for Scheme 3, had taken place between $TaSCl_3$ and HF. After standing at room temperature for 15 hours, all the yellow $TaSCl_3$ had been consumed, and only a pale yellow HF solution remained. Careful removal of the excess of HF by distillation resulted in the isolation of an off-white semi-crystalline material. Analysis by X-ray powder diffraction and infra-red spectroscopy showed this to be the complex $SH_3^+[Ta_2F_{11}]^-$, and not the expected thio-fluoride, $TaSF_3$ [Tables 8 and 9]. Further analysis of the off-white material by mass spectrometry confirmed these observations; the only ions formed being those particular to H_2S and TaF_5.

2.3.3 The reaction of $TaSBr_3$ with HF

Similar reaction conditions to those described in the preceding section were used to investigate the reaction of $TaSBr_5$ with an excess of anhydrous HF. Analysis of the solid isolated by X-ray powder diffraction and infra-red spectroscopy showed that, as in the case of the reaction of $TaSCl_3$ with an excess of HF, the complex $[SH_3]^+[Ta_2F_{11}]^-$ was the only solid species formed [Tables 8 and 9]. In no instance was evidence obtained for the formation of a thio-fluoride such as $TaSF_3$.

TABLE 8

X-ray powder diffraction data of the off-white solids isolated from the reaction of TaSX (X = Cl or Br) with an excess of anhydrous HF

Off-white solid from the reaction of $TaSCl_3$ with an excess of HF		Off-white solid from the reaction of $TaSBr_3$ with an excess of HF		$[SH_3]^+[Ta_2F_{11}]^-$ [a]	
d/A°	Intensity	d/A°	Intensity	d/A°	Intensity
5.748	15	5.751	15	5.746	15
5.461	15	5.440	15	5.457	15
5.187	40	5.201	40	5.191	40
5.017	40	5.014	40	5.010	40
4.149	100	4.152	100	4.152	100
3.819	15	3.820	15	3.814	15
3.579	90	3.581	90	3.584	90
3.472	15	3.476	15	3.481	15
3.109	10	3.108	10	3.100	10

[a] *See Table 10*

TABLE 9

Infra-red spectral data of the off-white solids isolated from the reaction of $TaSX_3$ (X = Cl or Br) with an excess of anhydrous HF, compared with those of $[SH_3]^+[Ta_2F_{11}]^-$

Frequency (cm^{-1})			Assignment[b]	
Off-white solid from the reaction of $TaSCl_3$ with an excess of HF	Off-white solid from the reaction of $TaSBr_3$ with an excess of HF	$[SH_3]^+[Ta_2F_{11}]^-$[b]	$[SH_3]^+, C_{3v}$	$[Ta_2F_{11}]^-$
2520 m, br	2520 m, br	2520 ms, br	(ν_1, ν_3)	
1025 mw	1026 m	1026 m	ν_2	
742 m[a]	742 ms[a]	740 m[a]		
722 ms	722 ms	722 ms		
700 s	700 s	700 s		
675 s	675 s	675 s		
645 s	645 s	645 s		
604 s, br	607 s, br	606 s, br		
505 s	505 ms	505 ms		
480 ms	481 m	482 ms		

[a] *Exhibit variable intensity;*
[b] *See Table 11.*

2.4 THE REACTION OF $TaSX_3$, X = Cl OR Br, WITH A 3 MOLAR EQUIVALENCE OF ANHYDROUS HF IN ACETONITRILE

2.4.1 General procedure

The reactions were carried out in ¼" Teflon FEP reactor tubes, pre-seasoned with fluorine, and fitted with Teflon needle valves. After addition of tantalum sulphide halide (0.2-0.5 mmoles), in a dry box, the FEP reactors were attached to the main vacuum manifold and evacuated to high vacuum. An excess of acetonitrile was distilled onto the respective sulphide at -196°C. Warming to room temperature followed by shaking for 0.5 hours afforded dark brown solutions of the respective sulphide dissolved in acetonitrile.[45] These solutions were cooled to -196°C and a 3 molar equivalence of anhydrous HF was metered into the reactor tubes.

2.4.2 The reaction of $TaSX_3$, X = Cl, Br, with HF in acetonitrile

The FEP reactor tube contents, $TaSX_3$, CH_3CN and HF, were allowed to warm to room temperature. On melting, a reaction between the HF and brown solutions of $TaSX_3$ in CH_3CN was indicated by the rapid formation of a colourless solution. This was allowed to stand at ambient temperature with occasional mixing for 2 hours. At the end of this period the solution remained unchanged and the reaction was deemed complete. Removal of the excess of solvent by distillation resulted in the isolation of a pale yellow oil. Analysis by infra-red spectroscopy showed three sets of strong absorptions in the regions 3500-3000 cm^{-1}, 1600-1500 cm^{-1} and 580 cm^{-1}. The former regions are normally associated with N-H stretching and N-H bending modes of amine and ammonium type compounds,[46] whilst the latter is characteristic of Ta-F stretching modes.[47] The precise nature of the oil was not ascertained but it appears likely that a polymeric species containing the groups =NH

or $\equiv\overset{+}{N}H$ is formed. Evidence for the formation of a tantalum thio-fluoride species was not obtained.

2.5 CONCLUSION

This study shows that the thio-fluoride species $TaSF_3$ cannot be prepared *via* fluorine exchange reactions between $TaSX_3$, X = Cl or Br, and anhydrous HF. In the case of the reaction of $TaSX_3$ with an excess of anhydrous HF, the previously uncharacterised species $[SH_3]^+[Ta_2F_{11}]^-$ is formed instead of the expected compound $TaSF_3$. The reason for the formation of $[SH_3]^+[Ta_2F_{11}]^-$ is not fully understood but it seems likely that reaction proceeds *via* the formation of TaF_5 which in the presence of HF, forms a super acid medium. The sulphur present is protonated in this medium to yield $[SH_3]^+$ which is stabilised by $[Ta_2F_{11}]^-$. This may also go some way to explaining the reaction of $TaSX_3$ in CH_3CN with a 3 molar equivalence of HF, in which oils are isolated. The presence of N-H stretching and bending modes in the infra-red spectra of these oils is indicative of this reaction proceeding *via* the protonation of CH_3CN. It is possible that TaF_5 is formed in the reaction which, in the presence of HF, catalyses the protonation of CH_3CN to yield species containing =NH and $\equiv NH^+$. This is further supported by the observation of a strong band at 580 cm^{-1} in the infra-red spectra of the oils, which is characteristic of ν_3 of the octahedral anion, $[TaF_6]^-$.[47]

It may be interesting to extend this study to the investigation of the reaction of TaF_5 with $Me_3Si\text{-}S\text{-}SiMe_3$. A recent report by Mironov *et al.*[48] has shown that $NbSCl_3$ can be conveniently prepared by the reaction of $NbCl_5$ with such a reagent.

2.6 THE PREPARATION AND CHARACTERISATION OF $[SH_3]^+[Ta_2F_{11}]^-$

The complex of tantalum $[SH_3]^+[Ta_2F_{11}]^-$ has been prepared by the reaction of H_2S with a solution of TaF_5 in anhydrous HF. The isolated off-white material has been characterised on the basis of X-ray powder diffraction and vibrational spectroscopy (Tables 10 and 11).

2.6.1 General procedure

Tantalum pentafluoride (1.2 mmoles) was introduced into a pre-seasoned ¼" Teflon FEP reactor tube, fitted with a Teflon needle valve, in a dry box. After addition of anhydrous HF (*ca.* 0.5 ml) *via* a 'parasite' fluoroplastic vacuum line (Chapter 8), a known excess of H_2S was metered into the reactor tube at -196°C. On warming to ambient temperature, the anhydrous HF was judiciously agitated to ensure dissolution of TaF_5 and H_2S. This resulted in the rapid formation of a pale yellow solution above an off-white solid. This was left standing at ambient temperature for 1 hour, with frequent mixing. At the end of this period, the excess of anhydrous HF solvent, and volatiles, were removed from the reactor tube *via* static vacuum distillation. The off-white, semi-crystalline material isolated was subject to analysis by X-ray powder diffraction and vibrational spectroscopy.

2.6.2 X-ray powder diffraction studies

The X-ray powder diffraction data of the off-white solid is recorded together with that of TaF_5 in Table 10. Comparison of the respective data confirms that the reaction of TaF_5 with H_2S in HF proceeds to completion and that the solid isolated is a new phase.

2.6.3 Vibrational spectroscopic studies

The infra-red spectrum of the off-white solid is shown in Figure 5. The infra-red and Raman data of this together with that of $[Ta_2F_{11}]^-$ in

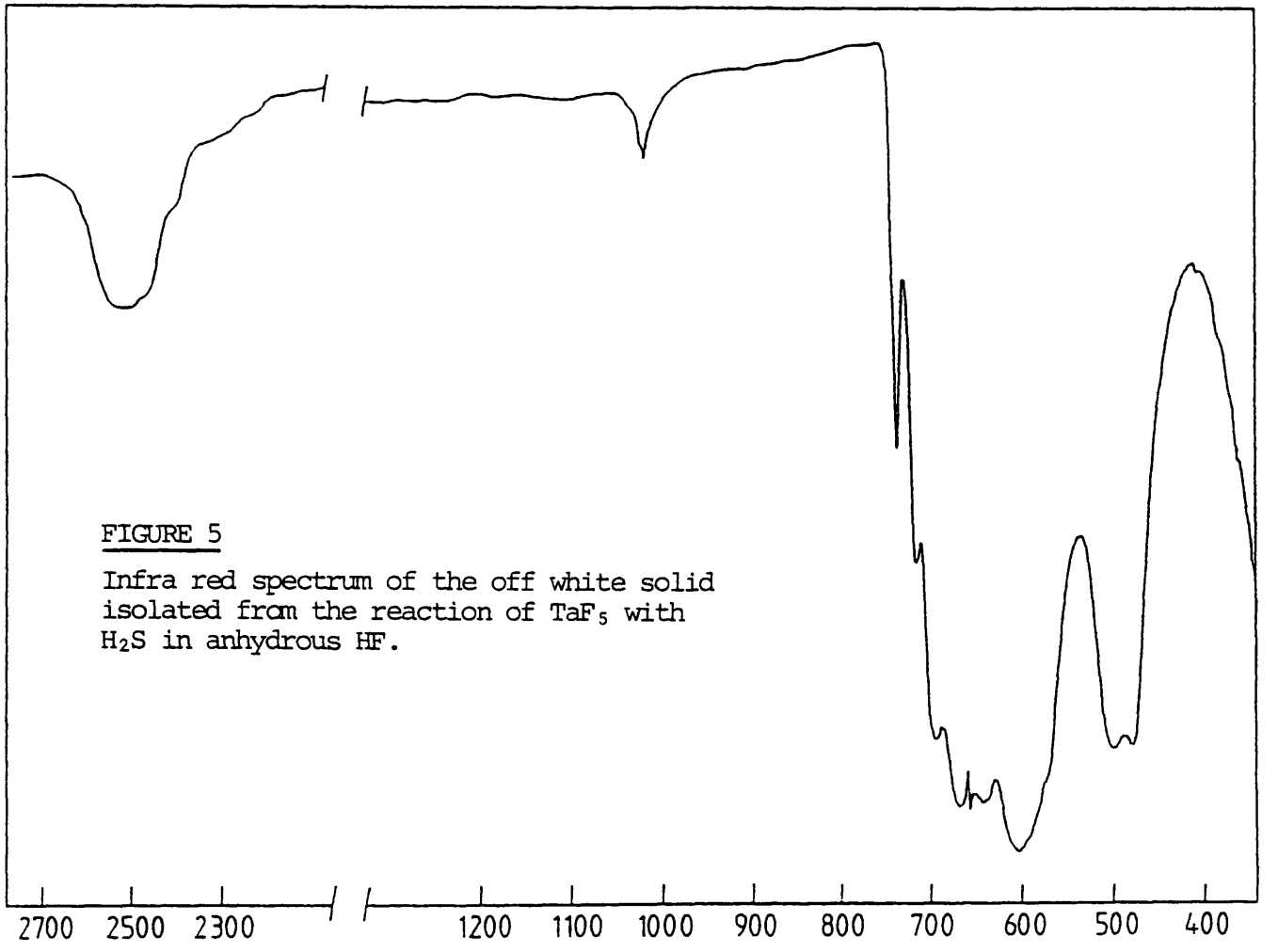

FIGURE 5

Infra red spectrum of the off white solid isolated from the reaction of TaF_5 with H_2S in anhydrous HF.

TABLE 10

X-ray powder diffraction pattern of the off-white solid isolated from the reaction of TaF_5 with H_2S in anhydrous HF

Off-white solid		TaF_5	
d/A°	Intensity	d/A°	Intensity
5.746	15	5.065	20
5.475	15	4.446	15
5.191	40	4.301	20
5.010	40	4.124	40
4.152	100	3.990	100
3.814	15	3.359	80
3.584	90	2.782	30
3.481	15	2.391	30
3.100	10	2.268	20

in $XeF_2.2TaF_5$[49] and $[SH_3]^+$ in $[SH_3]^+[SbF_6]^-$[50] are recorded in Table 11.

Comparison of the vibrational data of the off-white solid to that of $[Ta_2F_{11}]^-$ in $XeF_2.2TaF_5$[49] shows the bands associated with $[Ta_2F_{11}]^-$ are evident. Bands particular to the anion $[TaF_6]^-$ were not observed.[47,49] Further comparison with the vibrational data of $[SH_3]^+[SbF_6]^-$[50] permits assignment of the bands at 2520 and 1026 cm^{-1} to (ν_3,ν_1) and ν_3 of $[SH_3]^+$ respectively. The bands assigned to ν_2 and ν_4 in the Raman and ν_4 in the infra-red spectra of the cation in $[SH_3]^+[SbF_6]^-$ were not observed in the corresponding cation in the off-white solid due to their very low intensities.

2.7 THE ATTEMPTED PREPARATION OF $OsSF_4$ and $IrSF_4$

2.7.1 Present Study

The thermal reactions of MF_6, M = Os or Ir, with the sulphides ZnS and

TABLE 11

Vibrational spectral data of the off-white solid isolated from the reaction of TaF_5 with H_2S in anhydrous HF, compared with those of $[Ta_2F_{11}]^-$ and $[SH_3]^+$

Frequency cm^{-1}						Assignment[49,50]	
Off-white solid[c]		$[Ta_2F_{11}]^-$ in $XeF_2.2TaF_5$[49]		$[SH_3]^+$ in $[SH_3]^+[SbF_6]^-$[50]			
Ra	Ir	Ra	Ir	Ra	Ir	$[SH_3]^+ C_{3v}$	$[Ta_2F_{11}]^-$
				2520 (13)			
2500 (8, br)	2520 ms, br				2520 vs	(ν_3, ν_1)	
				2490 sh			
a					2360 sh	$2\nu_4$	
					1308 w		
					1222 w		
a				1180 (4)	1180 vw	ν_4	
a	1026 m			1025 (4)	1028 mw	ν_2	
725 (40)	740 m[b]	738 (53)	752 sh				
726 (100)	722 ms	726 (100)	735 sh				
	700 s	698 (8)	724 sh				
	675 s	680 (10)	669 mw				
668 (27)	645 s	667 (9)	667 m				
653 (4)	606 s, br	654 (4)	581 sh				
	505 ms	646 (5)	576 s				
	482 ms	628 (17)	564 sh				
		270 (9)	491 br, w				
251 (16)		253 (28)					
238 (sh)		240 (sh)					
219 (8)		218 (6)					
215 (sh)		200 (4)					
180 (5)							

[a] *Not measured due to low intensity;* [b] *Exhibits variable intensity;* [c] *Recorded at -120°C.*

and B_2S_3 have been investigated. Unlike the analogous reactions of WF_6 and ReF_6, thio-fluorides were not obtained. Instead, the reactions have resulted in the isolation of the previously identified adducts, $SF_4.OsF_5$[51] and $SF_4.IrF_5$.[51,52] These adducts have been fully characterised and are discussed in section 2.11.

Further attempts to prepare the thio-fluoride species via the reaction of the respective hexafluoride with Sb_2S_3, in anhydrous HF solvent, have also been made. However, these have shown that only lower oxidation-state fluorides, SbF_3 and unreacted Sb_2S_3, are obtained.

2.8 THE REACTION OF MF_6, M = Os OR Ir, WITH ZnS AND B_2S_3 AT ELEVATED TEMPERATURES

2.8.1 General procedure

Thermal reactions were carried out using between 0.8 and 3.0 mmoles of the hexafluoride (5% excess) in a pre-fluorinated stainless steel reactor. In accordance with the stoichiometry of the Schemes 6 and 7, the appropriate amounts of ZnS or B_2S_3 were loaded into the reactor in the dry box. After evacuation the hexafluoride was introduced at liquid nitrogen temperature.

$$MF_6 + ZnS \longrightarrow MSF_4 + ZnF_2, \quad M = Os \text{ or } Ir$$

SCHEME 6

$$3MF_6 + B_2S_3 \longrightarrow 3MSF_4 + 2BF_3, \quad M = Os \text{ or } Ir$$

SCHEME 7

2.8.2 The reaction of MF_6, M = Os or Ir, with ZnS

The investigation of the thermal reaction of ZnS with MF_6 was repeated several times. In each case the reactor was heated to 300°C, but the reaction period was varied between 7 and 11 hours [Table 12]. On cooling to room temperature the reactor was opened to the manifold,

TABLE 12

Thermal reactions of MF_6 (M = Os or Ir) with ZnS or B_2S_3

Reactions	Temp./°C	Duration/h	Products	
			Volatiles[53,54,55,56,57,58]	Solids
$IrF_6 + ZnS$	300	7–11	SF_4, SF_6, S_2F_{10}	$SF_4.IrF_5$, Ir metal
$OsF_6 + ZnS$	300	7–11	SF_4, SF_6, S_2F_{10}	$SF_4.OsF_5$, Os metal
$3IrF_6 + B_2S_3$	210	4–6	SF_4, SF_6, S_2F_{10}, BF_3	$SF_4.IrF_5$, Ir metal
$3OsF_6 + B_2S_3$	210	4–6	SF_4, SF_6, S_2F_{10}, BF_3	$SF_4.OsF_5$, Os metal

whereupon a pressure of between 50-60 mmHg was recorded. Analysis of the volatiles via gas-phase infra-red spectroscopy showed the volatile gas to consist of SF_4,[53,54] SF_6[55] and S_2F_{10}.[56,57] Mass spectroscopic analysis confirmed these results, and also showed that all the MF_6 had been consumed in reaction with the ZnS. Inspection of the reactor contents in a dry box revealed the presence of a dark powder in the upper, cooler regions of the reactor. Analysis by X-ray powder diffraction and infra-red spectroscopy showed that, in addition to the metal, M, the adducts $SF_4.MF_5$ had been formed. The $SF_4.MF_5$ adducts were characterised by comparing their infra-red spectra (Table 13) and X-ray powder diffraction patterns with those of the solid products from the reactions of the appropriate metal hexafluoride with SF_4, which are already known to produce these adducts[51,52] (section 2.11).

No evidence of the presence of thio-fluoride species such as MSF_4 was detected in these analyses.

2.8.3 The reaction of MF_6, M = Os or Ir, with B_2S_3

As with the reactions between MF_6 and ZnS, several reactions of MF_6 with B_2S_3 have been investigated. In each case the reactor was heated to ca. 210°C for times varying between 4 and 6 hours (Table 12). On cooling to room temperature, the reactor was opened to the manifold and the volatiles analysed by gas-phase infra-red spectroscopy. In addition to the presence of bands due to the expected fluoride, BF_3,[58] bands characteristic of the species SF_4,[53,54] SF_6[55] and S_2F_{10}[56,57] were also observed. Further analysis by mass spectrometry confirmed that all the MF_6 had reacted with the B_2S_3. On opening the reactor in a dry box a dark solid was isolated. Analysis of this by X-ray powder diffraction and infra-red spectroscopy showed that, as in the reaction of MF_6 with ZnS, the metal, M, and the adduct $SF_4.MF_5$ had been formed

TABLE 13

Comparison of infra-red spectra of solid products of reactions of MF_6 (M = Os or Ir) and ZnS or B_2S_3 with those of $SF_4.MF_5$

Solid from the reaction of OsF_6 with ZnS or B_2S_3	$SF_4.OsF_5$ [a]	Solid from the reaction of IrF_6 with ZnS or B_2S_3	$SF_4.IrF_5$ [a]	Assignments	
				$[SF_3]^+$ [a]	$[MF_6]^-$ [a]
922 ms	925 s, br	920 s, br	920 s, br	ν_1, ν_3	
	705 w, m				
640 s	~620 vs, br	635 s, br	635 s, br		ν_3
590 w, sh					
525 ms	528 s	522 s	522 s	ν_2	
-	400 s	400 m	400 ms	ν_4	

[a] *See Table 16*

(Table 13). The presence of the thio-fluoride species such as $OsSF_4$ and $IrSF_4$ were not detected.

2.9 THE REACTION OF MF_6, M = Os OR Ir, WITH Sb_2S_3 IN ANHYDROUS HF

2.9.1 General procedure

Antimony sulphide, Sb_2S_3 (0.15 mmoles) was introduced into a pre-fluorinated ¼" Teflon FEP reactor tube, fitted with a Teflon needle valve, in a dry box. The reactor was attached to a 'parasite' fluoro-plastic vacuum line (Chapter 8) and, after evacuation, ca. 0.5 ml of anhydrous HF was distilled onto the sulphide at -196°C. By maintaining the temperature at -196°C, the appropriate quantity of metal hexa-fluoride, according to the stoichiometry of Scheme 8, was metered into the reaction tube.

$$3MF_6 + Sb_2S_3 \xrightarrow{HF} 3MSF_4 + 2SbF_3, \ M = Os \text{ or } Ir$$

SCHEME 8

2.9.2 The reaction of OsF_6 with Sb_2S_3 in anhydrous HF

On warming to room temperature the yellow solution of OsF_6 dissolved in the HF solvent slowly discoloured to yield a blue/green solution above the black Sb_2S_3. By careful decantation and subsequent removal of the HF solvent by distillation, a blue/green solid was isolated. X-ray powder diffraction studies showed this to be OsF_5. Analysis of the residual black material left from decantation showed this to consist of SbF_3 and unreacted Sb_2S_3. No thio-fluoride species of osmium were detected (Table 14).

2.9.3 The reaction of IrF_6 with Sb_2S_3 in anhydrous HF

The reaction of IrF_6 with Sb_2S_3 in HF proceeds rapidly at room temperature to yield a pale yellow solution above a brown solid. Analysis of the solid isolated, after the removal of the HF solvent, by

X-ray powder diffraction revealed the presence of only SbF_3. Infra-red spectroscopy confirmed this observation. Removal of the SbF_3 by sublimation resulted in the isolation of a brown, involatile solid. This was shown to be amorphous to X-rays and did not yield an infra-red spectrum. Further analysis of the solid by X-ray fluorescence spectroscopy determined the presence of iridium, antimony and sulphur (Table 14). Although no definitive conclusions could be drawn concerning the nature of the solid, it is probable that it contains a low fluoride of iridium, e.g. IrF_4, and unreacted Sb_2S_3. In no instance during this study was a thio-fluoride species such as $IrSF_4$ observed.

TABLE 14

Reaction of MF_6 (M = Os or Ir) with Sb_2S_3 in anhydrous HF at room temperature

Reactants	Products
$3IrF_6 + Sb_2S_3$	SbF_3,[a] involatile brown powder which contains iridium, antimony and sulphur[b]
$3OsF_6 + Sb_2S_3$	SbF_3, OsF_5 and unreacted Sb_2S_3[a]

[a] *Determined by X-ray powder diffraction;*
[b] *Determined by X-ray fluorescence spectroscopy.*

2.10 CONCLUSION

It is apparent that the thio-fluorides of osmium and iridium cannot be formed by the analogous methods used to prepare group VIA and VIIA species, WSF_4 and $ReSF_4$. Instead of the expected sulphur substitution reactions which would have yielded $OsSF_4$ and $IrSF_4$, the hexafluorides, OsF_6 and IrF_6, appear to be partaking in oxidation/reduction reactions with the sulphide reagents used. The anomalous behaviour of OsF_6 and

IrF_6 can be explained as follows.

The transition metal hexafluorides increase in oxidant strength with increasing atomic number across any period of the Periodic table.[59,60] The trend for the 3rd. row transition series is:-

$$WF_6 < ReF_6 < OsF_6 < IrF_6 < PtF_6.$$

The greater electron affinity of PtF_6, compared with that of WF_6 correlates with the greater nuclear charge on the platinum and with the poor shielding of this charge from the ligands by the formally non bonding t_{2g} electrons. Since the non bonding t_{2g} valence electron configurations are:-

$$WF_6 = 0;\ \ ReF_6 = 1;\ \ OsF_6 = 2;\ \ IrF_6 = 3;\ \ PtF_6 = 4,$$

a regular increase in oxidising power may be anticipated. Thus, while WF_6 and ReF_6 can substitute sulphur to give WSF_4 and $ReSF_4$ respectively, it is not surprising that OsF_6 and IrF_6 readily oxidatively fluorinate B_2S_3 and ZnS to give SF_4 and that the reduced pentafluoride species, OsF_5 and IrF_5 then combine with this to give $SF_4.OsF_5$ and $SF_4.IrF_5$.

Since the attempts to prepare $OsSF_4$ and $IrSF_4$ by the means described in this study have proved unsuccessful, it may be of interest to investigate the reaction of the respective hexafluoride with the reagent $Me_3Si\text{-}S\text{-}SiMe_3$. A recent report by Mironov et al.[48] has shown this reagent to be extremely useful in preparing the group VA chalcogenide chloride, $NbSCl_3$, from $NbCl_5$.

2.11 THE PREPARATION AND CHARACTERISATION OF $SF_4.MF_5$, M = Os, Ir

The adducts, $SF_4.OsF_5$ and $SF_4.IrF_5$ have been prepared by the method of Jha,[51] in which the appropriate metal hexafluoride reacts with liquid sulphur tetrafluoride (Scheme 9). The isolated adducts have been characterised by mass balance, elemental analysis, infra-red

spectroscopy and X-ray powder diffraction. The infra-red and X-ray powder diffraction studies suggest that the adducts have contributions to the bonding from the ionic formulations $[SF_3]^+[OsF_6]^-$ and $[SF_3]^+[IrF_6]^-$. A ^{19}F nmr study also gives evidence for the latter in solution in anhydrous HF.

$$MF_6 \xrightarrow[\text{Excess}]{SF_4} SF_6 + SF_4.MF_5, \quad M = Os \text{ or } Ir$$

SCHEME 9

2.11.1 General preparative procedure

The reactions described here were carried out in prefluorinated ¼" Teflon FEP reactor tubes fitted with Teflon needle valves.

An approximately 4-fold excess of SF_4 was distilled onto the appropriate hexafluoride (1-3 mmoles) at liquid nitrogen temperature and the mixture warmed to -78°C. In the IrF_6 case, reaction was immediate and vigorous. The reaction involving OsF_6 did not take place until further warming to -30°C (ice/salt bath) had occurred, and the reaction was complete only after 48 hours. However, reaction was immediate at room temperature. In both the reactions of OsF_6 and IrF_6 fine crystalline products (Os, lilac; Ir, pale yellow) were obtained after the removal of SF_6 and the excess of SF_4. Monitoring of the reactions by mass balance showed that 1 mol of the hexafluoride reacts with 1 mol of SF_4 in each case. This result was confirmed by elemental analysis [Found: F, 42.1; Os, 47.9; S, 7.7. Calculated for $SF_4.OsF_5$: F, 43.5; Os, 48.4; S, 8.1 and F, 43.6; Ir, 47.9; S, 7.6. Calculated for $SF_4.IrF_5$: F, 43.3; Ir, 48.6; 8.1].

2.11.2 X-ray powder diffraction studies

The X-ray powder diffraction data for the adducts $SF_4.OsF_5$ and $SF_4.IrF_5$ prepared in this study are compared with those previously

published by Jha[51] in Table 15. Jha has discussed the cubic symmetry of these adducts and, on the basis of a preliminary X-ray study of the isomorphous adduct $SF_4.SbF_5$ by Bartlett et al.,[61] it has been suggested that they contain an ionic lattice composed of $[SF_3]^+$ and $[MF_6]^-$ ions.

2.11.3 Infra-red spectroscopic studies

The infra red spectral data of $SF_4.OsF_5$ and $SF_4.IrF_5$ have been recorded in Table 16 together with the previously published data for $[SF_3]^+$ in the adduct $SF_4.BF_3$.[62] Comparison of the two sets of data shows that for the adducts $SF_4.OsF_5$ and $SF_4.IrF_5$, the bands occurring in the regions 920, 525 and 400 cm^{-1} can be assigned to (ν_1,ν_3), ν_2 and ν_4 respectively of the pyramidal C_{3v} cation $[SF_3]^+$. The remaining band in the region of 630 cm^{-1} is assigned to ν_3 of the octahedral species $[MF_6]^-$.[63]

The absence of splitting of the bands assigned to ν_3 and ν_4 of $[SF_3]^+$ and of the ν_3 band of $[MF_6]^-$ agree with the X-ray diffraction studies in suggesting that bonding in these adducts has contributions from the ionic formulation, $[SF_3]^+[MF_6]^-$. However, it is very likely that significant interaction between the cation and anion occurs via fluorine bridging. A similar case exists for $[SeF_3]^+[NbF_6]^-$,[64] $[SeF_3]^+[Nb_2F_{11}]^-$,[64] $[SF_3]^+[BF_4]^-$[65] and $[SF_3]_2^+[GeF_6]^{2-}$.[66]

2.11.4 ^{19}F nmr study of $SF_4.IrF_5$ in anhydrous HF

The yellow solution of $SF_4.IrF_5$ in anhydrous HF has been analysed by low temperature ^{19}F nmr. The results are recorded in Table 17. The appearance of a high frequency singlet at 31.0 ppm has been assigned to the $[SF_3]^+$ cation on the basis of similar results obtained for the adducts $SF_4.BF_5$, $SF_4.2AsF_5$, and $SF_4.SbF_5$ in anhydrous HF.[62]

Attempts to measure the ^{19}F nmr spectrum of the lilac solutions of

TABLE 15

Comparison of d-spacings for $SF_4.OsF_5$ and $SF_4.IrF_5$

This work			Ref. 51		
$SF_4.OsF_5$	$SF_4.IrF_5$	Relative Intensities[a]	$SF_4.OsF_5$	$SF_4.IrF_5$	Relative Intensities
5.584	5.582	6	5.564	5.581	8
3.932	3.930	10	3.934	3.934	10
3.211	3.209	3	3.204	3.202	6
2.786	3.786	3	2.781	2.776	5
2.484	2.482	4	2.486	2.482	6
2.273	2.271	6	2.273	2.267	7
1.974	1.972	3	1.970	1.966	5
1.849	1.850	4	1.856	1.855	7
1.758	1.759	4	1.763	1.758	5
1.682	1.680	1	1.679	1.678	4

a *Visual estimations*

TABLE 16

Infra-red spectral data for the adducts $SF_4.MF_5$, M = Os or Ir

Frequency cm^{-1}		Assignments	
$SF_4.OsF_5$	$SF_4.IrF_5$	$[SF_3]^{+}$ 62	$[MF_6]^{-}$ 63
925 s, br	920 s, br	ν_1, ν_3	
705 w, m			ν_3
~620 vs, br	635 s, br		
528 s	522 s	ν_2	
400 s	400 ms	ν_4	

TABLE 17

^{19}F nmr data of some adducts containing SF_4 in anhydrous HF

Solute	T/°C	Chemical Shift (p.p.m. from $CFCl_3$)	
		$[SF_3]^{+}$	HF
$SF_4.BF_3$	-50[a]	26.7[a]	-194.2[a]
$SF_4.2AsF_5$	-60[a]	26.8[a]	-198[a]
$SF_4.SbF_5$	-60[a]	27.1[a]	-178.3[a]
$SF_4.IrF_5$	-29[b]	31.0[b]	-196[b]

[a] *Reference 62;*
[b] *This work.*

$SF_4.OsF_5$ in anhydrous HF were unsuccessful and no peaks were recorded. This observation has been attributed to the paramagnetism of the pentavalent osmium present in this adduct.

CHAPTER 3

Tungsten Thiotetrafluoride and its reaction with the Alkali Metal Fluorides in Anhydrous HF

3.1 INTRODUCTION

The oxidetetrafluorides of Cr, Mo and W are known to act as weak fluoride-ion acceptors, giving ionic adducts containing the anions $[MOF_5]^-$ and $[M_2O_2F_9]^-$ in the presence of strong fluoride-ion bases such as NF_4HF_2,[67] $ClOF_3$,[68] NOF[68,69] and CsF.[69,70]

Although identification of $[WSF_5]^-$ and $[W_2S_2F_9]^-$ in solution by ^{19}F nmr[26,27] provided some of the first evidence for transition metal thio-fluorides, no solids containing these anions have been reported.

3.2 PRESENT STUDY

In light of the observation of the species $[WSF_5]^-$ and $[W_2S_2F_9]^-$ in solution, it was clear that WSF_4 should parallel the chemistry of the oxidetetrafluorides of Cr, Mo and W, in providing ionic adducts with strong fluoride-ion bases.

In this study the reaction of the alkali metal fluorides, MF, M = Li, Na, K, Rb or Cs, with WSF_4 in anhydrous HF has been investigated and the first examples of solids containing $[WSF_5]^-$ and $[W_2S_2F_9]^-$ have been isolated and characterised.

3.3 THE PREPARATION OF THE IONIC ADDUCTS, $M^+[W_2S_2F_9]^-$ [M = Li, Na, K, Rb or Cs]

The ionic adducts $M^+[W_2S_2F_9]^-$ have been prepared as yellow solids by the reaction of WSF_4 with MF in anhydrous HF solvent at 25°C (Scheme 10).

Tungsten thiotetrafluoride (0.63 mmole) and the respective alkali metal fluoride, MF, (0.31 mmole) were introduced into a prepassivated ¼" Teflon FEP reactor tube, fitted with a Teflon needle valve, in a dry box. The reactor was fitted to a 'parasite' fluoroplastic vacuum line (Chapter 8) and evacuated to high vacuum. Approximately 0.5 ml of

anhydrous HF was then condensed onto the reactor contents at -196°C. Warming to room temperature followed by shaking, yielded a flocculent yellow solid below a pale yellow HF solution [Scheme 10(i)]. Removal of the HF solvent, first under static vacuum and then by pumping under dynamic vacuum, resulted in the isolation of a yellow powder [Scheme 10(ii)]. This was shown to be the new ionic adduct, $M^+[W_2S_2F_9]^-$ by X-ray powder diffraction, infra-red and ^{19}F nmr spectroscopy.

$$2\,WSF_4 + MF \xrightarrow{(i)} \begin{array}{c}\textbf{Yellow solid}\\ \textbf{under pale}\\ \textbf{yellow HF solution}\end{array} \xrightarrow{(ii)} \begin{array}{c}M^+[W_2S_2F_9]^-\\ \textbf{Yellow}\end{array}$$

(i) *In anhydrous HF solvent at 25°C;*
(ii) *Excess anhydrous HF solvent removed by distillation.*

SCHEME 10

3.3.1 X-ray powder diffraction studies

The X-ray powder diffraction patterns obtained for the yellow powders are clearly different from those of WSF_4 and the respective alkali metal fluoride, thus confirming the solids are new phases. None of the five solids isolated are isostructural. This observation can be rationalised by assuming that the solid-state structure of $M^+[W_2S_2F_9]^-$ is dependent on the size of the cation, M^+. This relationship between the size of the cation, M^+, and the adopted structure of salts is well known for the fluoride complexes $M'B^vF_6$, and has been reviewed in detail by Kemmitt, Russell and Sharp.[71]

3.3.2 Infra-red spectroscopic studies

The infra-red spectra of the ionic adducts $M^+[W_2S_2F_9]$, as fine powders between KBr discs, are shown in Figure 6. The data, together with those for $Cs^+[W_2O_2F_9]^-$[67] are recorded in Table 18.

Comparison of the infra-red spectral data of $M^+[W_2S_2F_9]^-$ with that of

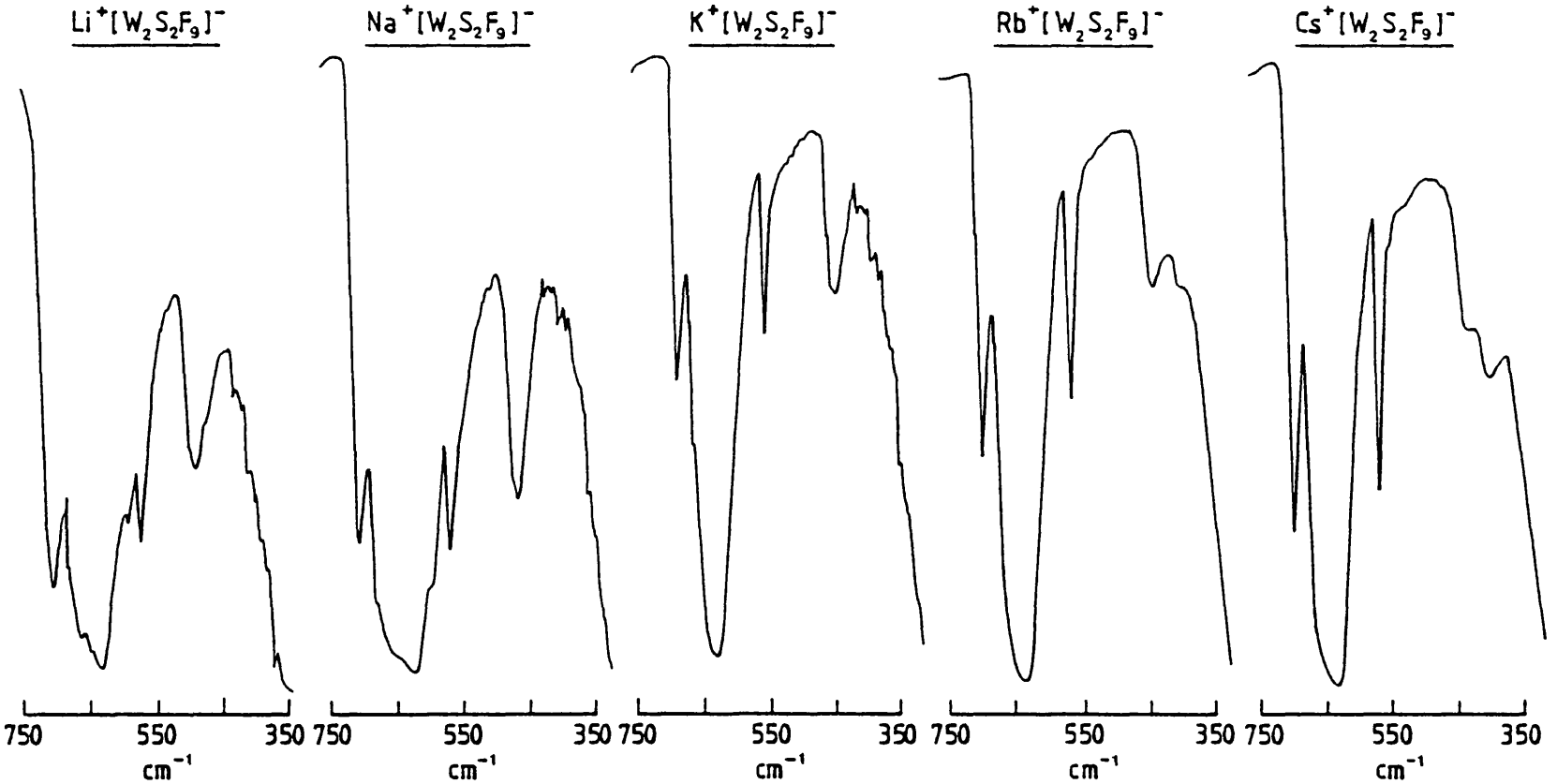

FIGURE 6

Infra-red spectra of $M^+[W_2S_2F_9]^-$, M = Li, Na, K, Rb or Cs.

TABLE 18

Infra-red spectral data of $M^+[W_2S_2F_9]^-$, M = Li, Na, K, Rb or Cs

Frequency cm^{-1}						
$Li^+[W_2S_2F_9]^-$ [a]	$Na^+[W_2S_2F_9]^-$ [a]	$K^+[W_2S_2F_9]^-$ [a]	$Rb^+[W_2S_2F_9]^-$ [a]	$Cs^+[W_2S_2F_9]^-$ [a]	$Cs^+[W_2O_2F_9]^-$ [67]	Assignment[67]
					1048 vs	ν(W=O) o.o.p.
					1035 vs	ν(W=O) i.p.
					822 vw	
					790 vw	
685 s	692 s	690 ms	682 ms	682 s	704 vs	$\nu_s(WF_4)$ i.p.
645 sh	642 s,sh					
615 vs	610 vs	620 vs	620 vs	620 vs	628 vs,br	$\nu_{as}(WF_4)$
575 ms	582 s,sh					
555 ms	555 ms	555 m	555 m	555 ms		ν(W=S)[30]
470 m	455 ms	447 m	430 m	415 m	440 vs	ν_{as}(WFW)
			385 sh	385 m		

[a] *Minor peaks due to trace amounts of tungsten oxide fluoride impurities have been removed.*

o.o.p. = out-of-phase; i.p. = in-phase.

$Cs^+[W_2O_2F_9]^-$ has permitted the assignment of $\nu_s(WF_4)_{in\text{-}phase}$, $\nu_{as}(WF_4)$ and the bridging stretch, $\nu_{as}(WFW)$. The stretching frequency of the W=S bond, assigned to the absorption at 555 cm^{-1}, is close to that observed in the solid complex, $WSF_4.CH_3CN$.[30] The position of the bridging stretch, $\nu_{as}(WFW)$ in $Cs^+[W_2S_2F_9]^-$ is some 25 cm^{-1} lower in frequency than the equivalent bond in $Cs^+[W_2O_2F_9]^-$. This can be attributed to the greater trans effect of the sulphur atom in the moiety, W=S, compared to that of oxygen in W=O. The relative positions of $\nu_s(WF_4)$ in phase and the bridging stretch, $\nu_{as}(WFW)$, are distinctly different; the latter occurring at ca. 300 cm^{-1} lower in frequency than the former. This is in agreement with similar observations made for the ionic adducts containing $[M_2O_2F_9]^-$, M = Mo or W, and is attributed to the greater ionic character of the metal-fluorine bridging bond.[68]

The regular increase in frequency of the bridging stretch, $\nu_{as}(WFW)$ for the sequence Cs < Rb < K < Na < Li observed for $M^+[W_2S_2F_9]^-$ (Table 18) is more difficult to explain, however, it is likely that the degree of ionic character of the adducts $M^+[W_2S_2F_9]^-$ plays an important rôle. It can be assumed that the ionic character of $M^+[W_2S_2F_9]^-$ increases in the sequence Li < Na < K < Rb < Cs. Thus $Li^+[W_2S_2F_9]^-$ will have the least ionic, and therefore, strongest tungsten-fluorine bridging bond, whereas $Cs^+[W_2S_2F_9]^-$ will have the most ionic, and, therefore, the weakest tungsten-fluorine bridging bond.

3.4 ^{19}F NMR STUDIES OF $M^+[W_2S_2F_9]^-$ IN CH_3CN

3.4.1 The characterisation of $[W_2S_2F_9]^-$ in solution

The ionic adducts, $M^+[W_2S_2F_9]^-$, exhibit high solubility in acetonitrile. Samples prepared for ^{19}F nmr studies yielded straw-coloured

solutions. This colour persists at temperatures ranging from 0 to -43°C, the freezing point of the solvent. When stored at room temperature, however, the solutions rapidly darken to yield a dark brown precipitate.

The ^{19}F nmr spectra were recorded at -12°C using a 'continuous wave' nmr spectrometer. The results from the study are recorded in Table 19. The spectra are typical of the AX_8 type pattern for the fluorine-bridged species, $[W_2S_2F_9]^-$, in solution,[26,27] (i.e. a bridging fluorine atom, Fb, between two tungsten atoms each bonded to four equivalent equatorial fluorine atoms, Fe, Figure 7a). The high-frequency doublet and low-frequency nonet (integration ratio 8:1) are the main peaks observed. The chemical shift parameters show the bridging fluorine atom, Fb, to be considerably more shielded than the equatorial fluorine atoms, Fe. This is consistent with similar observations made for $[M_2O_2F_9]^-$,[68] M = Mo or W, and confirms the inference from the infra-red spectroscopic data of the previous section, that the negative charge of the anion is localised mainly on the tungsten-fluorine bridging bond.

The comparison of the ^{19}F nmr chemical shift parameters of $[W_2S_2F_9]^-$ and $[W_2O_2F_9]^-$ by Buslaev et al.[26] shows the shielding of the bridging fluorine atom in the former anion to be greater than that in the latter. This observation confirms the results from the infra-red spectroscopic study, and shows the trans-effect of the sulphur atom in the moiety W=S to be greater than oxygen in W=O.

A detailed examination of $M^+[W_2S_2F_9]^-$, M = Li, K or Rb, in CH_3CN using a Fourier Transform nmr spectrometer yielded a fully resolved spectrum of the low-frequency nonet, Figure 8a. The doublets associated with each component of the nonet are a consequence of the bridging

TABLE 19

^{19}F nmr data for the ionic adducts $M^+[W_2S_2F_9]^-$, M = Li, Na, K, Rb or Cs in CH_3CN at -12°C

Sample	δ/ppm[a]	Multiplet[b] Structure	Coupling Constant/Hz	Assignment[c]
$Li^+[W_2S_2F_9]^-$	84.7	II	$^2J_{Fb-Fe}$ 70	$F_4WS-(\bar{F})-SWF_4$
	80.0	II[e]	$^2J_{Fa-Fe}$ 71	$WSF_4(\bar{F})$
	-158.8	IX[d]	$^2J_{Fb-Fe}$ 70	$(F_4)WS-\bar{F}-WS(F_4)$
$Na^+[W_2S_2F_9]^-$	84.3	II	$^2J_{Fb-Fe}$ 70	$F_4WS-(\bar{F})-SWF_4$
	76.7	II[e]	$^2J_{Fa-Fe}$ 74	$WSF_4(\bar{F})$
	-158.6	IX[d]	$^2J_{Fb-Fe}$ 70	$(F_4)WS-\bar{F}-SW(F_4)$
$K^+[W_2S_2F_9]^-$	84.1	II	$^2J_{Fb-Fe}$ 70	$F_4WS-(\bar{F})-SWF_4$
	77.0	II[e]	$^2J_{Fa-Fe}$ 75	$WSF_4(\bar{F})$
	-159.0	IX[d]	$^2J_{Fb-Fe}$ 70	$(F_4)WS-\bar{F}-SW(F_4)$
$Rb^+[W_2S_2F_9]^-$	84.3	II	$^2J_{Fb-Fe}$ 70	$F_4WS-(\bar{F})-SWF_4$
	77.2	II[e]	$^2J_{Fa-Fe}$ 75	$WSF_4(\bar{F})$
	-159.1	IX[d]	$^2J_{Fb-Fe}$ 70	$(F_4)WS-\bar{F}-SW(F_4)$
$Cs^+[W_2S_2F_9]^-$	84.5	II	$^2J_{Fb-Fe}$ 70	$F_4WS-(\bar{F})-SWF_4$
	77.4	II[e]	$^2J_{Fa-Fe}$ 75	$WSF_4(\bar{F})$
	-158.8	IX[d]	$^2J_{Fb-Fe}$ 70	$(F_4)WS-\bar{F}-SW(F_4)$

[a] *Spectrum run at 94.1 MHz and referenced with respect to external $CFCl_3$;*
[b] *II; doublet: IX; nonet;*
[c] *Symbols in parenthesis refer to those atoms not concerned by the chemical shift;*
[d] *Seven central lines of nonet identified by intensity ratio 10:30:55:65:55:28:9;*
[e] *$[WSF_5]^-$ present as ca. 8% impurity (Refs. 26 and 27).*

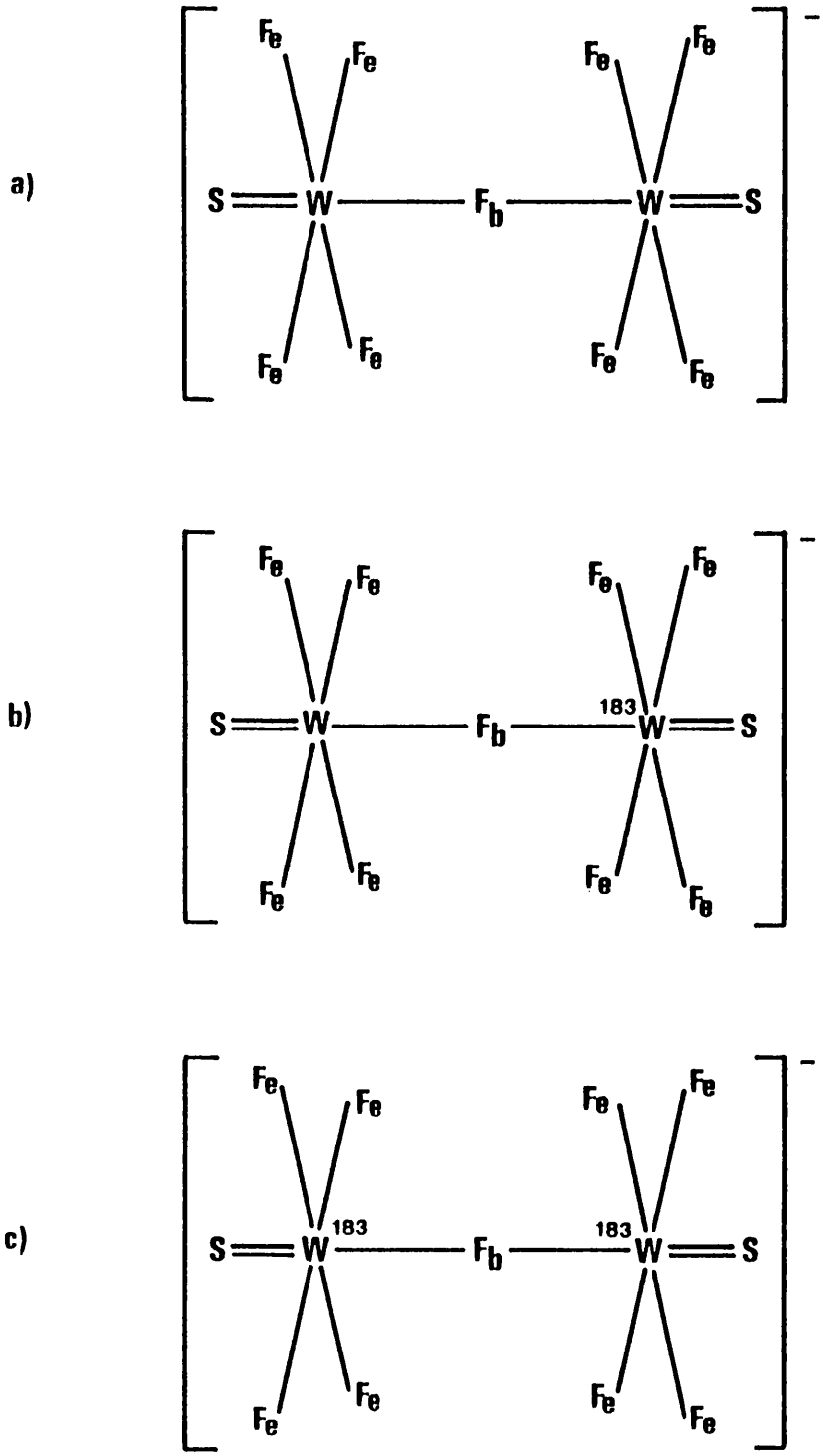

FIGURE 7

Proposed structure of $[W_2S_2F_9]^-$ in solution.

a)

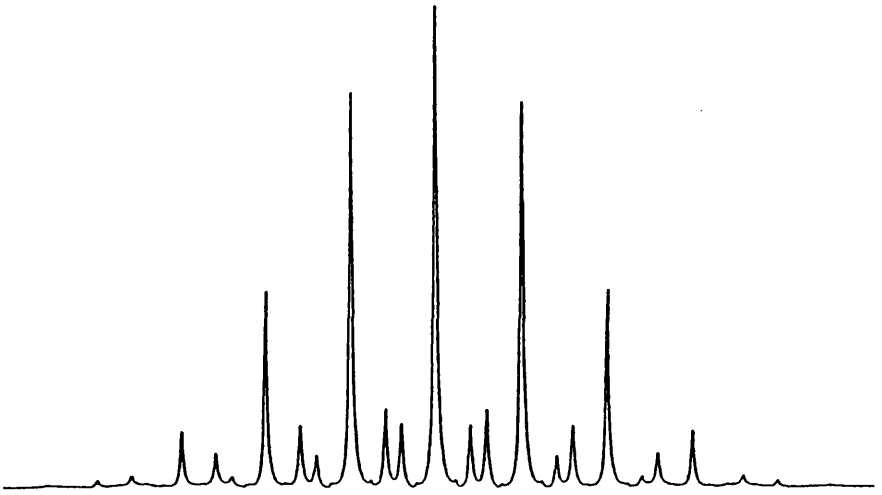

b)

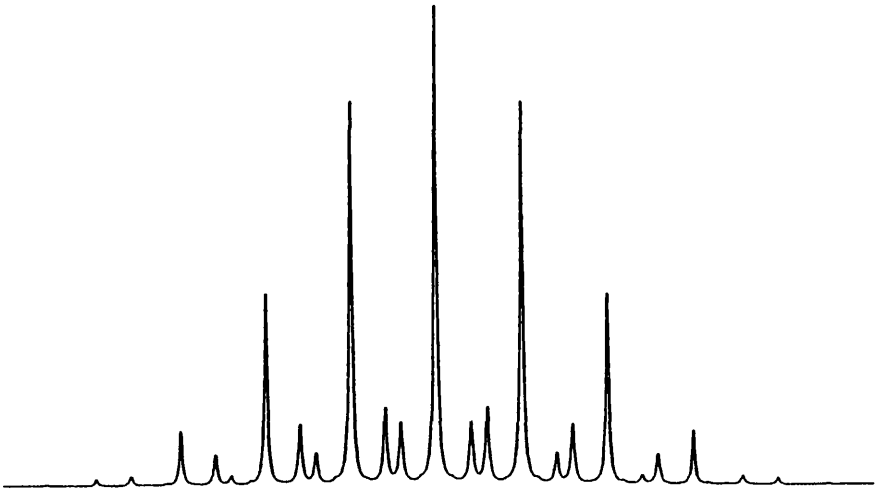

FIGURE 8

^{19}F n.m.r. spectrum of the bridging fluorine atom in $M^+[W_2S_2F_9]^-$ (M = Li, K, Rb); a) experimental in CH_3CN, b) simulated (parameters are given in Figure 9).

fluorine atom, Fb, coupling to tungsten-183, Figure 7b, $^1J[^{183}W-^{19}Fb]$ = 83 Hz [NB: W^{183}, I = ½, abundance = 14.3%]. Further lines of ca. 1% intensity present in the spectrum are due to the outer lines of the 1:2:1 triplets arising from coupling between the bridging fluorine atom, Fb, and two equivalent tungsten-183 atoms, Figure 7c, $^1J[^{183}W-^{19}Fb]$ = 83 Hz. The central lines of the 1:2:1 triplets are obscured by the main components of the nonet.

Simulations of the three coupling systems associated with the bridging fluorine atom, Fb, namely, $^2J[^{19}Fe-^{19}Fb]$, which gives rise to the nonet, $^1J[^{183}W-^{19}Fb]$, which gives rise to the nonet of doublets, and $^1J[^{183}W-^{19}Fb]$, which gives rise to the nonet of triplets, are shown in Figure 9a, b and c respectively. Values for the respective coupling constants used in the simulation are 70 Hz for the ^2J coupling and 83 Hz for ^1J. The resulting combination of these, assuming their respective intensities, is shown in Figure 8b and is in excellent agreement with the observed spectrum of the tungsten-fluorine bridging atom, Fb, of $[W_2S_2F_9]^-$.

Examination of the high-frequency doublet reveals the expected satellites from the coupling of the tungsten-fluorine equatorial atoms, Fe, with tungsten-183, (Figure 7b), $^1J[^{183}W-^{19}Fe]$ = 33 Hz.

3.4.2 The characterisation of $[W_2OSF_9]^-$ in solution

The species examined in this study, $M^+[W_2S_2F_9]^-$ show extreme sensitivity to traces of moisture, forming oxide-fluorides of tungsten. The ^{19}F nmr spectra recorded using the Fourier Transform nmr spectrometer show a low intensity signal, which is attributable to the anion $[WOF_5]^-$, but signals due to the fluorine-bridged anion $[W_2O_2F_9]^-$ are absent. Instead, a low intensity A_4B_4X spectrum (ca. 7%), two high-frequency doublets and a low-frequency multiplet, are observed (Figure 11a). The

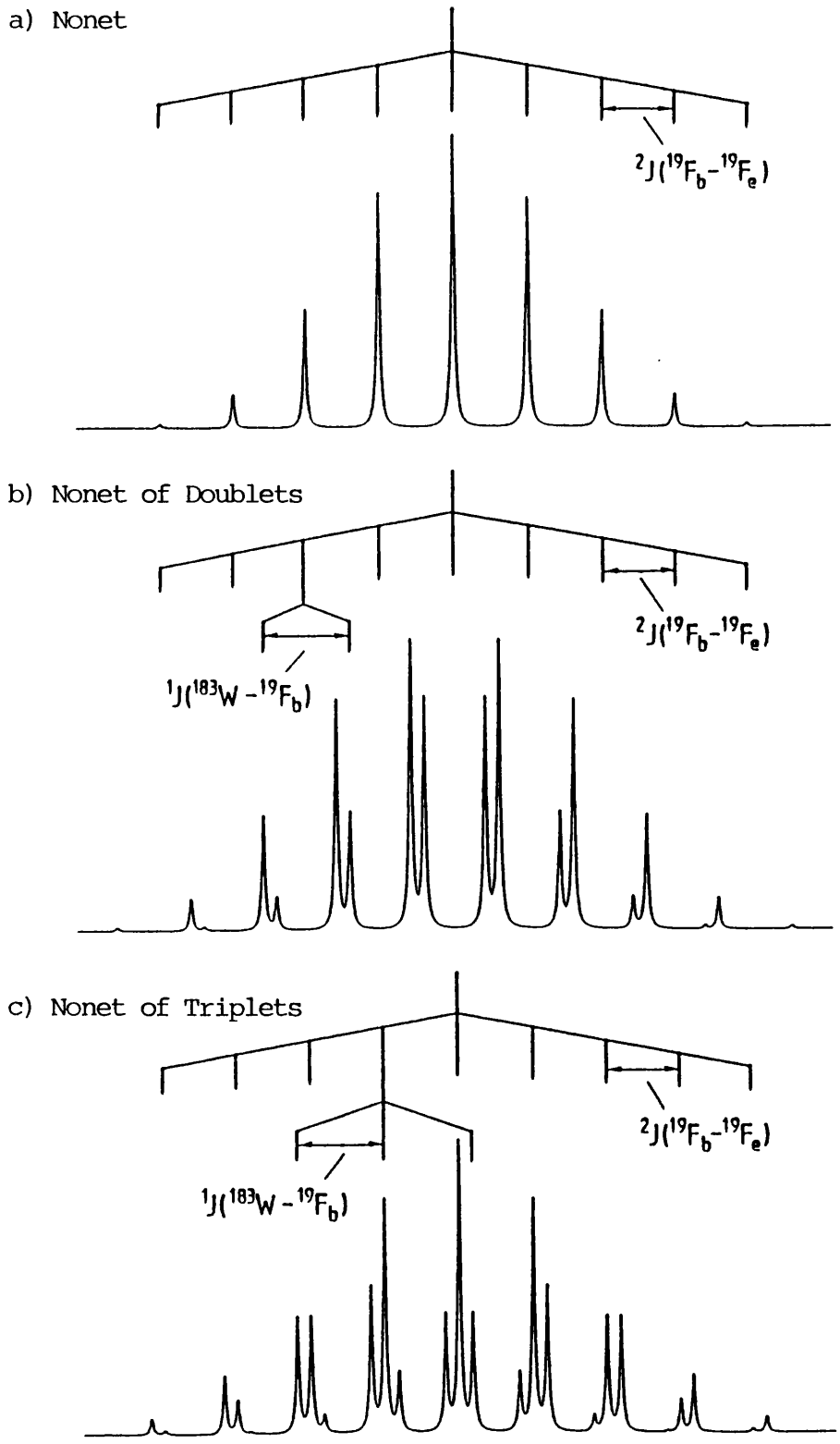

FIGURE 9

Simulated spectra of the bridging fluorine in a) $[W_2S_2F_9]^-$, b) $[^{183}WWS_2F_9]^-$, c) $[^{183}W_2S_2F_9]^-$ with the following coupling parameters:

$^2J(^{19}F_b-^{19}F_e)$ = 70 Hz, $^1J(^{183}W-^{19}F_b)$ = 83 Hz.

data are recorded in Table 20. This has been assigned to the new fluorine-bridged mixed oxide-sulphide anion, $[W_2OSF_9]^-$.

Based on the proposed structure of $[W_2OSF_9]^-$ in solution, Figure 10a, in which two non-equivalent sets of four equatorial fluorine atoms, Feo and Fes ('o' denoting Fe bonded to 'W=O' and, similarly, 's' denoting Fe bonded to 'W=S') are present, the signal due to the fluorine-bridged atom, Fb, should appear as a quintet of quintets. Further splitting of each component into doublets by the two non-equivalent tungsten-183 atoms of the moieties 'WSF_4' and 'WOF_4' (^{183}Ws and ^{183}Wo respectively) is also expected; Figure 10b and c. The doublet of doublets expected when both tungsten atoms are of the isotope 183 is unlikely to be observed due to the complexity of the spectrum.

Simulation of the three coupling systems associated with the bridging fluorine atom, Fb, $^2J[^{19}Fb-^{19}Feo] = 57$ Hz[2] and $^2J[^{19}Fb-^{19}Fes] =$ 70 Hz, which gives rise to the quintet of quintets, $^1J[^{183}Ws-^{19}Fb] = 86$ Hz, which gives rise to the quintet of quintets of doublets and $^1J[^{183}Wo-^{19}F] = 52$ Hz[72] which gives rise to the quintet of quintet of doublets are shown in Figure 12a, b and c respectively. Combination of the simulated spectra, assuming their relative intensities, results in the simulated spectrum shown in Figure 11b. This is in excellent agreement with the observed spectrum of the low frequency multiplet, Figure 11a, thus confirming the presence of the anion, $[W_2OSF_9]^-$.

The outer lines were not resolved due to low concentration of the species and the subsequent high signal-to-noise ratio. It should be noted that the infra-red spectra of $M^+[W_2S_2F_9]^-$ did not reveal any bands that could be assigned to $M^+[W_2OSF_9]^-$. Weak bands appearing in the region of 1000 cm^{-1} could only be given the general assignment of $\nu(W=O)$.

TABLE 20

^{19}F nmr data for the species $[W_2OSF_9]^-$ observed during the study of $M^+[W_2S_2F_9]^-$, M = Li, K, Rb, in CH_3CN

Sample	δ/ppm[a]	Multiplet[b] Structure	Coupling Constant/Hz		Assignment[a]
$Li^+[W_2S_2F_9]^-$	-	-[c]	$^2J_{Fb-Fes}$	-	$F_4WO-(\bar{F})-SWF_4$
	61.1	II	$^2J_{Fb-Feo}$	57	
			$^1J_{W^{183}-Feo}$	70	
	-147.4	M	$^2J_{Fb-Fes}$	70	$(F_4)WO-\bar{F}-SW(F_4)$
			$^2J_{Fb-Feo}$	57	
$K^+[W_2S_2F_9]^-$	86.2	II	$^2J_{Fb-Fes}$	70	$F_4WO-(\bar{F})-SWF_4$
	61.1	II	$^2J_{Fb-Feo}$	57	
			$^1J_{W^{183}-Feo}$	70	
	-147.7	M	$^2J_{Fb-Fes}$	70	$(F_4)WO-\bar{F}-SW(F_4)$
			$^2J_{Fb-Feo}$	57	
$Rb^+[W_2S_2F_9]^-$	86.2	II	$^2J_{Fb-Fes}$	70	$F_4WO-(\bar{F})-SWF_4$
	61.1	II	$^2J_{Fb-Feo}$	57	
			$^1J_{W^{183}-Feo}$	70	
	-147.7	M	$^2J_{Fb-Fes}$	70	$(F_4)WO-\bar{F}-SW(F_4)$
			$^2J_{Fb-Feo}$	57	

[a] *See Table 19;* [b] *II; doublet: M; multiplet;*
[c] *Expected doublet obscured by main peak of* $[W_2S_2F_9]^-$.

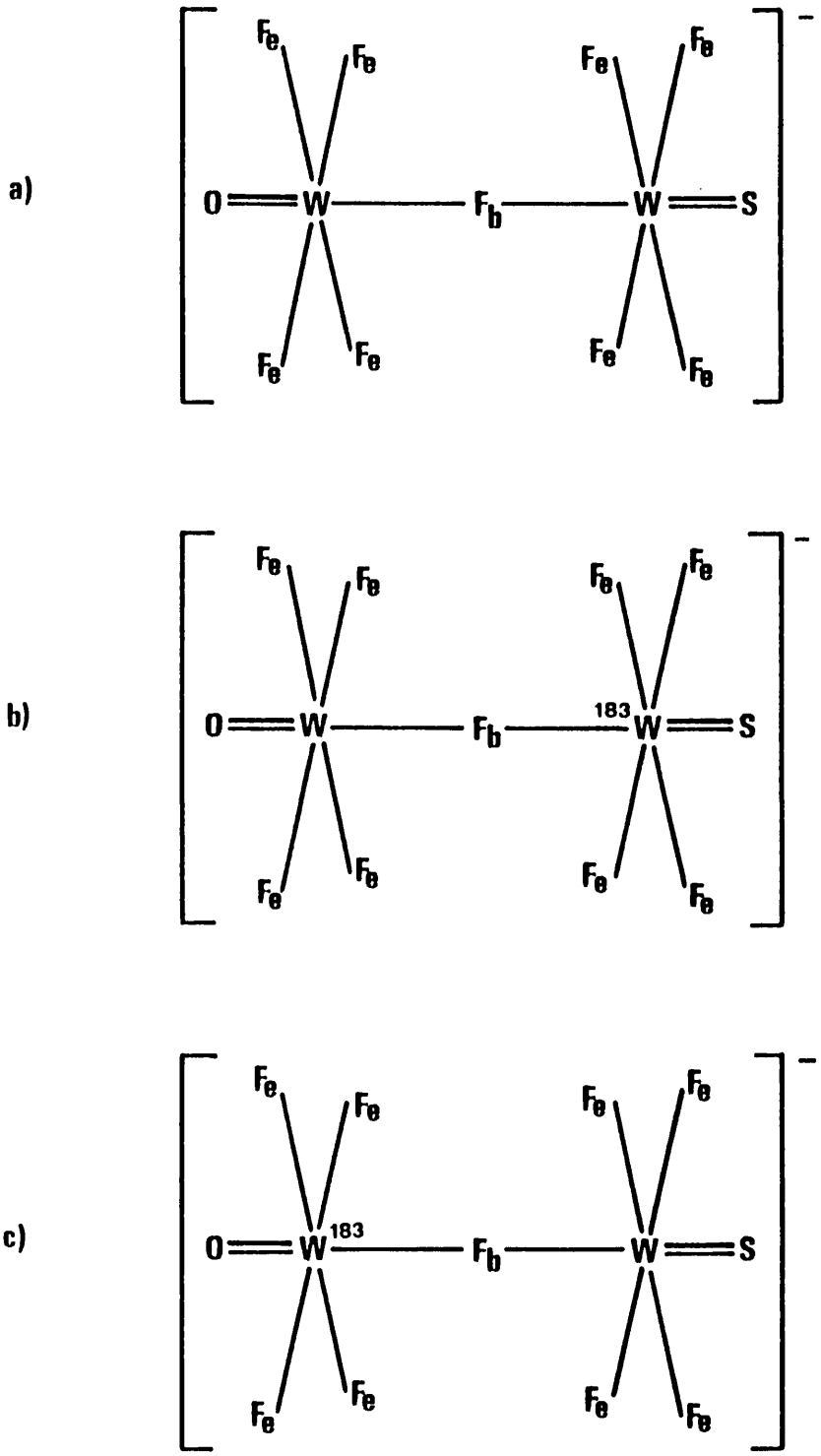

FIGURE 10

Proposed structure of $[W_2OSF_9]^-$ in solution.

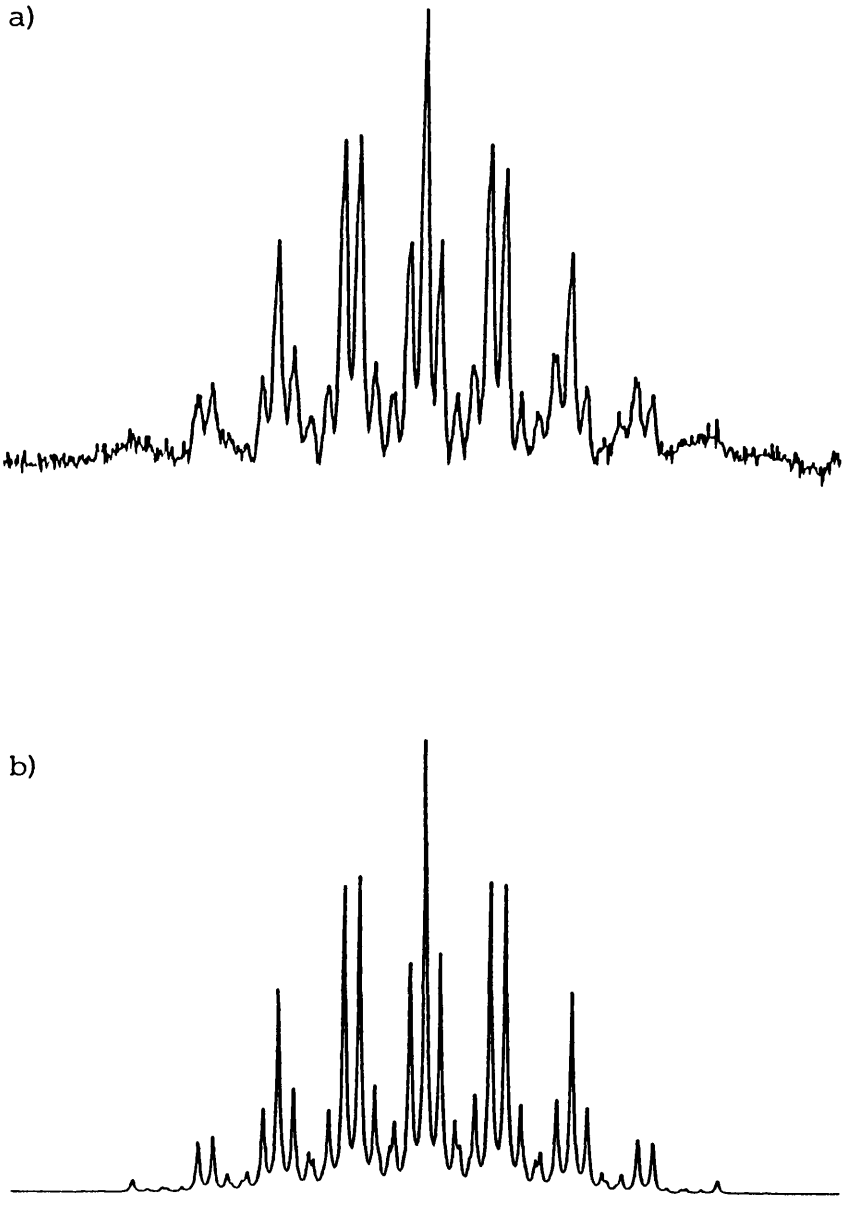

FIGURE 11

^{19}F n.m.r. spectrum of the bridging fluorine atom in $[W_2OSF_9]^-$; a) experimental in CH_3CN, b) simulated (parameters are given in Figure 12).

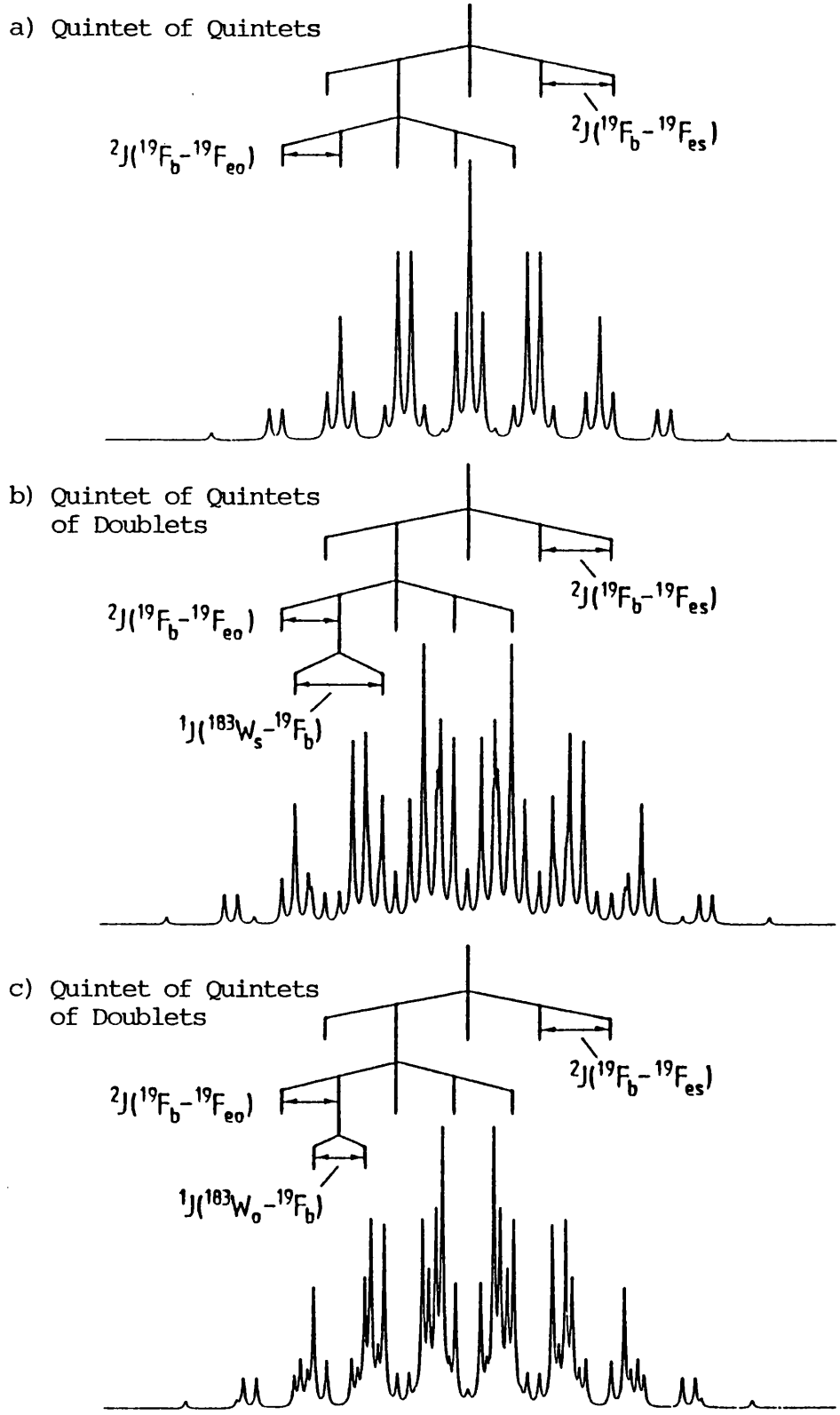

FIGURE 12

Simulated spectra of the bridging fluorine in a) $[W_2OSF_9]^-$, b) $[^{183}W_sWOSF_9]^-$, c) $[^{183}W_oWOSF_9]^-$ with the following coupling parameters:
$^2J(^{19}F_b-^{19}F_{es})$ = 70 Hz, $^2J(^{19}F_b-^{19}F_{eo})$ = 57 Hz,
$^2J(^{183}W_s-^{19}F_b)$ = 86 Hz, $^2J(^{183}W_o-^{19}F_b)$ = 52 Hz.

3.5 THE PREPARATION OF THE IONIC ADDUCTS $M^+[WSF_5]^-$, M = Rb or Cs

The ionic adducts, $M^+[WSF_5]^-$ have been isolated from a reaction of tungsten thiotetrafluoride with the respective alkali metal fluoride in anhydrous HF at 25°C (Scheme 11).

At liquid nitrogen temperature, anhydrous HF, ca. 0.5 ml, was distilled onto a mixture of WSF_4 (0.32 mmoles) and the respective alkali metal fluoride (0.31 mmoles) contained in a ¼" Teflon-FEP reactor tube, fitted with a Teflon needle valve, as described previously [Section 3.3]. Warming to room temperature followed by judicious shaking yielded a yellow solid below a pale yellow HF solution [Scheme 11(i)]. Removal of the HF solvent, first under static vacuum and then by pumping under dynamic vacuum, yielded a yellow, granular solid [Scheme 11(ii)]. X-ray powder diffraction, infra-red and ^{19}F nmr spectroscopy and mass balance have shown this to be a mixture of $M^+[W_2S_2F_9]^-$, $M^+[WSF_5]^-$ and $MF(HF)_{\sim 3}$. When this solid mixture was allowed to stand in an atmosphere of dry nitrogen at room temperature for 5 weeks, further spectroscopic investigation of the mixture revealed that almost complete conversion of $M^+[W_2S_2F_9]^-$ to $M^+[WSF_5]^-$ had occurred [Scheme 11(iii)].

The existence of an equilibrium reaction between $M^+[WSF_5]^-$ and $M^+[W_2S_2F_9]^-$ in anhydrous HF has been demonstrated by Schemes 11(iv) and (v). Thus, when the solid from Scheme 11(i) is isolated via decantation of the pale yellow HF solution, Scheme 11(iv), spectroscopic investigation has shown that $M^+[W_2S_2F_9]^-$ is the major component, whilst addition of an excess of anhydrous HF to $M^+[WSF_5]^-$ isolated from Scheme 11(iii), followed by decantation of excess solvent, also results in the formation of $M^+[W_2S_2F_9]^-$.

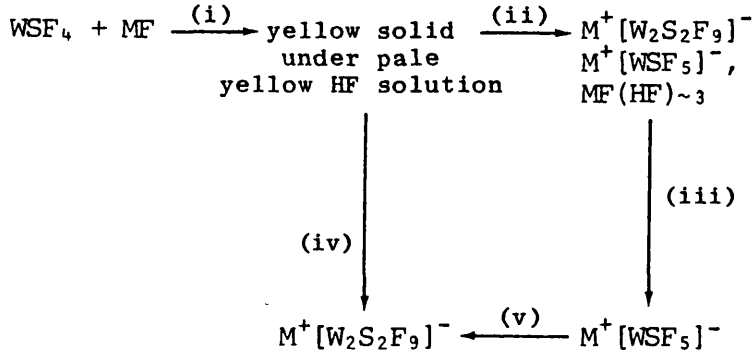

(i) *In anhydrous HF at 25°C;*
(ii) *Excess anhydrous HF solvent removed by distillation;*
(iii) *After standing in an atmosphere of dry nitrogen for 5 weeks;*
(iv) *Anhydrous HF solvent removed by decantation;*
(v) *Addition of excess HF solvent, followed by decantation of excess HF solvent.*

SCHEME 11

3.6 THE SOLID MIXTURE OF $M^+[WSF_5]^-$ AND $M^+[W_2S_2F_9]^-$

3.6.1 Infra-red spectroscopic studies

The infra-red spectra of the solid mixtures isolated from Scheme 11(ii) were recorded as previously described [Section 3.3.2]. The spectra are shown in Figure 13a and the data are recorded together with those for $Cs^+[WOF_5]^-$ [78] and $M^+[W_2S_2F_9]^-$, M = Rb or Cs, in Table 21.

In addition to bands ascribed to $M^+[W_2S_2F_9]^-$, the solid mixtures exhibit new bands that are not observed in the spectra of MHF_2 [73,74] and WSF_4. [27] Comparison of the spectra to that of $Cs^+[WOF_5]^-$ [78] permits tentative assignment of the new bands to $\nu_s(WF_4)_{in\text{-}phase}$, $\nu_{as}(WF_4)$ and $\nu(WF)_{axial}$ of $M^+[WSF_5]^-$. The absorptions at 539 and 537 cm^{-1} are assigned to $\nu(W{=}S)$ of $Rb^+[WSF_5]^-$ and $Cs^+[WSF_5]^-$ respectively.

As expected for the ionic adducts $M^+[WSF_5]^-$, $\nu_s(WF_4)_{in\text{-}phase}$ is much higher in frequency than $\nu(WF)_{axial}$, (c.f. $M^+[W_2S_2F_9]^-$, Section 3.3.2).

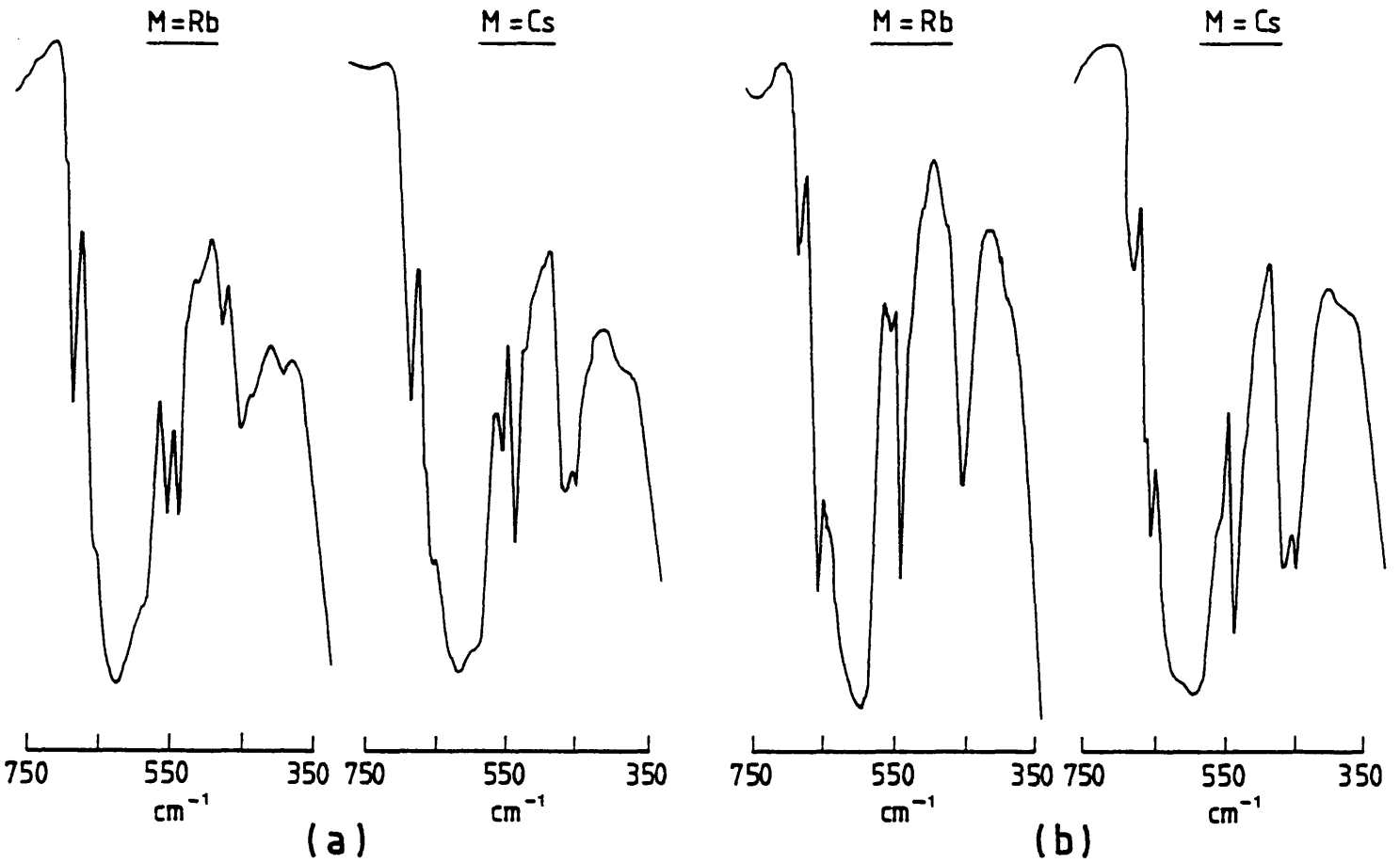

FIGURE 13

Infra-red spectra of a) the mixture of $M^+[W_2S_2F_9]^-$ and $M^+[WSF_5]^-$ isolated from Scheme 11(ii) and b) $M^+[WSF_5]^-$ isolated from Scheme 11(iii).

TABLE 21

Infra-red spectral data for the solid mixture of $M^+[WSF_5]^-$ and $M^+[W_2S_2F_9]^-$ and $M^+[WSF_5]^-$, M = Rb or Cs

Frequency, cm^{-1}							Assignment	
Solid mixture of $M^+[W_2S_2F_9]^-$ and $M^+[WSF_5]^-$ isolated from Scheme 11(ii)		$M^+[WSF_5]^-$ isolated from Scheme 11(iii)						
M = Rb	M = Cs	M = Rb	M = Cs	$Cs^+[WOF_5]^-$ [78]	$Cs^+[W_2S_2F_9]^-$ [a]	$Rb^+[W_2S_2F_9]^-$ [a]	$[WXF_5]^-$ [78]	$[W_2S_2F_9]^-$ [a]
				987 vs			ν(W=O)	
685 s	685 ms	685 w	684 w		682 s	682 ms		$\nu_s(WF_4)$ i.p.
655 sh	655 m	656 s	655 ms	686 vs			$\nu_s(WF_4)$ i.p.	
622 vs	618 vs				620 vs	620 vs		$\nu_{as}(WF_4)$
587 sh	587 sh	596 vs	595 vs	608 vs			$\nu_{as}(WF_4)$	
555 ms	555 ms	555 vw	557 sh		555 ms	555 m		ν(W=S)
539 ms	537 ms	540 s	535 s				ν(W=S)	
480 vw								
452 m	465 m 450 m	455 s	465 s 450 s	507 m			ν(WF) axial	
432 sh	415 sh				415 m	430 m		$\}\ \nu_{as}(WFW)$
390 vw	385 sh				385 m	385 sh		

i.p. = in-phase;
X = S or O.

[a] *See Table 18.*

This is attributed to the greater ionic character of the tungsten fluorine axial bond. The decrease in frequency of $\nu(WF)_{axial}$ from $Cs^+[WOF_5]^-$ to $Cs^+[WSF_5]^-$ is consistent with the similar trend observed for the bridging stretch, $\nu_{as}(WFW)$ of $Cs^+[W_2O_2F_9]^-$ and $Cs^+[W_2S_2F_9]^-$ [Section 3.3.2], i.e. the sulphur atom of the moiety W=S exerts a greater trans effect than oxygen in W=O.

It is interesting to compare the infra-red spectra of the ionic adducts $M^+[W_2S_2F_9]^-$ and $M^+[WSF_5]^-$. Although both show the same characteristic features, the bands assigned to $\nu_s(WF_4)_{in\text{-}phase}$, $\nu_{as}(WF_4)$ and $\nu(W{=}S)$ of $M^+[WSF_5]^-$ occur at lower frequency than the respective bands in $M^+[W_2S_2F_9]^-$. It is probable that this is due to greater electron density on the central tungsten atom of $M^+[WSF_5]^-$, compared to that of $M^+[W_2S_2F_9]^-$, which effectively weakens the fluorine and sulphur tungsten bonds.

3.6.2 X-ray powder diffraction studies

The X-ray powder diffraction patterns of the solid mixtures obtained from Scheme 11(ii) confirm the infra-red data of the preceding section. In addition to the patterns attributed to the respective ionic adducts $M^+[W_2S_2F_9]^-$, the X-ray powder diffraction patterns reveal the presence of new, isostructural phases which are assigned to $Rb^+[WSF_5]^-$ and $Cs^+[WSF_5]^-$. Patterns particular to MF were not observed.

3.6.3 ^{19}F nmr studies in CH_3CN

The ^{19}F nmr spectra of the solid mixtures obtained from Scheme 11(ii) in acetonitrile solvent, at -12°C, were recorded as previously described [Section 3.4]. The data are recorded in Table 22.

In addition to the AX_8 spectrum of $[W_2S_2F_9]^-$, and of comparable intensity, an AX_4 type spectrum consisting of a high-frequency doublet

TABLE 22

^{19}F nmr data for the solid mixture of $M^+[W_2S_2F_9]^-$ and $M^+[WSF_5]^-$, M = Rb or Cs, in CH_3CN at -12°C

Sample	M	δ/ppm[a]	Multiplet[b] Structure	Coupling Constant/Hz	Assignment[c]
Solid mixture of $M^+[W_2S_2F_9]^-$ and $M^+[WSF_5]^-$ isolated from Scheme 11(ii)	Rb	84.5	II	$^2J_{Fb-Fe}$ 70	$F_4WS-(\bar{F})-SWF_4$
		76.7	II	$^2J_{Fa-Fe}$ 76	$WSF_4(\bar{F})$
		-121.3	V[d]	$^2J_{Fa-Fe}$ 75	$WS(F_4)\bar{F}$
		-158.6	IX	$^2J_{Fb-Fe}$ 70	$(F_4)WS-\bar{F}-SW(F_4)$
	Cs	85.1	II	$^2J_{Fb-Fe}$ 69	$F_4WS-(\bar{F})-SWF_4$
		78.0	II	$^2J_{Fa-Fe}$ 74	$WSF_4(\bar{F})$
		-115.0	V[d]	$^2J_{Fa-Fe}$ 76	$WS(F_4)\bar{F}$
		-154.1	IX	$^2J_{Fb-Fe}$ 70	$(F_4)WS-\bar{F}-SW(F_4)$

[a],[b],[c] *See Table 19;* [d] *V; Quintet.*

and a low frequency quintet (integration ratio 4:1) was also observed. On the basis of chemical shift parameters and coupling constants this was assigned to $[WSF_5]^-$[26,27] [Figure 14]. The chemical shift parameters show the axial fluorine atom, Fa, to be considerably more shielded than the equatorial fluorine atom, Fe. This is consistent with similar observations made for the anion $[MOF_5]^-$, (M = Mo or W)[68] and confirms the infra-red data of Section 3.6.1 that the negative charge of the anion is localised mainly on the tungsten-fluorine axial bond. As observed for the anions $[W_2S_2F_9]^-$ and $[W_2O_2F_9]^-$,[26] [Section 3.4], the variation in chemical shift of the axial fluorine atoms, Fa, of $[WSF_5]^-$ and $[WOF_5]^-$ is a result of the greater trans effect of the sulphur atom in the moiety W=S than oxygen in W=O.[26]

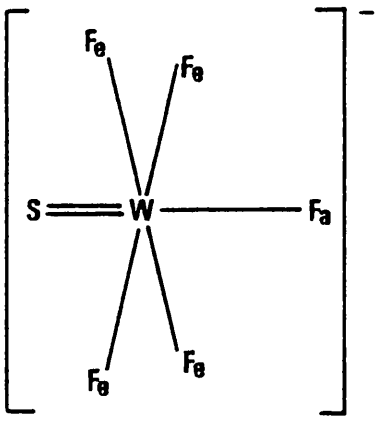

FIGURE 14
Proposed structure of $[WSF_5]^-$ in solution.[26]

3.7 THE CONVERSION OF $M^+[W_2S_2F_9]^-$ TO $M^+[WSF_5]^-$ IN THE SOLID STATE

After standing in an atmosphere of dry nitrogen at room temperature for 5 weeks, further investigation of the solid mixture of $M^+[W_2S_2F_9]^-$ and $M^+[WSF_5]^-$ isolated from Scheme 11(ii) revealed that almost complete conversion of $M^+[W_2S_2F_9]^-$ to $M^+[WSF_5]^-$ had occurred, Scheme 11(iii).

3.8 EVIDENCE FOR THE CONVERSION OF $M^+[W_2S_2F_9]^-$ TO $M^+[WSF_5]^-$ IN THE SOLID STATE

3.8.1 Infra-red spectroscopic studies

The infra-red spectra of the solids isolated from Scheme 11(iii) are shown in Figure 13b and the data recorded in Table 21.

The spectra show that the features attributed to $\nu_s(WF_4)_{in\text{-}phase}$, $\nu_{as}(WF_4)$, $\nu(W{=}S)$ and $\nu(WF)_{axial}$ of $M^+[WSF_5]^-$ are all clearly enhanced, whereas those ascribed to $M^+[W_2S_2F_9]^-$ are greatly diminished. Bands particular to MHF_2 and WSF_4 were not observed.

3.8.2 X-ray powder diffraction studies

The X-ray powder diffraction patterns obtained for the solids from Scheme 11(iii) show enhancement in intensity for the new phases, $M^+[WSF_5]^-$, whereas the patterns of $M^+[W_2S_2F_9]^-$ are diminished in intensity.

3.8.3 ^{19}F nmr studies in CH_3CN

The results of the ^{19}F nmr study of the solids isolated from Scheme 11(iii) in acetonitrile at -12°C are recorded in Table 23.

The spectra are typical of the AX_4 type pattern expected for the species $[WSF_5]^-$ in solution [Section 3.6.3]. Only a low intensity doublet assigned to the equatorial fluorine atoms, Fe, of $[W_2S_2F_9]^-$ is observed.

3.9 DISCUSSION OF THE CONVERSION OF $M^+[W_2S_2F_9]^-$ TO $M^+[WSF_5]^-$ IN THE SOLID STATE

It is apparent from the 1:1 molar stoichiometry of the reactants, WSF_4 and MF, of Scheme 11, that a quantity of MF is present in the solid mixture of $M^+[W_2S_2F_9]^-$ and $M^+[WSF_5]^-$ isolated from Scheme 11(ii). The probability of either MF or the bifluoride, MHF_2, being present in this mixture has been excluded by the X-ray powder diffraction and infra-

TABLE 23

^{19}F nmr data for $M^+[WSF_5]^-$, M = Rb or Cs, in CH_3CN at -12°C

Sample	M	δ/ppm[a]	Multiplet[b] Structure	Coupling Constant/Hz	Assignment[c]
$M^+[WSF_5]^-$ isolated from Scheme 11(iii)	Rb	84.3	II	$^2J_{Fb-Fe}$ 70	$F_4WS-(\bar{F})-SWF_4$
		77.2	II	$^2J_{Fa-Fe}$ 74	$WSF_4(\bar{F})$
		-116.0	V	$^2J_{Fa-Fe}$ 74	$WS(F_4)\bar{F}$
	Cs	84.6	II	$^2J_{Fb-Fe}$ 70	$F_4WS-(\bar{F})-SWF_4$
		77.1	II	$^2J_{Fa-Fe}$ 74	$WSF_4(\bar{F})$
		-117.4	V	$^2J_{Fa-Fe}$ 74	$WS(F_4)\bar{F}$

a,b,c *See Table 22.*

spectroscopic studies of Sections 3.6.1 and 3.6.2.

Using identical conditions employed in the isolation of the mixture of the tungsten containing species, Scheme 11(ii), the reaction of MF with an 8-fold excess of anhydrous HF was investigated. Mass balance showed the pasty solids isolated to contain MF and HF in a ca. 1:3 molar ratio. This observation is consistent with similar work carried out by Prideaux et al.[75] The infra-red spectra of the solids between KBr discs show broad, featureless bands. Attempts to assign these bands were not made. On the basis of these results it is tentatively suggested that the MF present in the mixture of $M^+[W_2S_2F_9]^-$ and $M^+[WSF_5]^-$ is formulated as $MF(HF)_{\sim 3}$.

For the conversion of $M^+[W_2S_2F_9]^-$ to $M^+[WSF_5]^-$ in the solid state, the alkali metal fluoride, MF, must be consumed, and it is proposed that the HF present in $MF(HF)_{\sim 3}$ is catalytically involved in this conversion, Scheme 12.

$$M^+[W_2S_2F_9]^-_{(s)} + MF(HF)_{\sim 3\,(s)} \xrightarrow{(i)} 2M^+[WSF_5]_{(s)} + HF\uparrow$$

(i) *After standing in an atmosphere of dry nitrogen at room temperature for 5 weeks.*

SCHEME 12

3.10 THE EQUILIBRIUM REACTION OF $M^+[WSF_5]^-$ IN ANHYDROUS HF

Wilson and Christe[67] have demonstrated the existence of the equilibrium reaction for $Cs^+[WOF_5]^-$ in anhydrous HF (Scheme 13).

$$2\,Cs^+[WOF_5]^- + HF \rightleftharpoons Cs^+[W_2O_2F_9]^-\downarrow + CsHF_2$$

SCHEME 13

Thus, a large excess of HF solvent shifts the equilibrium to the right, and the insoluble $Cs^+[W_2O_2F_9]^-$ can be removed by filtration. Removal of the HF solvent by distillation shifts the equilibrium to the left

which results in the isolation of mostly $Cs^+[WOF_5]^-$.

It has been shown by the spectroscopic investigations of Sections 3.6.1 and 3.6.3 that distillation of the HF solvent from the reaction of WSF_4 with MF, Scheme 11(ii), affords a mixture of the tungsten containing species, $M^+[W_2S_2F_9]^-$ and $M^+[WSF_5]^-$. However, examination by infra-red and ^{19}F nmr spectroscopy of the dried solid after decantation of the HF solvent from the same reaction, Scheme 11(iv), shows $M^+[W_2S_2F_9]^-$ to be the major component. Further, when an excess of HF solvent is added to $M^+[WSF_5]^-$ obtained from Scheme 11(iii), the solid isolated after decantation of the HF solvent has also been shown to be $M^+[W_2S_2F_9]$, Scheme 11(v). Thus, these results demonstrate that an equilibrium reaction similar to that of $Cs^+[WOF_5]^-$ is occurring for $M^+[WSF_5]^-$ in anhydrous HF (Scheme 14).

$$2M^+[WSF_5]^- + HF \rightleftharpoons M^+[W_2S_2F_9]^-\downarrow + MF \text{ solvated}$$

SCHEME 14

It should be noted that during this study of the equilibrium reaction of $M^+[WSF_5]^-$ in anhydrous HF solvent, in no instance were the alkali metal bifluorides, MHF_2, observed. Residues isolated from the decanted HF solvents from Schemes 11(iv) and 11(v) gave broad, featureless infra-red spectra which are similar to those observed for $MF(HF)_{\sim 3}$ [Section 3.9]. It is very likely that the alkali metal fluoride, MF, present in solution in Scheme 14 is solvated by the MF solvent and is not present in the form of the bifluoride as described by Wilson and Christe[67] in Scheme 13.

3.11 THE ATTEMPTED PREPARATION OF $M^+[WSF_5]^-$, M = Li, Na or K

The reaction of tungsten thiotetrafluoride with the respective alkali metal fluoride in anhydrous HF, at 25°C, has been shown to afford

$M^+[W_2S_2F_9]^-$ and MHF_2, and not $M^+[WSF_5]^-$ as expected from the reaction stoichiometry [Scheme 15].

At liquid nitrogen temperature, anhydrous HF (ca. 0.5 ml) was distilled onto a mixture of WSF_4 (0.32 mmole) and the respective alkali metal fluoride (0.31 mmole) contained in a ¼" Teflon FEP reactor tube, fitted with a Teflon needle valve as described in Section 3.3. Warming to room temperature, followed by shaking yielded a yellow solid below a pale yellow HF solution [Scheme 15(i)]. Removal of the HF solvent first under static vacuum and then by pumping under dynamic vacuum yielded a yellow powder [Scheme 15(ii)]. This was shown to be a mixture of $M^+[W_2S_2F_9]^-$ and MHF_2 by X-ray powder diffraction and infra-red spectroscopy.

$$WSF_4 + MF \xrightarrow{(i)} \text{Yellow solid under pale yellow HF solution} \xrightarrow{(ii)} M^+[W_2S_2F_9]^- + MHF_2$$

(i) *In anhydrous HF at 25°C;*
(ii) *Excess anhydrous HF solvent removed by distillation.*

SCHEME 15

3.12 THE MIXTURE OF $M^+[W_2S_2F_9]$ AND MHF_2

3.12.1 X-ray powder diffraction studies

X-ray powder diffraction patterns obtained for the solids isolated from Scheme 15(ii) are identical to those of the respective ionic adducts, $M^+[W_2S_2F_9]^-$, M = Li, Na or K. No other patterns were observed.

3.12.2 Infra-red spectroscopic studies

The infra-red spectra of the solids isolated from Scheme 15(ii) were recorded as previously described [Section 3.3.2]. These data together with those for MHF_2[73,74] and $M^+[W_2S_2F_9]^-$ are recorded in Table 24.

TABLE 24

Infra-red spectral data for the mixture of $M^+[W_2S_2F_9]^-$ and MHF_2, M = Li, Na or K

Frequency, cm^{-1}									Assignment	
Mixture of $M[W_2S_2F_9]$ and MHF_2 isolated from Scheme 15(ii)										
M = Li	M = Na	M = K	$LiHF_2$ [73,74]	$NaHF_2$ [73,74]	KHF_2 [73,74]	$Li[W_2S_2F_9]$ [c]	$Na[W_2S_2F_9]$ [c]	$K[W_2S_2F_9]$ [c]	$[FHF]^-$ [73,74]	$[W_2S_2F_9]^-$ [c]
2300 vbr, w	2150 vbr, m	[a]	2190 vbr, m	2110 vbr, m	2055 vbr, m				$\nu_3+\nu_1$	
[b]	[b]	1780 vbr, m	[b]	1880 vbr, w	1830 vbr				$\nu_2+\nu_1$	
1800 vbr, w	1620 vbr, ms	1400 vbr, m	1800 vbr, m	1550 vbr, m	1450 vbr, m				ν_3	
1172 s	1210 s	1160 mw	1170 s	1200 s	1223 s				ν_2	
685 s	692 s	690 ms				685 s	692 s	690 ms		$\nu_s(WF_4)$ i.p.
645 s	640 s, sh					645 s	640 s, sh			
615 vs	610 vs	620 vs				615 vs	610 vs	620 vs		$\nu_{as}(WF_4)$
573 ms	580 s, sh					575 ms	582 s, sh			
555 ms	555 ms	555 ms				555 ms	555 ms	555 ms		$\nu(W=S)$
								542 sh		
470 m	455 m	447 m				470 m	455 m	447 m		$\nu_{as}(WFW)$

[a] $\nu_1+\nu_3$ *not observed;* [b] ν_3 *and* $(\nu_2+\nu_1)$ *are very broad in these regions;* [c] *See Table 18.*

i.p. = in-phase.

Each spectrum exhibits high frequency absorptions in the region 2300 to 1100 cm^{-1}, which are assigned to the alkali metal bifluorides, MHF_2.[73,74] This observation alone indicates that the bifluorides formed are non-crystalline and, therefore, transparent to X-ray radiation. The low-frequency region of the spectra, 700 to 350 cm^{-1}, is identical to that of the ionic adducts, $M^+[W_2S_2F_9]^-$, and thus confirms the observations from the X-ray powder diffraction study, that $M^+[W_2S_2F_9]^-$ is the only tungsten containing species formed from Scheme 15.

3.12.3 ^{19}F nmr studies in CH_3CN

The ^{19}F nmr spectra of the solids from Scheme 15(ii) in acetonitrile, at -12°C, were recorded as previously described [Section 3.4]. The results are recorded in Table 25.

Initially, only the AX_8 spectrum of $[W_2S_2F_9]^-$ was observed, but after 3-4 minutes an AX_4 spectrum appeared, a high-frequency doublet and a low-frequency quintet (integration ratio 4:1). On the basis of chemical shift parameters and coupling constants [Tables 22 and 23] this was assigned to $[WSF_5]^-$. The appearance of this latter anion is most probably a consequence of a reaction similar to that depicted in Scheme 16 occurring in the acetonitrile solvent.

$$F^- + [W_2S_2F_9]^- \xrightarrow{CH_3CN} 2[WSF_5]^-$$

SCHEME 16

Thus, an increase in fluoride ion concentration resulting from the presence of the alkali metal bifluoride subsequently increases the concentration of $[WSF_5]^-$. A similar observation was made by Atherton and Holloway.[27] ^{19}F nmr studies of a reaction of HF with $WSCl_4$ in acetonitrile shows that a 6:1 molar ratio of HF to $WSCl_4$ produces both $[W_2S_2F_9]^-$ and $[WSF_5]^-$, whereas when the ratio is 12:1 only $[WSF_5]^-$ is

TABLE 25

^{19}F nmr data for the mixture of $M^+[W_2S_2F_9]$ and MHF_2, M = Li, Na or K, in CH_3CN, at -12°C

Sample	M	δ/ppm[a]	Multiplet[b] Structure	Coupling Constant/Hz	Assignment[c]
Mixture of $M^+[W_2S_2F_9]^-$ and MHF_2 isolated from Scheme 15(ii)	Li	85.9	II	$^2J_{Fb-Fe}$ 70	$F_4WS-(\bar{F})-SWF_4$
		80.6	II[d]	$^2J_{Fa-Fe}$ 74	$WSF_4(\bar{F})$
		-	V[e,g]	$^2J_{Fa-Fe}$ -	$WS(F_4)\bar{F}$
		-156.4	IX[f]	$^2J_{Fb-Fe}$ 69	$(F_4)WS-\bar{F}-SW(F_4)$
	Na	84.7	II	$^2J_{Fb-Fe}$ 69	$F_4WS-(\bar{F})-SWF_4$
		77.1	II[d]	$^2J_{Fa-Fe}$ 74	$WSF_4(\bar{F})$
		-127.8	V[e]	$^2J_{Fa-Fe}$ 73	$WS(F_4)\bar{F}$
		-158.6	IX[f]	$^2J_{Fb-Fe}$ 69	$(F_4)WS-\bar{F}-SW(F_4)$
	K	84.6	II	$^2J_{Fb-Fe}$ 70	$F_4WS-(\bar{F})-SWF_4$
		76.3	II[d]	$^2J_{Fa-Fe}$ 75	$WSF_4(\bar{F})$
		-124.1	V[e]	$^2J_{Fa-Fe}$ 76	$WS(F_4)\bar{F}$
		-159.0	IX[f]	$^2J_{Fb-Fe}$ 70	$(F_4)WS-\bar{F}-SW(F_4)$

[a,b,c] *See Table 22;*
[d,e] *Signals due to $[WSF_5]^-$ appeared 3-4 minutes after CH_3CN solvent had melted;*
[f] *Central five lines of nonet identified by intensity ratio 30:55:65:55:28;*
[g] *Quintet not observed.*

observed.

3.13 DISCUSSION

The failure to isolate $M^+[WSF_5]^-$ from Scheme 15 shows that the reverse step of the equilibrium reaction in Scheme 14 [Section 3.10] does not occur for $M^+[W_2S_2F_9]^-$ and MHF_2, M = Li, Na or K, in anhydrous HF. A possible explanation for this observation is discussed below.

For the complexes M_2PtF_6[76] and M_2GeF_6,[77] M = Li, Na, K, Rb or Cs, it is known that their solubility in anhydrous HF increases with increasing ionic radius of the cation. Thus the lithium salts are less soluble than the caesium salts. Extrapolating this phenomenon to the ionic adducts $M^+[W_2S_2F_9]^-$, it is plausible to assume that the degree of solubility of $M^+[W_2S_2F_9]^-$ in anhydrous HF solvent increases in the series Li < Na < K < Rb < Cs. Thus $Li^+[W_2S_2F_9]^-$ has the least solubility and $Cs^+[W_2S_2F_9]^-$ the greatest. It is probable, therefore, that $M^+[W_2S_2F_9]^-$, M = Li, Na or K, are insoluble to an extent which prevents a reaction with MF present in the anhydrous HF solvent of Scheme 15, hence prohibiting the reverse step of the equilibrium reaction in Scheme 14 [Section 3.10]. Thus on removal of the anhydrous HF solvent by distillation, only $M^+[W_2S_2F_9]^-$ and MF, in the form of the bifluoride, are formed.

Finally, it is worth noting that even after 5 weeks in an atmosphere of dry nitrogen, at room temperature, no evidence was obtained for the formation of $M^+[WSF_5]^-$ from the mixture of MHF_2 and $M^+[W_2S_2F_9]^-$.

3.14 OVERALL CONCLUSION TO THE REACTION OF WSF_4 WITH MF, M = Li, Na, K, Rb, Cs, IN ANHYDROUS HF

This study has produced the first examples of solids containing the anions $[W_2S_2F_9]^-$ and $[WSF_5]^-$, viz. $M^+[W_2S_2F_9]^-$, M = Li, Na, K, Rb or Cs

and $M^+[WSF_5]^-$, M = Rb or Cs.

The infra-red and ^{19}F nmr spectroscopic data both show that the trans effect of the sulphur atom of $[W_2S_2F_9]^-$ and $[WSF_5]^-$ to be greater than that of oxygen in $[W_2O_2F_9]^-$ and $[WOF_5]^-$. Thus, WSF_4 is a weaker fluoride-ion acceptor than WOF_4.

Like $Cs^+[WOF_5]^-$,[67] $M^+[WSF_5]^-$ in anhydrous HF sets up an equilibrium reaction, Scheme 14, but this has been shown to be confined to the ionic adducts of M = Rb or Cs.

$$2M^+[WSF_5]^- + HF \rightleftharpoons M^+[W_2S_2F_9]^-\downarrow + MF \text{ solvated}$$

SCHEME 14

An unusual solid state reaction in which $M^+[W_2S_2F_9]^-$ and what is thought to be $M(HF)_{\sim 3}$ are converted to $M^+[WSF_5]^-$ has been observed for M = Rb or Cs. It is very likely that the HF present in $MF(HF)_{\sim 3}$ catalyses the reaction, but further work is required to confirm this theory.

All of the tungsten sulphide fluoride species isolated in this study show extreme sensitivity to moisture. On exposure to the atmosphere, H_2S and HF gases are rapidly evolved (cf. WSF_4[27]). However, when moisture is present in low concentrations, the primary hydrolysis products appear to be oxide-fluorides of tungsten.[32]

During the detailed ^{19}F nmr study of $M^+[W_2S_2F_9]^-$, M = Li, K or Rb, [Section 3.4], in CH_3CN, a product from primary hydrolysis of $[W_2S_2F_9]^-$ was identified as the new mixed oxide sulphide species, $[W_2OSF_9]^-$. An interesting route for further investigation would be the synthesis of the anion $[W_2OSF_9]^-$ in the solid state. This may be achieved via the reaction of MF, M = Li, Na, K, Rb or Cs, with a mixture of WOF_4 and WSF_4 in anhydrous HF solvent.

CHAPTER 4

Tungsten Thiotetrafluoride and its interaction with Nitrosyl Fluoride

4.1 INTRODUCTION

Nitrosyl fluoride, NOF, is a colourless gas at ambient temperature and pressure (b.pt. -59.9°C).[79] It condenses to form a colourless liquid which freezes at -132.5 C.[79] It can be prepared by a variety of methods but is usually prepared by the method of Faloon and Kenna,[80] which involves the direct fluorination of nitric oxide by elemental fluorine.

Nitrosyl fluoride is well known as a strong fluoride ion base. It reacts with a wide range of Lewis acid fluorides to produce salts, e.g. with SbF_5 it gives $[NO]^+[SbF_6]^-$ and with WF_6 it yields $[NO]^+[WF_7]^-$ and $[NO]_2^+[WF_8]^{2-}$.[1,81,82] Some further examples of this type of reaction are given in Table 26.

Bartlett *et al.*[83] have accounted for the high basicity of NOF by considering the three steps in the process from which the F^- separation

TABLE 26

Some reactions of NOF with fluoride ion acceptors

Fluoride Ion Acceptor	NOF Product
BF_3	$[NO]^+[BF_4]^-$ [81]
ClF_3	$[NO]^+[ClF_4]^-$ [81]
VF_5	$[NO]^+[VF_5]^-$ [81]
CrO_2F_2	$[NO]^+[CrO_2F_3]^-$ [87]
$CrOF_4$	$[NO]^+[CrOF_5]^-$ [69]
BrF_3	$[NO]^+[BrF_4]^-$ [81]
$MoOF_4$	$[NO]^+[MoOF_5]^-$, $[NO]^+[Mo_2O_2F_9]^-$, $[NO]_2^+[MoOF_6]^{2-}$ [68]
TcF_6	$[NO]_2^+[TcF_8]^{2-}$ [88]
SbF_5	$[NO]^+[SbF_6]^-$ [89]
XeF_6	$[NO]_2^+[XeF_8]^{2-}$ [90,91]
WF_6	$[NO]^+[WF_7]^-$, $[NO]_2^+[WF_8]^{2-}$ [59,81,82]
WOF_4	$[NO]^+[WOF_5]^-$, $[NO]^+[W_2O_2F_9]^-$, $[NO]_2^+[WOF_6]^{2-}$ [68]
PtF_6	$[NO]^+[PtF_6]^-$, $[NO]_2^+[PtF_6]^{2-}$ [81]

enthalpy of hypervalent fluorides EFx, such as SF_4, XeF_2 and XeF_6, is derived. These are:-

a) the conversion of the resonance hybrid of the two canonical forms of a three-centre - four-electron bond $[(F\text{-}E)^+F^- \leftrightarrow F^-(E\text{-}F)^+]$ to the ion pair, $(F\text{-}E)^+F^-$,

b) the contraction of $(E\text{-}F)^+$ and the strengthening of that bond,

c) the work necessary to separate $(E\text{-}F)^+$ and F^-, of the ion pair $(E\text{-}F)^+F^-$, to infinity.

It has been shown that the first and last steps are the determining steps in the F^- separation energy. Thus, in the case of NOF (a molecule which can be considered as the ion pair $[NO]^+F^-$) resonance stabilisation, step a), does not occur, and only the last step, ion pair separation is important.

Nitrosyl fluoride also reacts as a powerful oxidising fluorinating agent, reacting with a wide range of elements to yield nitric oxide and the respective fluoride.[79,81.84,85] However, Sokol'skii et al.[86] have shown the compound to be tractable in apparatus made of copper, nickel and some nickel alloys.

4.2 PRESENT STUDY

The preceding chapter demonstrates the fluoride-ion acceptor ability of WSF_4. Its reaction with the alkali metal fluorides, MF, M = Li, Na, K, Rb or Cs, in anhydrous HF has led to the isolation of the new ionic adducts, $M^+[W_2S_2F_9]^-$ and $M^+[WSF_5]^-$.

In an attempt to further categorise the reaction of WSF_4 with strong fluoride-ion donors, its reaction with the strong fluoride-ion donor, NOF, has been investigated.

This Chapter describes a low temperature ^{19}F nmr study of a reaction of WSF_4 with an excess of NOF, and the attempts made to isolate the new

ionic adducts $[NO]^+[W_2S_2F_9]^-$ and $[NO]^+[WSF_5]^-$. This study requires much further work, especially a Raman investigation of intermediates formed. Without this further data, discussion of the results obtained can only be regarded as speculative.

4.3 PREPARATION OF NOF

Nitrosyl fluoride was prepared by the method described by Faloon and Kenna[80] in which nitric oxide, at just above its melting point, is fluorinated with elemental fluorine. The ensuing reaction is extremely vigorous and takes place with the emission of light.

Because of the refractory nature of the reactants, NO and F_2, and the reaction product, NOF, a detailed description of the method of preparation of NOF will be given here.

4.3.1 Procedure

The apparatus used to prepare nitrosyl fluoride in this study was constructed from stainless steel needle valves and 'T's, nickel tubing, Teflon connectors and 6 mm o.d. Kel-F tubing [Chapter 8].

4.3.2 Purification of NO

The apparatus used for the purification of NO is shown in Figure 15. After evacuation and passivation of the apparatus, valve B was kept closed for the duration of the purification process.

Nitric oxide was introduced into the apparatus *via* valve A. The likely impurities present in nitric oxide, nitrogen dioxide (NO_2: m.pt. -11°C) and nitrous oxide (N_2O: m.pt. -91°C) were removed by passing the gas through a Kel-F 'U' trap, F, which was maintained at -160°C by an isopentane/liquid nitrogen slush bath. The resulting, pure NO (m.pt. -164°C) was trapped in the ¾" Kel-F reactor tube, E, at -196°C. After *ca.* 0.5 hours, valve D was closed and the reactor

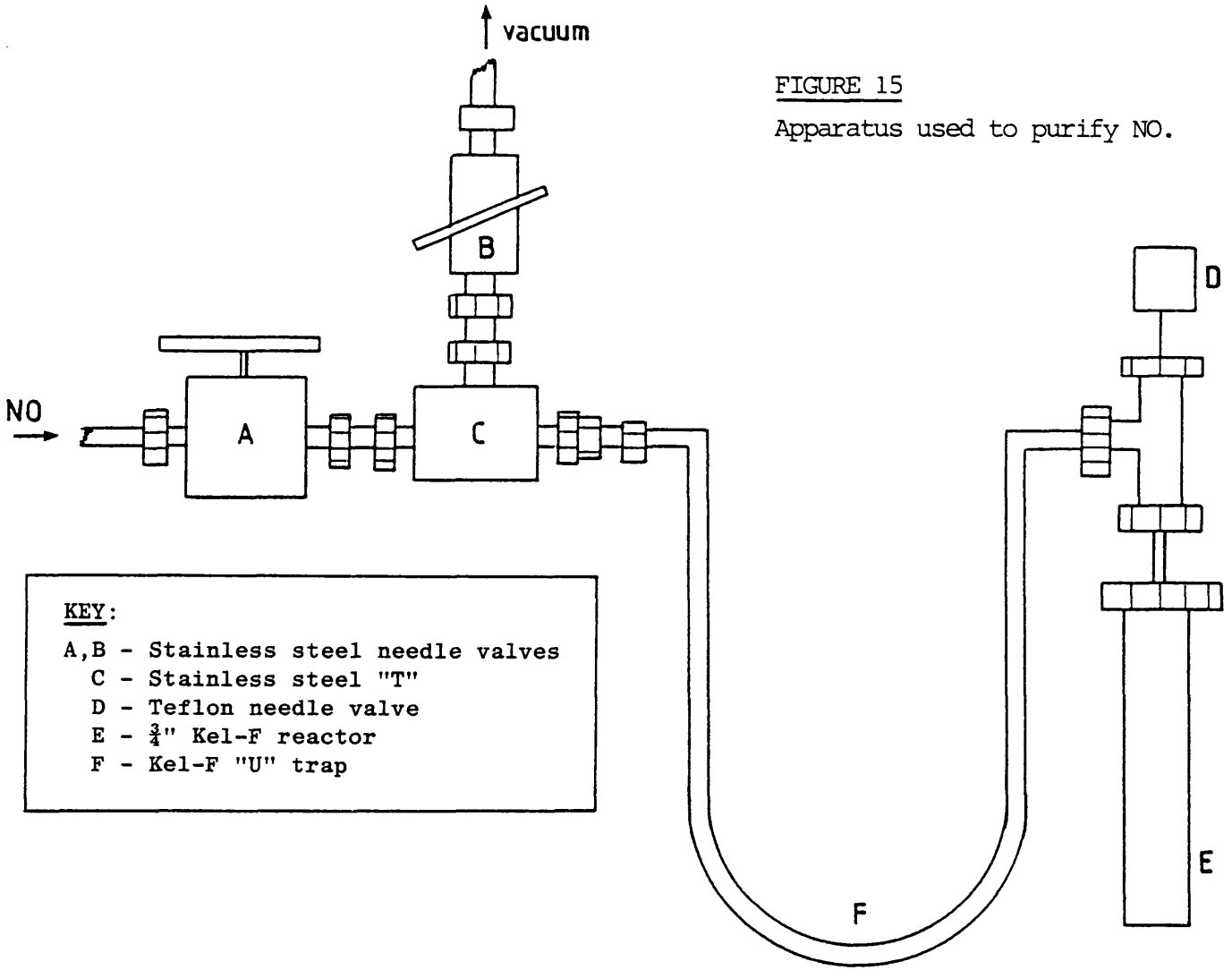

KEY:

A,B - Stainless steel needle valves
C - Stainless steel "T"
D - Teflon needle valve
E - ¾" Kel-F reactor
F - Kel-F "U" trap

FIGURE 15

Apparatus used to purify NO.

tube, E, warmed to -160°C. On melting the NO was observed as a clear liquid of approximately 5 cm^3 in volume.

4.3.3 Formation of NOF

The apparatus used for the reaction of NO with F_2 is shown in Figure 16. It is similar in design to that used for the purification of NO [Figure 15] except that now a nickel can containing ca. two atmospheres pressure of F_2 is attached to valve A, and the ¾" Kel-F reactor containing pure NO is attached directly to the stainless steel 'T', C.

The temperature of the reactor tube, E, containing pure NO, was maintained at -160°C using an isopentane/liquid nitrogen slush bath. Keeping valves B and D closed, approximately two atmospheres pressure of F_2 were admitted through valve A. Valve A was then closed. On opening valve D, the ensuing reaction of NO with F_2 was indicated by the appearance of small yellow flames on the surface of the liquid NO. It was found that this reaction could be rapidly quenched by replacing the isopentane/liquid nitrogen slush bath with liquid nitrogen. The addition of F_2 into reactor tube E was repeated until no further reaction occurred. After cooling to -196°C the excess F_2 from reactor tube E was removed by evacuation. The NOF formed was stored in reactor tube E at -78°C.

4.3.4 Determination of the purity of NOF

Attempts to determine the purity of gaseous NOF by infra-red spectroscopy were unsuccessful. Nitrosyl fluoride contained in a copper gas-cell, closed with AgCl windows reacted quickly with its surroundings. This resulted in the formation of NO[93] and ClF_3.[94] Only small bands assignable to NOF[95] were observed.

An investigation by ^{19}F nmr at -100°C proved the NOF to be of high purity. The ^{19}F nmr chemical shift obtained, 460 ± 10 p.p.m., is in

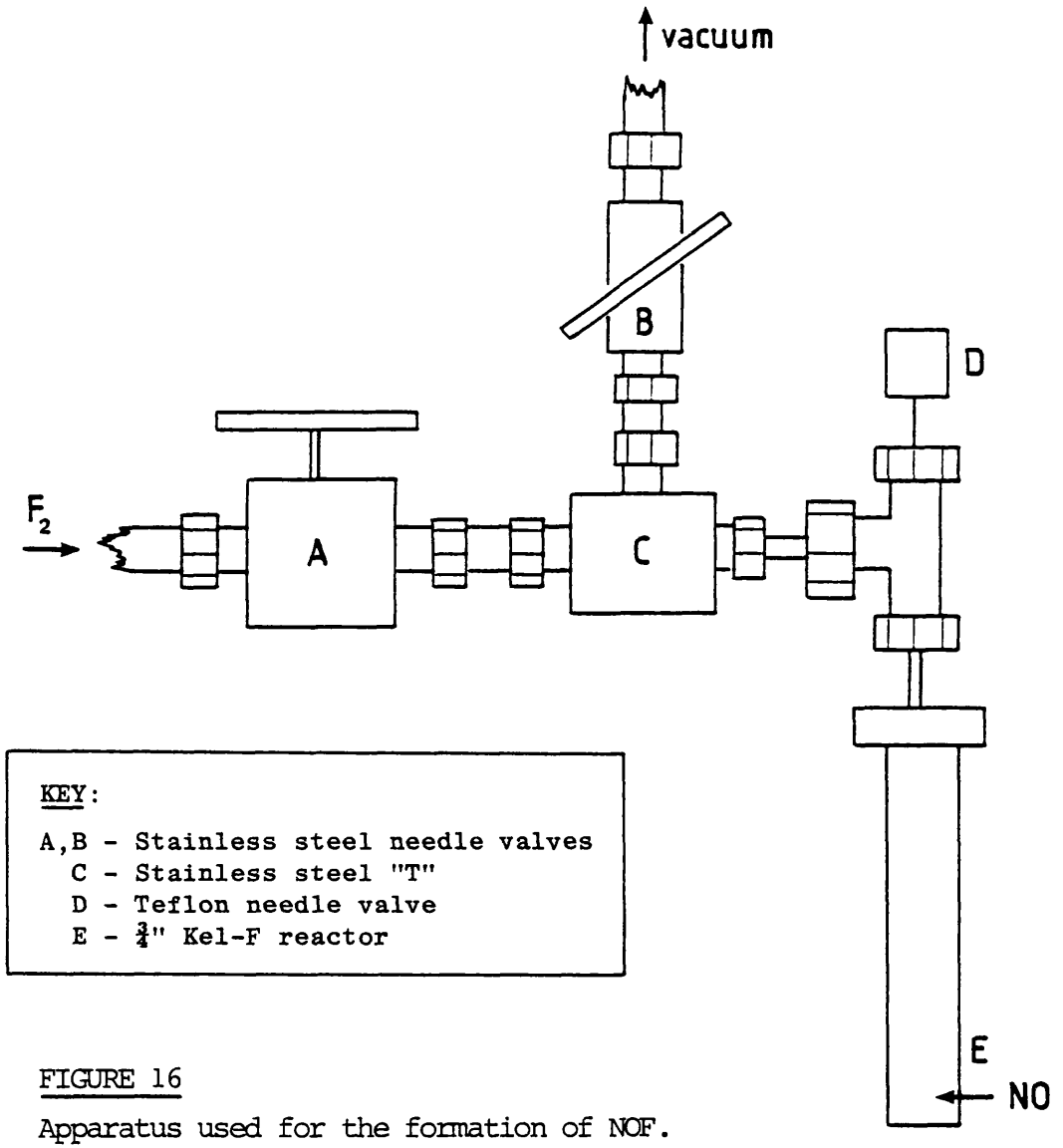

KEY:

A,B - Stainless steel needle valves
C - Stainless steel "T"
D - Teflon needle valve
E - ¾" Kel-F reactor

FIGURE 16

Apparatus used for the formation of NOF.

good agreement with the value of 479 ± 1 p.p.m. obtained by Holmes et al.[96]

However, the most convenient and reliable method of purity determination was found to be the reaction of WF_6 with a slight excess of NOF. The resulting white solid isolated from the reaction was shown to contain only $[NO]_2^+[WF_8]^{2-}$ [59,81,82] by infra-red spectroscopy, thus proving the NOF to be of high purity.

4.4 THE REACTION OF WSF_4 WITH AN EXCESS OF NOF

4.4.1 General procedure

Tungsten thiotetrafluoride, WSF_4, (0.2 mmole), was introduced into either a preseasoned 4 mm Kel-F nmr tube or a ¼" Teflon FEP reactor tube fitted with a Teflon needle valve, in a dry box. This was then attached to a 'parasite' fluoroplastic vacuum line [Chapter 8], containing the ¾" Kel-F reactor tube of NOF. After evacuation and passivation, an excess of NOF was condensed onto the sulphide at -196°C. The Kel-F nmr tubes containing samples for ^{19}F nmr analysis were heat sealed *in situ* and stored at -196°C.

A preliminary investigation established the reaction of WSF_4 with an excess of NOF to be extremely vigorous. On warming a sample from -196°C to -78°C, the melting of the NOF is accompanied by a spontaneous reaction with WSF_4, which yields a dark green solution above a dark solid. Warming to -30°C is followed by rapid discolouration of the green solution which results in the formation of a white solid. Infra-red spectroscopy and X-ray powder diffraction show this to be a mixture of $[NO]_2^+[WF_8]^{2-}$ [59,81,82] and $[NO]^+[WOF_5]^-$ [68] [Tables 28 and 29]. [N.B. Due to the small volume of the fluoroplastic reactor tubes used, and the high volatility of NOF, extreme caution was employed during this study.]

4.4.2 The low-temperature ^{19}F nmr study of the reaction of WSF_4 with an excess of NOF

It should be noted that reliable integration of peak area during this ^{19}F nmr study was not obtained, therefore a quantitative comparison of the concentrations of the species present in solution was not possible. Figure 17 shows the relative intensities of the high-frequency peaks within each spectrum, which are expressed in percentages.

A sample of WSF_4 and excess of NOF contained in a sealed 4 mm Kel-F nmr tube was transferred from storage at -196°C to the probe of a 'continuous wave' nmr spectrometer, which was maintained at -110°C. After ca. 3 minutes a reaction of WSF_4 with NOF was indicated by the appearance of 4 multiplets and 1 singlet in the nmr spectrum [Table 27, Figure 17a].

A doublet at 85.6 p.p.m. and a nonet at -164 p.p.m., $^2J[^{19}Fb-^{19}Fb]$ = 70 Hz, reveals the presence of the fluorine-bridged species, $[W_2S_2F_9]^-$ [27,28] [see also Tables 19 and 25], whilst the doublet and quintet at 76.3 p.p.m. and -117 p.p.m., $^2J[^{19}Fa-^{19}Fe]$ = 74 Hz, respectively are assigned to the species $[WSF_5]^-$.[27,28] Both species are present in solution in approximately equal concentration. The assignment of the low-intensity singlet at 69.1 p.p.m. is tentative, but it is likely that it is due to the presence of SOF_2[97] formed via the oxidative fluorination of the sulphur present in WSF_4 (by NOF). This is discussed further in Section 4.4.3.

After standing in the nmr probe at -110°C for 4 hours it was observed that a further reaction had occurred, Figure 17b. The signals due to the $[WSF_5]^-$ species are greatly reduced, whilst the singlet of SOF_2 shows an increase in intensity. The reason for this diminution

TABLE 27

^{19}F nmr data for the initial reaction of WSF_4 with an excess of NOF at -110°C

Sample	δ/ppm[a]	Multiplet[b] Structure	Coupling Constant/Hz[c]	Assignment[d]
WSF_4 + excess NOF	85.6	II	$^2J_{Fb-Fe}$ 70	$F_4WS-(\bar{F})-SWF_4$
	76.3	II	$^2J_{Fa-Fe}$ 74	$WSF_4(\bar{F})$
	69.1	I	-	SOF_2 [97]
	-117.0	V	$^2J_{Fa-Fe}$ 74	$WS(F_4)\bar{F}$
	-164.0	IX[e]	$^2J_{Fb-Fe}$ 70	$(F_4)WS-\bar{F}-SW(F_4)$

a,b,c,d *See Tables 19 and 25;*
e *Seven central lines of nonet identified by intensity ratio 10:30:55:65:55:28:9.*

TABLE 28

Infra-red data for the white solid isolated from the reaction of WSF_4 with excess NOF compared to those for $[NO]_2^+[WF_8]^{2-}$ and $[NO]^+[WOF_5]^-$

White solid from the reaction of WSF_4 with excess NOF	Frequency, cm^{-1}		Assignment[68,82]
	$[NO]_2^+[WF_8]^{2-}$ [82]	$[NO]^+[WOF_5]^-$ [68]	
2320 m	2320 m	2320 m	$\nu(NO)^+$
1000 s		1003 s	$\nu(W{=}O)$
680 s,sh		680 sh	$\nu_s(WF_4)$ i.p.
618 s,sh	620 s		$\nu(WF_8)^{2-}$
610 s,sh		610 vs,br	$\nu_{as}(WF_4)$ i.p.
558 vs	555 vs		$\nu(WF_8)^{2-}$
458 m		455 m	$\nu(WF)$ axial

i.p. = In-phase.

TABLE 29

X-ray powder diffraction data for the white solid isolated from the reaction of WSF_4 with excess NOF compared with that of $[NO]^+[WOF_5]^-$

White solid from the reaction of WSF_4 with excess NOF			$[NO]^+[WOF_5]^-$ [68]		
hkl	dA°	Intensity	hkl	dA°	Intensity
100	5.19	s	100	5.18	s
002	4.91	ms	002	4.87	ms
101	4.58	s	101	4.57	s
110	3.67	m	110	3.67	m
102	3.54	s	102	3.56	s
111	3.41	m	111	3.41	m
112	2.93	m	112	2.94	m
103	2.74	mw	103	2.76	mw
200		a	200	2.59	w,br
201			201	2.49	mw
004			004	2.45	w
113			113		
210			210	2.29	vvw
211	2.25	mw	211	2.24	m
104	2.19	mw	104	2.21	w
212	2.10	m	212	2.10	m
114	2.03	m	114	2.03	s,br
203			203		

[a] *Lines too weak to be measured.*

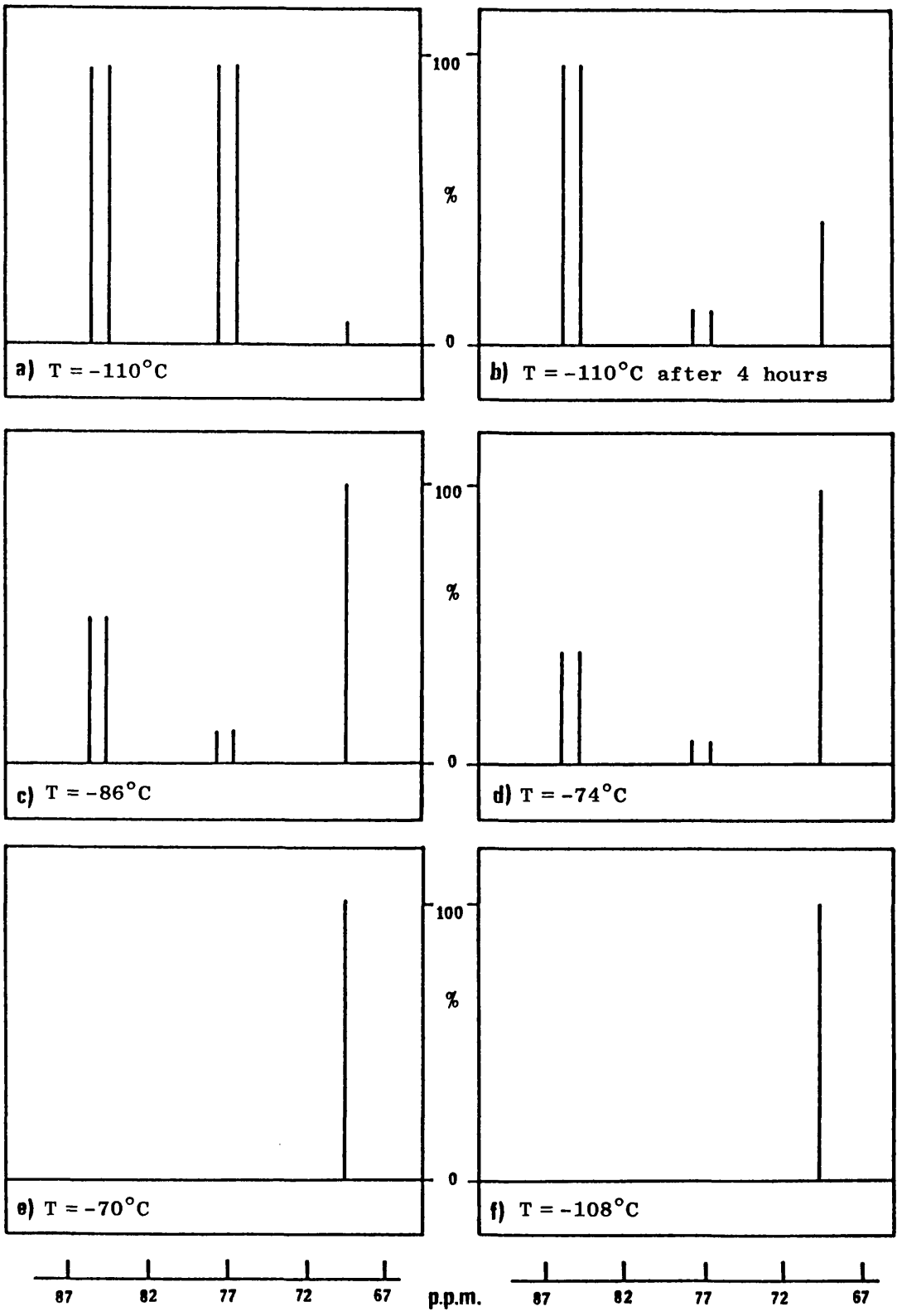

FIGURE 17

^{19}F nmr spectra of the green solution from the reaction of WSF_4 with an excess of NOF (high-frequency region).

of $[WSF_5]^-$ is not fully understood, but it is likely to be a consequence of two reaction processes occurring in the NOF solvent. Firstly, NOF is reacting preferentially with $[WSF_5]^-$ to yield oxidative fluorination products which include SOF_2. Secondly, the $[WSF_5]^-$ formed is kinetically unstable in the presence of NOF, and at -110°C slowly forms the (more stable) species, $[W_2S_2F_9]^-$. In light of observations made for the reaction of $M^+[WSF_5]^-$, M = Rb or Cs, in an excess of anhydrous HF [Section 3.10], in which $M^+[W_2S_2F_9]^-$ is preferentially formed, Scheme 14, the latter process for the diminution of $[WSF_5]^-$ in NOF solvent is preferred.

$$2M^+[WSF_5]^- + HF \rightleftharpoons M^+[W_2S_2F_9]^-\downarrow + MF \text{ solvated}$$

SCHEME 14

On warming to -86°C, Figure 17c, the signals due to $[W_2S_2F_9]^-$ slowly decrease while the singlet of SOF_2 continues to increase in intensity. At -74°C, Figure 17d, only a small concentration of tungsten thio-fluoride species remains in solution, and at -70°C, Figure 17e, the only species present is that giving rise to the singlet, namely SOF_2. On cooling to -108°C, Figure 17f, the spectrum remains unchanged.

This sequence of observations demonstrates that, even at moderately low temperatures, the tungsten thio-fluoride species, $[WSF_5]^-$ and $[W_2S_2F_9]^-$, formed in the excess NOF are extremely unstable, and react rapidly to yield SOF_2. During this study, peaks other than those assigned were not observed, therefore the tungsten fluoride species formed as a consequence of the oxidative fluorination of $[WSF_5]^-$ and $[W_2S_2F_9]^-$ by NOF cannot be defined. However, on the basis of the results from the preliminary reaction [Section 4.4.1], it is suggested that the tungsten fluoride species formed is a mixture of $[NO]_2^+[WF_8]^{2-}$ and $[NO]^+[WOF_5]^-$.

4.4.3 The attempted isolation of the ionic adducts $[NO]^+[W_2S_2F_9]^-$ and $[NO]^+[WSF_5]^-$

Attempts to isolate ionic adducts of the type $[NO]^+[W_2S_2F_9]^-$ and $[NO]^+[WSF_5]^-$ from the reaction of WSF_4 with excess of NOF have proved unsuccessful. During a further study of this reaction a green solid was isolated at -120°C. This decomposes at -78°C to yield a white solid and a gas. Analysis of the gas *via* infra-red spectroscopy shows it to consist of mainly NO[93] and SOF_2[98] and to a minor extent NOF.[95] On the basis of this evidence and that of the ^{19}F nmr study, it is probable that the green solid contains the ionic adducts $[NO]^+[W_2S_2F_9]$ and $[NO]^+[WSF_5]$.

Interestingly, infra-red spectroscopic and X-ray powder diffraction studies [Tables 28 and 29] have shown the white solid to consist of a mixture of $[NO]^+[WOF_5]^-$ and $[NO]_2^+[WF_8]^{2-}$. The presence of the former species and indeed SOF_2, implies that an oxygen exchange reaction is occurring between the tungsten thio-fluoride species and NOF. The nature of such an exchange has not been ascertained but it is thought to parallel a similar oxygen exchange process observed by Geichman *et al.*[99] in which the reaction of MF_6, M = Mo, W or U, with N_2O_4 affords $[NO]^+[MOF_5]^-$.

4.5 CONCLUSION

Although this study has demonstrated that WSF_4 is acting as a weak fluoride-ion acceptor in NOF solvent, the tungsten thio-fluoride species formed, $[W_2S_2F_9]^-$ and $[WSF_5]^-$ are very unstable and it appears that NOF rapidly oxidises the sulphur present in these species.

Attempts to isolate ionic adducts of the type $[NO]^+[W_2S_2F_9]^-$ and $[NO]^+[WSF_5]^-$ were unsuccessful, but an unstable green solid isolated at low temperatures is thought to contain such adducts. Scheme 17

SCHEME 17

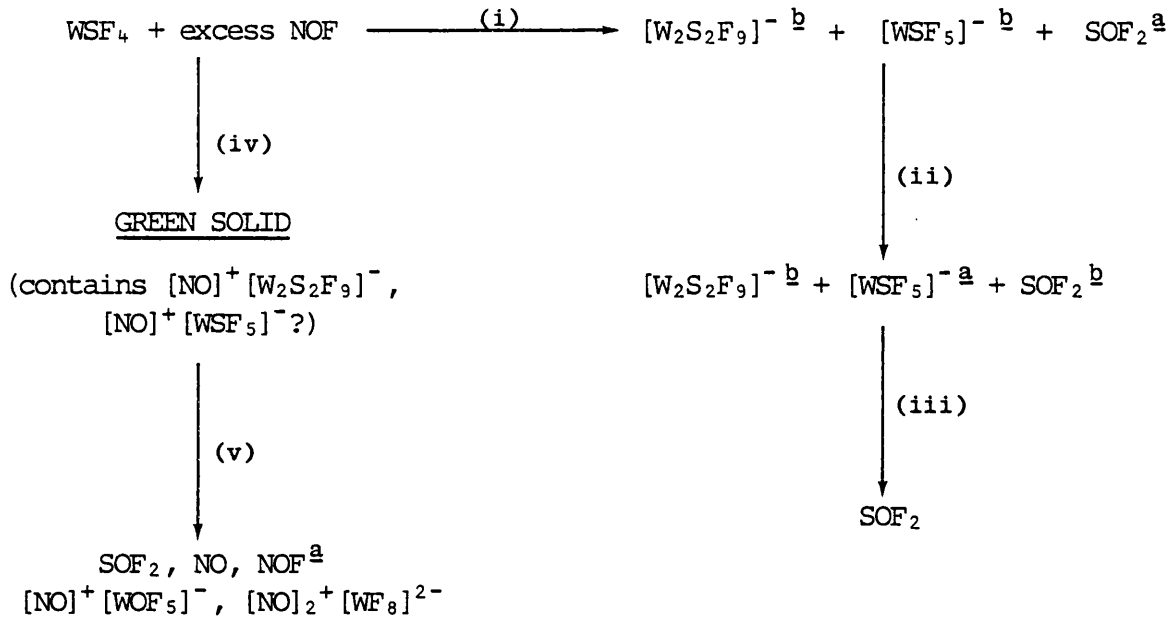

a) *Minor product;*
b) *Major product.*

---

i) *Solution analysed immediately after warming from -196°C to -110°C;*
ii) *Solution analysed after standing at -110°C for 4 hours;*
iii) *Solution analysed at -70°C;*
iv) *Excess of NOF solvent removed immediately after warming from -196°C to -120°C;*
v) *After warming to -78°C.*

summarises the results from this study.

4.6 FURTHER WORK

It is apparent from the results of this study that much further work is required. A low temperature Raman investigation of the solutions and solids isolated during this study might definitely identify the species formed.

It may be interesting to investigate indirect methods for preparing the ionic adducts, $[NO]^+[W_2S_2F_9]^-$ and $[NO]^+[WSF_5]^-$. One such method may be the reaction of $[NO]^+[WF_7]^-$ with H_2S in CH_3CN or HF solvent in which two fluorine atoms of $[NO]^+[WF_7]^-$ are replaced with sulphur from H_2S, thus yielding $[NO]^+[WSF_5]^-$ (cf. $WF_6 + H_2S \xrightarrow{CH_3CN} WSF_4$[29]).

CHAPTER 5

The Reaction of Tungsten Oxidetetrafluoride
and Tungsten Thiotetrafluoride with
Sulphur Tetrafluoride

5.1 INTRODUCTION

Sulphur tetrafluoride is a colourless gas at ambient temperatures and pressures (b.pt. -40°C). It condenses to a colourless liquid which solidifies at -121°C.[100] It is extremely sensitive to moisture, rapidly hydrolysing to HF and SO_2 via SOF_2.[101] Sulphur tetrafluoride can be prepared by a variety of methods,[100] but the most favoured laboratory preparation is the fluorination of SCl_2 by NaF in the presence of CH_3CN at 70-80°C.[101]

The reactions of SF_4 fall into three main categories. First, SF_4 is a Lewis acid; its reaction with $(CH_3)_4NF$[102] and CsF[103] to yield 1:1 adducts, $(CH_3)_4NF.SF_4$ and $Cs^+[SF_5]^-$ have been reported. A vibrational spectroscopic study of $Cs^+[SF_5]^-$ by Christe et al.[103] has shown the $[SF_5]^-$ anion to be square pyramidal with a point group symmetry of C_{4v}.

Sulphur tetrafluoride also reacts as a fluorinating agent; its reaction with organic molecules to selectively replace functional groups with fluorine has been extensively studied.[104-106] At elevated temperature, SF_4 reacts with inorganic oxides to afford the respective fluoride and SOF_2.[107,108] For example, with SeO_2 it produces SeF_4 and SOF_2 and with WO_3 it gives WF_6 and SOF_2. A similar reaction occurs with inorganic sulphides[107] but the reaction is characterised by the formation of elemental sulphur. For example, with P_4S_{10} it yields PF_5 and S, and with SnS_2, SnF_4 and S are formed.

In the presence of Lewis acid fluorides, SF_4 behaves as a fluoride-ion donor to produce adducts. For example with BF_3, GeF_4, AsF_5, SbF_5 and UF_5 the adducts $SF_4.BF_3$, $(SF_4)_2.GeF_4$, $SF_4.AsF_5$, $SF_4.SbF_5$ and $SF_4.3UF_5$ are formed.[62,66,107,109,110] The vibrational spectra of the adducts $SF_4.BF_3$ and $SF_4.MF_5$, (M = P, As or Sb) have been assigned by Azeem et al.[62] on the basis of the ionic models, $[SF_3]^+[BF_4]^-$ and

$[SF_3]^+[MF_6]^-$, in which $[SF_3]^+$ has the point group symmetry, C_{3v}. The occurrence of forbidden bands in the assignment of $[BF_4]^-$ and $[MF_6]^-$, and the additional splittings of the bands assigned to $[SF_3]^+$, is thought to be a consequence of fluorine bridging between the ions which lowers their symmetry in the crystal. Indeed, for the adducts $SF_4.BF_3$ and $(SF_4)_2.GeF_2$, solid state structure determination[65,66] has revealed that contributions to the bonding via fluorine does occur. A further study of the adducts $SF_4.BF_3$ and $SF_4.MF_5$ (M = P, As or Sb) in anhydrous HF by ^{19}F nmr[62] has revealed a singlet in the region 25 to 30 p.p.m. This has been assigned to the ion, $[SF_3]^+$.

Finally, Mallouk et al.[66] have determined the value of the F^- separation enthalpy for gaseous SF_4 from lattice enthalpy calculations [Scheme 18].

$$\Delta H^\circ(SF_{4(g)} \rightarrow SF_3^+{}_{(g)} + F^-{}_{(g)}) = 883 \pm 33 \text{ kJ mol}^{-1}$$

SCHEME 18

It is interesting to note that the value of $\Delta H^\circ F^-sep.SF_4$ is close to that of $\Delta H^\circ F^-sep.XeF_2$[111] (902 kJ mol^{-1}).

5.2 PRESENT STUDY

Tungsten oxidetetrafluoride, WOF_4, is known to act as a weak fluoride-ion acceptor. In the presence of strong fluoride ion bases such as NF_4HF_2, NOF and CsF, ionic adducts are formed which contain the anions $[W_2O_2F_9]^-$ and $[WOF_5]^-$.[67,68,112] In the presence of XeF_2, the adducts $XeF_2.nWOF_4$, n = 1 or 2, are formed. Spectroscopic investigation has shown these species to be essentially covalent, containing Xe-F-W bridges in the solid state and in solution.[113-115] The covalent nature of $XeF_2.WOF_4$ has been confirmed by single crystal structure determination.[116]

Tungsten thiotetrafluoride, WSF_4, however, has only recently been shown to act as a fluoride-ion acceptor, forming ionic adducts containing the anions $[W_2S_2F_9]^-$ and $[WSF_5]^-$ [Chapter 3]. Spectroscopic investigation has revealed that WSF_4 is a weaker fluoride-ion acceptor than WOF_4; this is discussed in detail in Chapter 3. The reaction with NOF further demonstrates the fluoride-ion acceptor ability of WSF_4 [Chapter 4] but, due to oxidative fluorination of the sulphur by NOF, solids containing either $[W_2S_2F_9]^-$ or $[WSF_5]^-$ were not isolated.

Although SF_4 reacts with a wide variety of Lewis acid fluorides to yield adducts, no such interaction with Lewis acid oxide fluorides or sulphides of the transition metals has been reported. In light of the fluoride-ion acceptor properties of WOF_4 and WSF_4, it appeared probable that WOF_4 and WSF_4 might produce new adducts on reaction with SF_4.

In this study, the reaction of WOF_4 and WSF_4 with an excess of SF_4 has been investigated. In the case of WOF_4 a new adduct has been isolated but with WSF_4 no adduct formation was observed.

5.3 THE REACTION OF WOF_4 WITH AN EXCESS OF SF_4

The ionic adduct $[SF_3]^+[W_2O_2F_9]^-$ has been prepared as a white, crystalline material from the reaction of WOF_4 and excess of SF_4. The adduct has been characterised by mass balance, infra-red spectroscopy, X-ray powder diffraction and low temperature ^{19}F nmr spectroscopy. The infra-red spectrum of the solid has been assigned on the basis of the ionic formulation $[SF_3]^+[W_2O_2F_9]^-$ in which bonding contributions from fluorine bridging are minimal. The low temperature ^{19}F nmr spectrum in SO_2 shows the ions $[SF_3]^+$ and $[W_2O_2F_9]^-$ to be discrete, any interaction *via* fluorine bridging being absent.

5.3.1 The preparation of $[SF_3]^+[W_2O_2F_9]^-$

The ionic adduct $[SF_3]^+[W_2O_2F_9]^-$ was prepared by the reaction of WOF_4 with an excess of SF_4 [Scheme 19]. Tungsten oxidetetrafluoride, WOF_4, (ca. 3.0 mmole) was introduced into a prepassivated ¼" Teflon FEP reactor tube, fitted with a Teflon needle valve, in the dry box. The reactor and manifold were pumped to high vacuum before an excess of SF_4 was condensed onto the oxide at -196°C. On warming to -78°C, the oxide slowly dissolved in the liquid SF_4, and at -30°C complete dissolution had occurred. Careful removal of the excess of SF_4 under static vacuum at -30°C resulted in the isolation of a white, crystalline material. Mass balance of repeated experiments was in accord with the formulation $[SF_3]^+[W_2O_2F_9]^-$ in which WOF_4 and SF_4 are present in a 2:1 molar ratio.

$$WOF_4 + \text{Excess } SF_4 \xrightarrow{(i)} \underline{[SF_3]^+[W_2O_2F_9]^-}$$

(i) *Excess of SF_4 removed at -30°C under static vacuum.*

SCHEME 19

5.3.2 Infra-red spectroscopic studies

The infra-red spectrum of $[SF_3]^+[W_2O_2F_9]^-$ is shown in Figure 18 and these data together with those for $Cs^+[W_2O_2F_9]^-$ [67] and $[SF_3]^+$ in $SF_4.BF_3$ [62] are recorded in Table 30. The infra-red spectrum of $[SF_3]^+$-$[W_2O_2F_9]^-$ was recorded as a fine powder pressed between KBr discs.

Comparison of the infra-red data of $[SF_3]^+[W_2O_2F_9]^-$ with that of $Cs^+[W_2O_2F_9]^-$ show the two to be in excellent agreement. Therefore, the bands at 1027, 707, 638 and 448 cm^{-1} present in the infra-red spectrum of $[SF_3]^+[W_2O_2F_9]^-$ can be assigned to $\nu(W{=}O)$, $\nu_s(WF_4)_{in\text{-}phase}$, $\nu_{as}(WF_4)$ and the bridging stretch $\nu_{as}(WFW)$, respectively, of the fluorine bridged anion, $[W_2O_2F_9]^-$. Further comparison of the infra-red

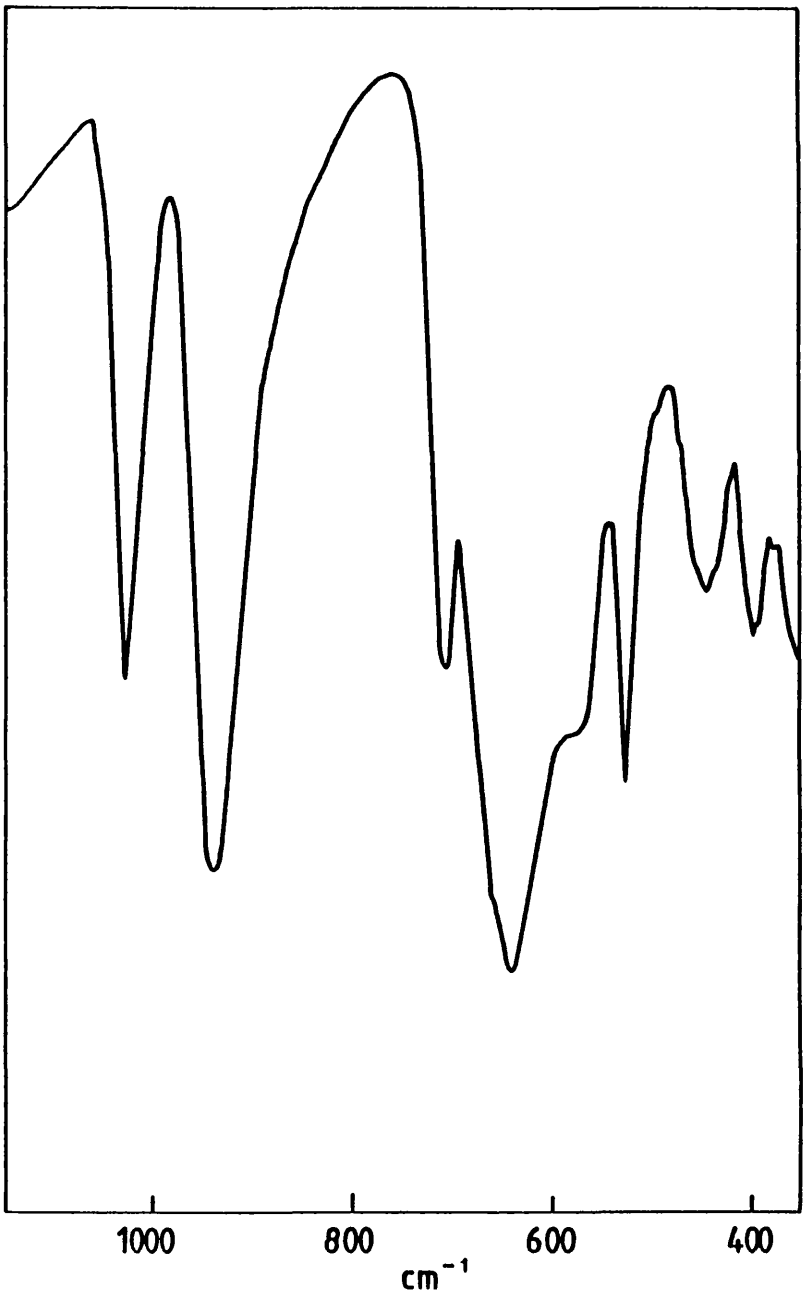

FIGURE 18

Infra-red spectrum of $[SF_3]^+[W_2O_2F_9]^-$.

TABLE 30

Infra-red data for the ionic adduct $[SF_3]^+[W_2O_2F_9]^-$ compared with those for $Cs^+[W_2O_2F_9]^-$ and $[SF_3]^+$ in $SF_4.BF_3$

Frequency, cm^{-1}			Assignment	
$[SF_3]^+[W_2O_2F_9]^-$	$Cs^+[W_2O_2F_9]^-$ [67]	$[SF_3]^+$ in $SF_4.BF_3$ [62]	$[SF_3]^+C_{3v}$ [62]	$[W_2O_2F_9]^-$ [67]
1027 s	1048 vs 1035 vs			ν(W=O)
937 vs		935 vs 910 vs	(ν_1, ν_3)	
	822 vw 790 vw			
707 s	704 s			$\nu_s(WF_4)$ i.p.
638 vs	628 vs,br			$\nu_{as}(WF_4)$
575 sh				
525 s		520 vs	ν_2	
448 ms	440 vs			ν_{as}(WFW)
400 ms		409 m	ν_4	

i.p. = in-phase.

data with those for $[SF_3]^+$ in $SF_4.BF_3$ permits assignment of the bands at 937, 525 and 400 cm^{-1} to the normal modes of vibration (ν_1,ν_3), ν_2 and ν_4 of the pyramidal $[SF_3]^+$ cation [Figure 19]. N.B. This assignment is based on $[SF_3]^+$ possessing the point group symmetry C_{3v} in the solid state.[66]

It is interesting to note that splitting of the modes ν_3 and ν_4 [Figure 19], which is diagnostic of the lowering of symmetry of the C_{3v} point group,[117] is not observed. This indicates that significant interaction arising from fluorine bridging between $[SF_3]^+$ and $[W_2O_2F_9]^-$ in the solid state is minimal.

5.3.3 X-ray powder diffraction studies

The X-ray powder diffraction patterns obtained for $[SF_3]^+[W_2O_2F_9]^-$ confirms that it is a new phase. Comparison with the X-ray powder diffraction of the ionic adduct $[NO]^+[W_2O_2F_9]^-$[68] shows the two ionic adducts are not isostructural.

5.3.4 ^{19}F nmr spectroscopic studies in SO_2

The ^{19}F nmr spectrum of $[SF_3]^+[W_2O_2F_9]^-$ in SO_2 at -70°C is shown in Figure 20. These data are recorded together with those for $[NO]^+[W_2O_2F_9]^-$[68] in propylene carbonate and $SF_4.SbF_5$[62] in anhydrous HF in Table 31. The ionic adduct $[SF_3]^+[W_2O_2F_9]^-$ exhibits high solubility in SO_2; brief examination of the sample at -70°C reveals a clear, colourless solution.

The high-frequency doublet at 64.3 p.p.m., $^2J[^{19}Fb-^{19}Fe] = 57$ Hz, and low-frequency nonet at -146.3 p.p.m., $^2J[^{19}Fb-^{19}Fe] = 56$ Hz, integration ratio 8:1, for $[SF_3]^+[W_2O_2F_9]^-$ in SO_2 compares well with similar data for $[NO]^+[W_2O_2F_9]^-$ in propylene carbonate.[68] Therefore, these resonances are assigned to the typical AX_8 type spectrum of the fluorine-bridged species $[W_2O_2F_9]^-$, Figure 21. Further comparison of the ^{19}F nmr data of

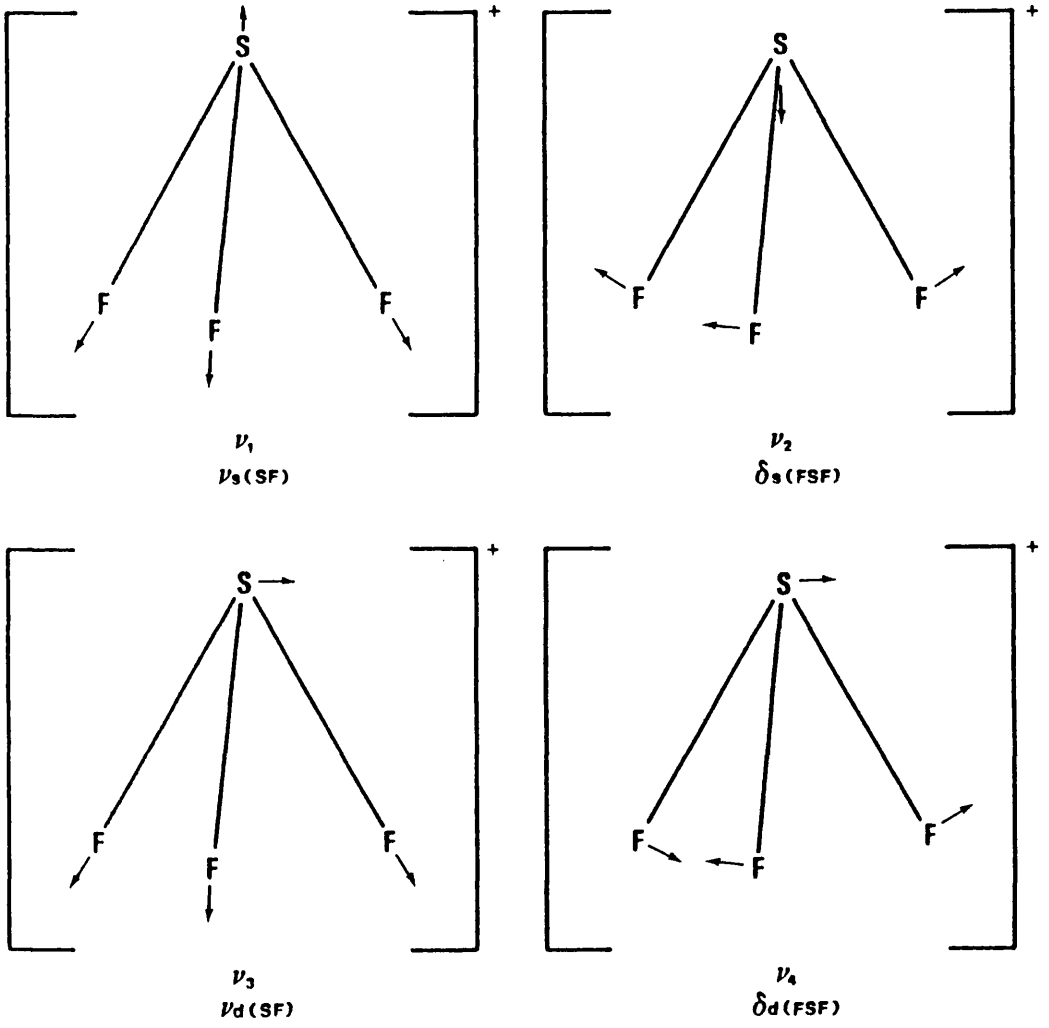

FIGURE 19

Normal modes of vibration of the pyramidal $[SF_3]^+$ cation [Ref. 117].

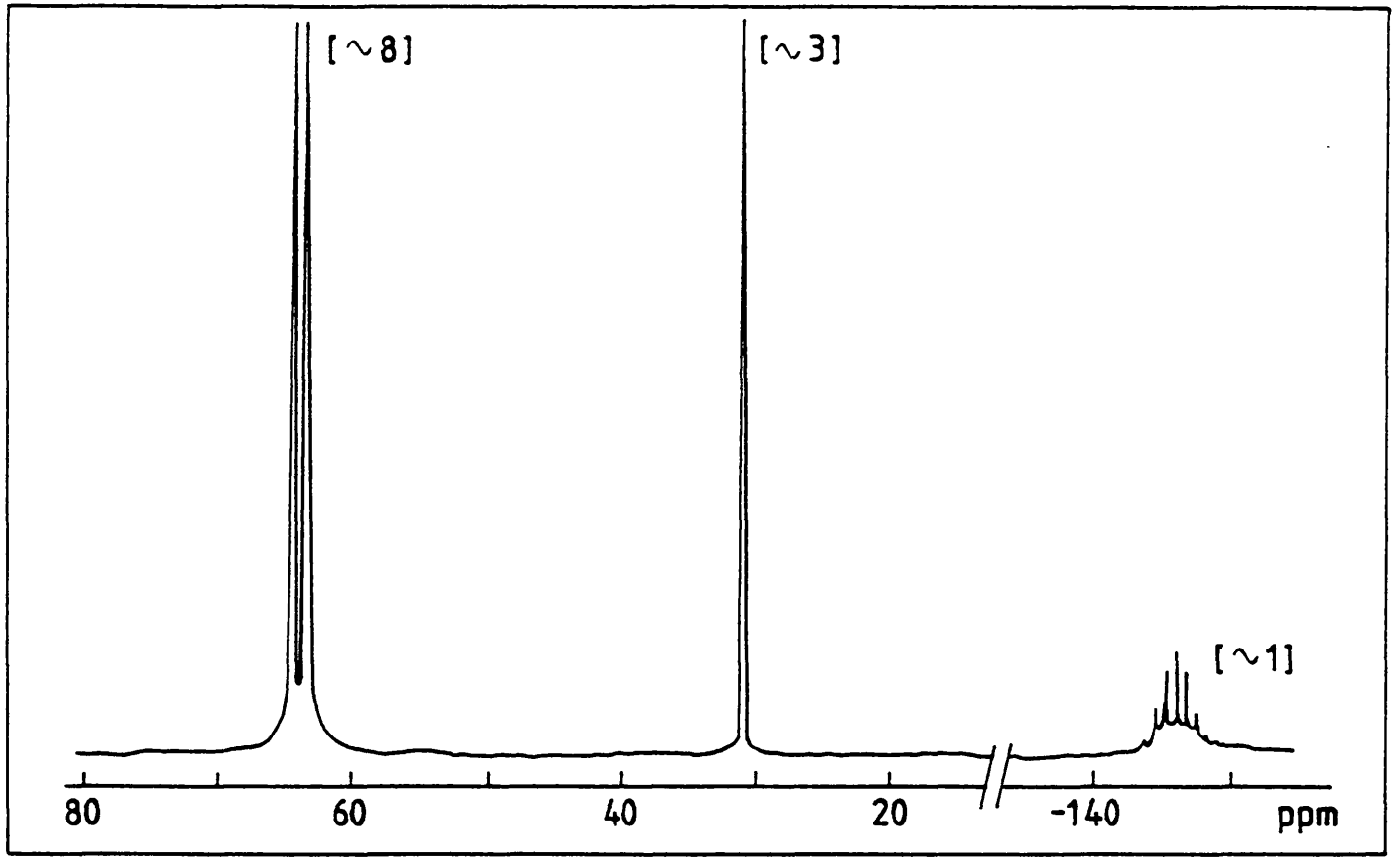

FIGURE 20

^{19}F n.m.r. spectrum of $[SF_3]^+[W_2O_2F_9]^-$ in SO_2 at -70°C.

TABLE 31

^{19}F nmr data for $[SF_3]^+[W_2O_2F_9]^-$ in SO_2 compared with those for $[NO]^+[W_2O_2F_9]^-$ and $SF_4.SbF_5$

Sample	Temperature °C	Solvent	δ/ppm[a]	Multiplet[b] Structure	Coupling Constant/Hz	Assignment[62,68]
$[NO]^+[W_2O_2F_9]^-$[68]	10	propylene carbonate	62.0	II	$^2J_{Fb-Fe}$ 58	$F_4WO-(\bar{F})-OWF_4$
			-145.5	IX	$^2J_{Fb-Fe}$ 58	$(F_4)WO-\bar{F}-OW(F_4)$
$SF_4.SbF_5$[62]	-60	anhydrous HF	27.1	I	-	SF_3^+
			-198	I	-	HF
$[SF_3]^+[W_2O_2F_9]^-$	-70	SO_2	64.3	II	$^2J_{Fb-Fe}$ 57	$F_4WO-(\bar{F})-OWF_4$
			31.2	I	-	SF_3^+
			-146.3	IX[c]	$^2J_{Fb-Fe}$ 56	$(F_4)WO-\bar{F}-OW(F_4)$

[a],[b] *See Table 19;*
[c] *Seven central lines of nonet identified by intensity ratio 10:30:55:65:55:29:9.*

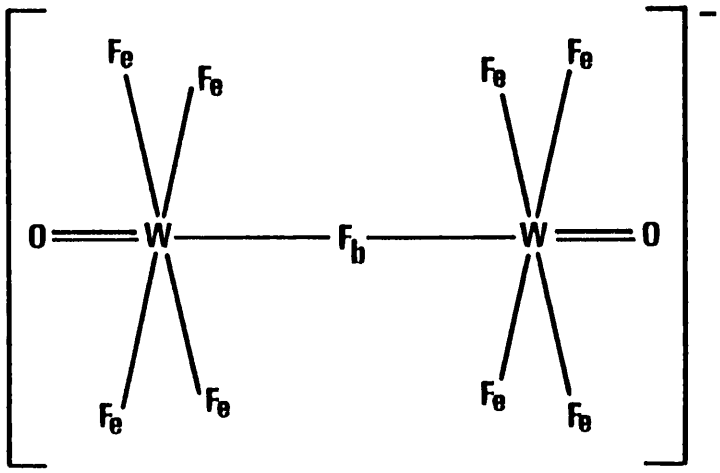

FIGURE 21

Proposed structure of $[W_2O_2F_9]^-$ in solution.[68]

$[SF_3]^+[W_2O_2F_9]^-$ in SO_2 to those for $SF_4.SbF_5$ in anhydrous HF, permits assignment of the sharp singlet at 31.2 p.p.m. to the cation $[SF_3]^+$.

Integration ratios of the respective resonances for $[SF_3]^+[W_2O_2F_9]^-$ in SO_2 are shown in parentheses in Figure 20. These are in excellent agreement with the expected values for the ions $[SF_3]^+$ and $[W_2O_2F_9]^-$ present in a 1:1 molar ratio.

The appearance of the high-frequency doublet and low-frequency nonet of $[W_2O_2F_9]^-$ and the sharp singlet of $[SF_3]^+$ implies that any interaction between the two ions via fluorine bridging is absent. Thus, in SO_2 the two ions $[SF_3]^+$ and $[W_2O_2F_9]^-$ are discrete.

5.4 THE REACTION OF WSF_4 WITH AN EXCESS OF SF_4

Although the reaction of WSF_4 with an excess of SF_4 did not yield an isolable adduct, the procedure of reaction and analysis of reaction products will be discussed here.

The samples of WSF_4 and excess of SF_4 were prepared using the method previously described [Section 5.3.1]. For the ^{19}F nmr studies, samples were prepared in 4 mm Kel-F nmr tubes.

The warming of a sample of WSF_4 and an excess of SF_4 from -196°C to -78°C was accompanied by the slow formation of an orange, flocculent precipitate. Removal of all volatiles at this temperature resulted in the isolation of an orange material. On warming to -30°C, rapid discolouration occurred with the bulk of the orange material being consumed. At 0°C no further reaction was apparent; the final products being a straw coloured solid and a volatile colourless liquid. Analysis of the volatiles by mass spectrometry showed unequivocally that the colourless liquid is WF_6. Analysis of the straw coloured solid by mass spectrometry and infra-red spectroscopy showed it to consist of elemental sulphur and unreacted WSF_4. Spectra assignable to adduct

formation between SF_4 and WSF_4 were absent.

5.4.1 ^{19}F nmr studies in SO_2, SO_2ClF and SF_4 solvents

In attempts to ascertain the nature of the orange material, low temperature ^{19}F nmr studies of the orange material in the solvents SO_2, SO_2ClF and SF_4 were conducted. The results from the studies are recorded in Table 32.

The high-frequency singlet in the region of 160 p.p.m., which appears as the strongest peak in each spectrum, is assigned to the resonance of WF_6. The assignment of the weak singlet in the region of 80 p.p.m. is tentative, but it is probably due to WSF_4. Increasing the temperature of the samples was accompanied by an increase in the intensity of the resonance assigned to WF_6. In all samples studied, species other than those stated above were not observed. Scheme 20 summarises the results from the study of the reaction of WSF_4 with an excess of SF_4.

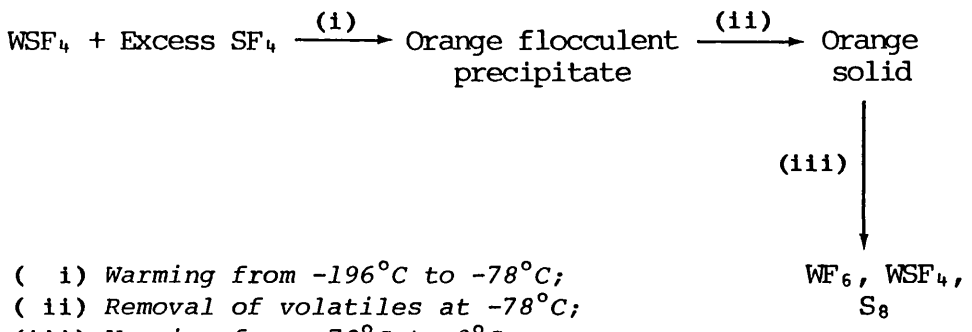

SCHEME 20

5.5 OVERALL CONCLUSION TO THE REACTION OF WOF_4 AND WSF_4 WITH AN EXCESS OF SF_4

This study has produced the new ionic adduct, $[SF_3]^+[W_2O_2F_9]^-$, the first example of a complex between SF_4 and a transition metal oxide-fluoride. Infra-red spectroscopy shows there to be considerable ionic contribution to the bonding in the solid state, with fluorine bridging between $[SF_3]^+$ and $[W_2O_2F_9]^-$ being minimal. The ^{19}F nmr spectrum in SO_2

TABLE 32

^{19}F nmr data for the orange material in SF_4, SO_2ClF and SO_2 solvents

Sample	Temperature °C	Solvent	δ/ppm[a]	Multiplet[b] Structure	Assignment
orange material from the reaction of WSF_4 with an excess of SF_4	-110	SF_4	162.0	I	WF_6
			75.8	I	WSF_4 ?
	-115	SO_2ClF	168.4	I	WF_6
			81.6	I	WSF_4 ?
	-70	SO_2	164.2	I	WF_6
			87.8	I	WSF_4 ?

[a] *See Table 19;*
[b] *I; Singlet.*

shows the ions $[SF_3]^+$ and $[W_2O_2F_9]^-$ to be discrete, any interaction between $[SF_3]^+$ and $[W_2O_2F_9]^-$ via fluorine bridging being absent.

Although no evidence has been found for the formation of the adduct containing $[WOF_5]^-$ and $[SF_3]^+$ during this study, it might be possible to prepare such an adduct by the addition of SF_4 to $[SF_3]^+[W_2O_2F_9]^-$ in anhydrous HF. The subsequent reaction might be in the form of the equilibrium, Scheme 21.

$$[SF_3^+, HF_2^-] + [SF_3]^+[W_2O_2F_9]^- \rightleftharpoons 2[SF_3]^+[WOF_5]^- + HF$$

SCHEME 21

Thus on removal of the anhydrous HF by distillation, $[SF_3]^+[WOF_5]^-$ will be formed. Such equilibrium reactions have been shown to exist for $Cs^+[WOF_5]^-$ [67] and $M^+[WSF_5]^-$, (M = Rb or Cs), in anhydrous HF, and are discussed in Chapter 3.

It may be interesting to extend this study to the investigation of the interaction of SF_4 with other oxide-fluorides of the transition metals, e.g. $MoOF_4$, $ReOF_4$, $ReOF_5$, $OsOF_4$ and $OsOF_5$.

This study has also demonstrated the fluorinating ability of SF_4. The reaction of WSF_4 with an excess of SF_4 has been shown to afford an unstable orange material which on decomposition yields WF_6, S_8 and unreacted WSF_4. Although adduct formation was not observed in this study, the probability of the orange material being a loosely bound adduct of WSF_4 and SF_4 cannot be excluded. The next obvious stage in this investigation would be the low temperature Raman study of the orange material. This might definitely identify the species present.

CHAPTER 6

Tungsten Thiotetrafluoride and its reaction with Xenon Difluoride

6.1 INTRODUCTION

The reactions of XeF_2 can be broadly divided into two categories. First XeF_2 is a mild fluorinating agent reacting with a wide variety of organic compounds, generally unsaturated, to yield fluoro-substituted or addition compounds.[118] It also reacts with organic compounds containing $\equiv P$, $\equiv Sb$, $=S$ and $-I$.[119] These are oxidatively fluorinated to yield $\equiv PF_2$, $\equiv SbF_2$, $=SF_2$ and $-IF_2$ respectively. A review by Burns et al.[120] has demonstrated the utility of the XeF_2/HF system as a mild fluorinating agent for simple transition metal compounds. For example, with ReO_2, $ReOF_4$ is formed and with $Ru(CO)_3Cl_2$ it initially yields $Ru(CO)_3F_2$, which reacts further to give $Ru(CO)_2F_3$. Holloway et al.[121] have contrasted the reactivity of F_2 with XeF_2 via their reaction with $Ru_2(CO)_{10}$. With F_2, $Re_2(CO)_{10}$ reacts explosively, whereas with XeF_2 in Genetron-113, the novel adduct $Re(CO)_5F.ReF_5$ can be isolated.

Xenon difluoride also reacts with a wide variety of main group and transition metal Lewis acid pentafluorides to yield adducts. In general, adducts of the type $XeF_2.2MF_5$, $XeF_2.MF_5$ and $2XeF_2.MF_5$ are formed,[122-129] although other more complex stoichiometries have been reported.[127-130] X-ray crystallographic and vibrational spectroscopic studies[122,125,126,129,130,131] of these adducts indicate that in addition to contributions to the bonding from the ionic formulations $[XeF]^+[M_2F_{11}]^-$, $[XeF]^+[MF_6]^-$ and $[Xe_2F_3]^+[MF_6]^-$, a significant contribution from fluorine bridging also occurs.

In a more recent study it has been shown that when XeF_2 is fused, at 50°C, with stoichiometric amounts of MOF_4, (M = Mo or W), the adducts $XeF_2.nMOF_4$, n = 1 or 2, can be isolated.[113-116] Vibrational and ^{19}F nmr spectroscopy[113-116] has demonstrated that these adducts are essentially covalent and contain Xe-F-M bridges in the solid state and in solution.

The covalent nature of the adduct $XeF_2.WOF_4$ has been determined by a single crystal structure determination.[116] Longer chain species, n = 1-4, have been characterised by low temperature ^{19}F nmr studies in SO_2ClF solvent, and evidence for isomerisation between oxygen and fluorine bridged Xe-F groups has been obtained.[114]

6.2 PRESENT STUDY

In this study the reaction of WSF_4 with XeF_2 has been investigated both in the solid state and in SO_2ClF solvent.

In light of the weak fluoride ion acceptor ability of WSF_4 [as demonstrated in Chapters 3 and 4] and the mild fluorinating properties of XeF_2, it was anticipated that, in such a system, the following types of reaction might occur.

i) Adduct formation: The interaction of WSF_4 and XeF_2 to yield adducts analogous to those formed by WOF_4, i.e. $XeF_2.nWSF_4$, n = 1 or 2.

ii) Oxidative fluorination: The fluorination of the sulphur of the terminal tungsten-sulphur bond in WSF_4 to yield a compound of the type, F_4WSF_2.

However, evidence for the formation of neither species was not obtained. Instead the reaction of WSF_4 with XeF_2 in the solid state yielded only WF_6, SF_4, S_2F_{10}, SF_6 and Xe, whilst the reaction in SO_2ClF solvent was shown to yield WF_6 and the radical cation $S_8^{+\bullet}$ at low temperatures.

In addition an initial investigation of the reaction of WSF_4 with XeF_2 in anhydrous HF solvent has led to the isolation of a red-orange material. This is stable up to temperatures of ca. -70°C, but above this, rapid decomposition occurs to yield tungsten and sulphur fluorides.

6.3 THE REACTION OF WSF_4 WITH XeF_2 IN THE SOLID STATE

The reaction between WSF_4 and XeF_2 in the solid state [Scheme 22] was attempted by mixing stoichiometric quantities of the reagents in a fluorine dried, Pyrex reaction vessel [Figure 22].

$$WSF_4 + XeF_2 \longrightarrow XeF_2.WSF_4$$

SCHEME 22

Tungsten thiotetrafluoride and XeF_2 were introduced into tubes A and B respectively in the dry box. These were cooled to -78°C whilst the apparatus was evacuated to high vacuum on the main vacuum manifold. After closing Teflon valve C, tube B was warmed to ambient temperature whereupon the XeF_2 distilled into tube A containing the sulphide. On warming tube A to ambient temperature, a violent reaction occurred with the emission of light and the formation of copious quantities of a white vapour. Analysis of the volatile material taken from tube A *via* mass spectrometry and gas phase infra-red spectroscopy revealed the presence of WF_6, SF_4, S_2F_{10}, SF_6 and Xe. Evidence for the formation of species of the type $XeF_2.WSF_4$ or F_4WSF_2 was not obtained. In light of this, attempts to investigate the reaction between XeF_2 and WSF_4 in the solid state were discontinued.

6.4 THE REACTION OF WSF_4 WITH XeF_2 IN SO_2ClF

Due to the vigorous nature of the reaction between WSF_4 and XeF_2 in the solid state, it was decided to investigate the reaction in SO_2ClF solvent *via* low temperature ^{19}F nmr spectroscopy. The reactions were investigated using 1:1 and 2:1 mixtures of WSF_4 and XeF_2.

6.4.1 General procedure

Known amounts of XeF_2 and WSF_4 were introduced into the Pyrex side-arm and Kel-F nmr tube respectively, of the apparatus shown in Figure

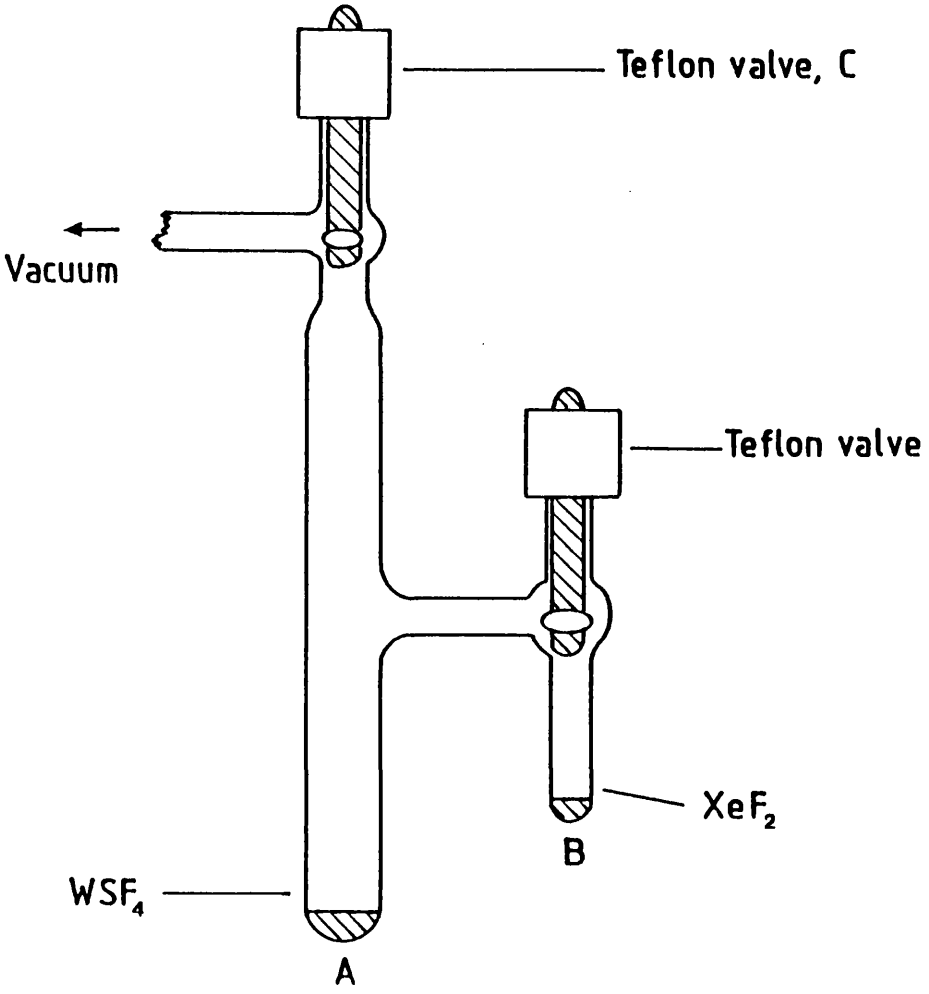

FIGURE 22

Pyrex apparatus used to study the reaction of WSF_4 with XeF_2 in the solid state.

23, in the dry box. After evacuation of the apparatus, SO_2ClF was distilled onto the sulphide at -196°C. Keeping Teflon valve D closed, Teflon valve C was opened and the XeF_2 crystals admitted into the Kel-F nmr tube. Brief warming of the solvent to its melting point permitted dissolution of XeF_2 and WSF_4 which resulted in the formation of an intense red-brown solution. The Kel-F nmr tubes were heat sealed and stored in liquid nitrogen.

6.4.2 ^{19}F nmr studies

Several samples of the red-brown mixtures of WSF_4 and XeF_2 in SO_2ClF have been extensively studied by ^{19}F nmr at temperatures ranging from the melting point of SO_2ClF, -121°C, to -50°C. In spite of this, in no instance during this study was ^{19}F nmr evidence obtained for the formation of the expected species, $XeF_2.nWSF_4$, n = 1 or 2, or F_4WSF_2. The peaks that were observed in the spectra were readily assigned to WF_6, and unreacted WSF_4 and XeF_2. The latter was unequivocally identified by its characteristic singlet at -189.8 p.p.m. flanked by xenon-129 satellites, $^1J[^{129}Xe-^{19}F] = 5537$ Hz. [N.B. ^{129}Xe, I = ½, natural abundance = 26.24%.] Interestingly at lower temperatures, peaks were observed in the regions associated with the adducts $XeF_2.nWOF_4$, n = 1 or 2;[114] these probably arising from the inevitable trace impurity of WOF_4 present in the samples of WSF_4 used.

6.4.3 E.s.r. studies

It has been well established that a red-brown colouration can be formed from solutions of sulphur in oxidising media such as 25%[132] and 65%[133] oleum, and AsF_5 in SO_2,[134] and that such solutions exhibit e.s.r. spectra. A very recent study by Chandra *et al.*[135] has conclusively shown the species present in these solutions to be the radical cation, $S_8^{+\bullet}$.

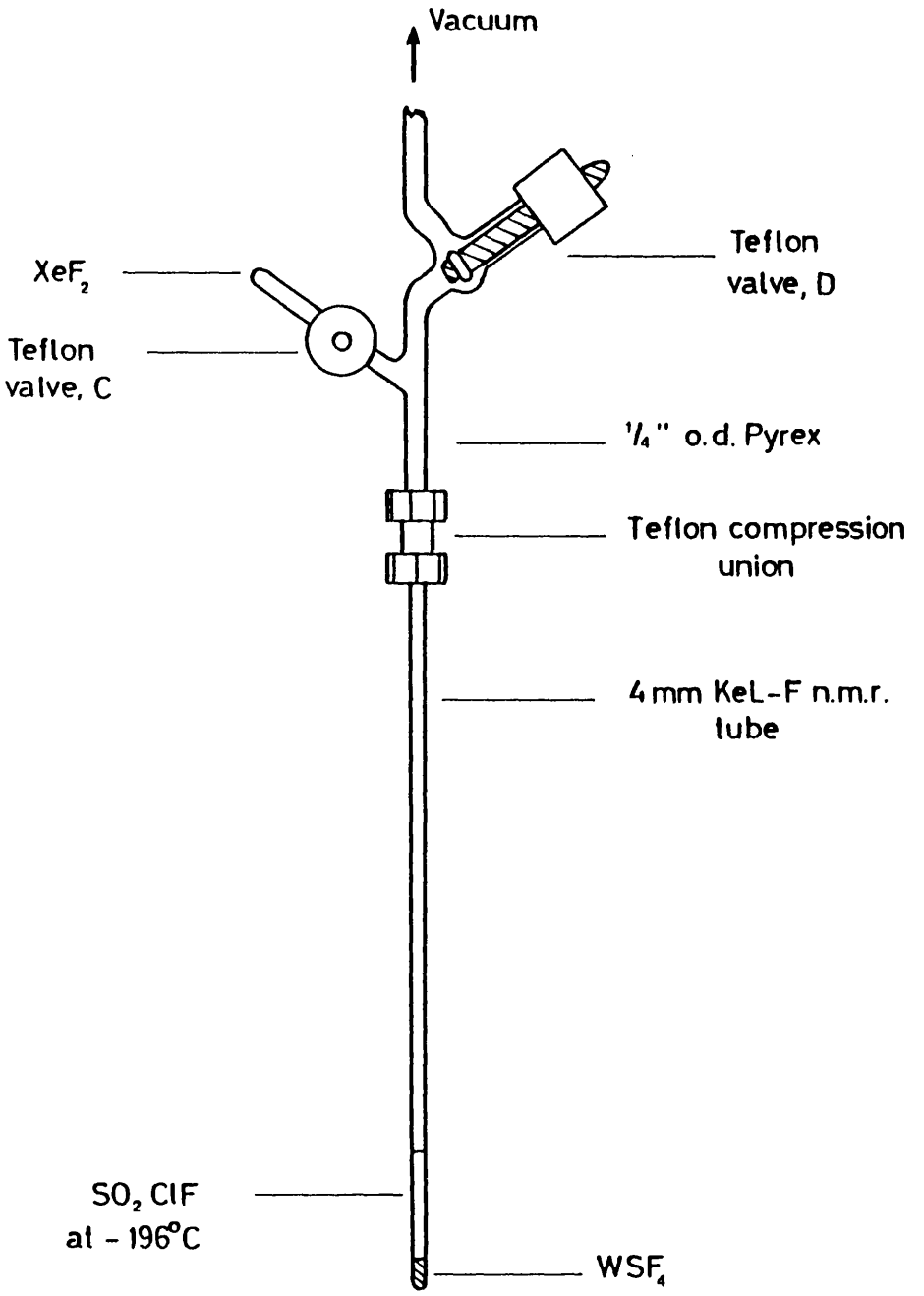

FIGURE 23

Apparatus used to study the reaction of XeF_2 with WSF_4 in SO_2ClF.

The lack of peaks other than those due to WF_6, WSF_4 and XeF_2 observed in the ^{19}F nmr spectroscopic study (previous section) coupled with the intense red-brown colour of the solutions investigated prompted speculation that a paramagnetic species such as a radical cation of sulphur was present in the solutions of WSF_4 and XeF_2 in SO_2ClF.

In light of these factors a low temperature e.s.r. study of a 1:1 mixture of WSF_4 and XeF_2 in SO_2ClF was carried out. The e.s.r. spectra are shown in Figure 24 and the data are recorded in Table 33. Figure 24a shows the e.s.r. spectrum of the red-brown solution frozen at -196°C. This spectrum is similar in many respects to that reported for the radical cation, $S_8^{+\bullet}$, by Chandra et al., (Table 33), g-values of 2.043, 2.031 and 2.004 being obtained (these being characteristic of a non-axially symmetric g-tensor). In addition a second species giving rise to three distinct resonances was detected. The g-values designated as $g\alpha_1$, $g\alpha_2$ and $g\alpha_3$ occur at 2.059, 2.019 and 2.002 respectively and, as yet, this species has not been identified. However, it is worth noting that the values are not characteristic of the radical $XeF^{\bullet}$.[136] After warming the sample to ca. -100°C, followed by quenching to -196°C, the e.s.r. spectrum shows enhancement of the features assigned to $S_8^{+\bullet}$ and diminution of $g\alpha_1$, $g\alpha_2$ with $g\alpha_3$ being lost altogether [Figure 24b]. This tentatively suggests that the species giving rise to the $g\alpha$ values is an intermediate to the formation of the radical cation, $S_8^{+\bullet}$. It has been postulated[137] that this species may be a dimer of the type $RS^{\bullet}\text{-}SR$ (where R is a group containing tungsten and fluorine) which breaks down to yield WF_6 and $S_8^{+\bullet}$, but further e.s.r. studies are required to confirm this.

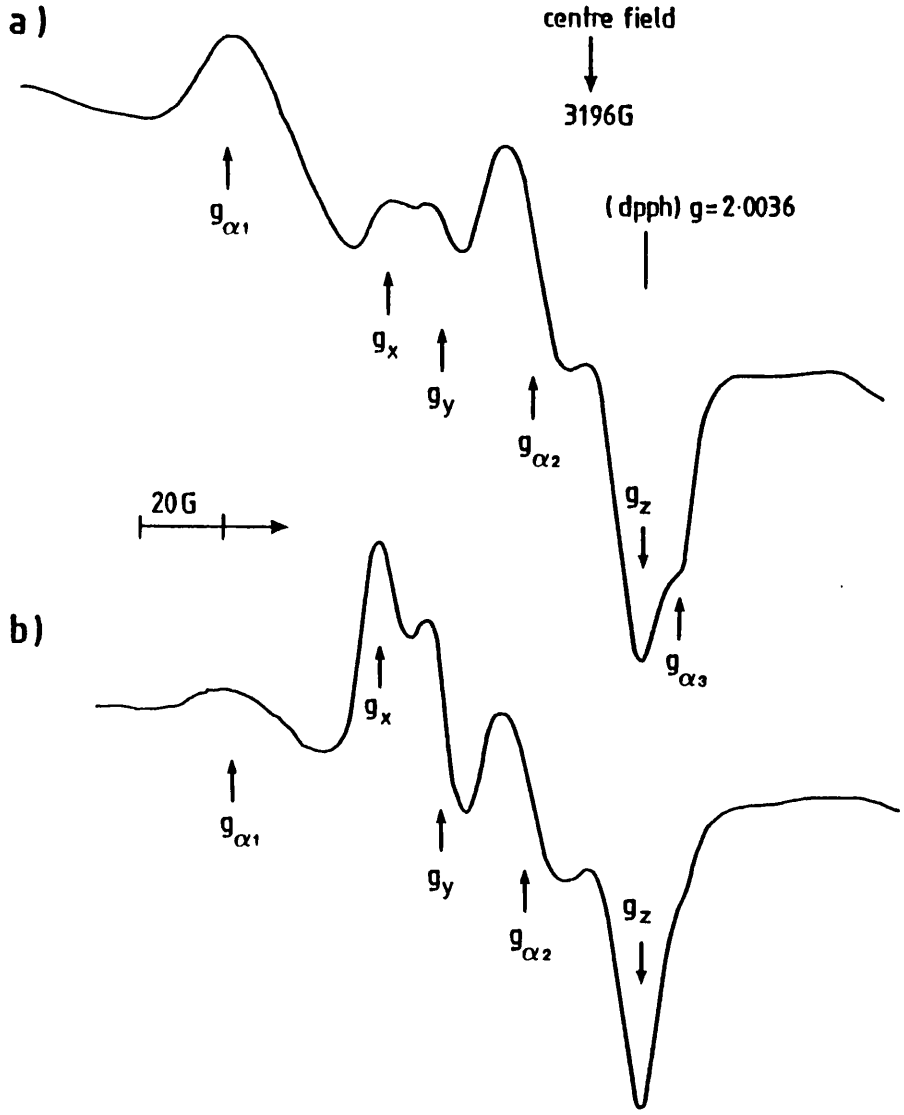

FIGURE 24

E.s.r. spectrum of the red-brown solution;
a) at -196°C,
b) after warming to ca. -100°C, followed by quenching to -196°C.

TABLE 33

ESR spectral data for the reaction of XeF_2 with WSF_4 (1:1) in SO_2ClF

Species	g-value	Method of preparation	Reference
$S_8^{+\bullet}$	$g_x = 2.044$; $g_y = 2.034$; $g_z = 2.0035$	exposure of S_8 in $CFCl_3$ to ^{60}Co γ-rays at 77 K	135
$S_8^{+\bullet}$	$g_x = 2.043$; $g_y = 2.031$; $g_z = 2.0040$	low temperature reaction of WSF_4 with XeF_2 (1:1) in SO_2ClF	This work
?	$g\alpha_1 = 2.059$; $g\alpha_2 = 2.019$; $g\alpha_3 = 2.002$		

6.5 THE REACTION OF WSF_4 WITH XeF_2 IN ANHYDROUS HF

Preliminary investigations into the reaction of XeF_2 with WSF_4 (1:1) in anhydrous HF solvent have shown that a red-orange material can be isolated at temperatures below -78°C. This decomposes when warmed to ca. -30°C to yield WF_6, fluorides of sulphur and Xe which were identified by gas-phase infra-red and mass spectrometry. In light of the results obtained for the reaction between WSF_4 and XeF_2 in SO_2ClF it appears likely that the red-orange material contains the radical cation, $S_8^{+\bullet}$.

6.6 CONCLUSION

This study shows that the reaction of WSF_4 with XeF_2 in either the solid state or in solution in SO_2ClF, does not yield either the adducts $XeF_2.nWSF_4$, n = 1 or 2, or the fluorination product, F_4WSF_2. In the case of the solid state reaction only WF_6 and fluorides of sulphur are formed. However, in SO_2ClF at low temperatures, in addition to the formation of WF_6, the radical cation, $S_8^{+\bullet}$, is formed. The red-orange material from the reaction of XeF_2 with WSF_4 in anhydrous HF has not been fully characterised, but on the basis of the evidence obtained from the reaction in SO_2ClF, it is likely that the radical cation, $S_8^{+\bullet}$, is formed.

It may be interesting to investigate the synthesis of the adducts $XeF_2.nWSF_4$, n = 1 or 2, via more indirect methods, viz. the interaction of either $Cs^+[WSF_5]^-$ or $Cs^+[W_2S_2F_9]^-$ with $XeF_2.SbF_5$ in SbF_5. This should yield $Cs^+[Sb_2F_{11}]^-$ and $XeF_2.nWSF_4$, n = 1 or 2.

CHAPTER 7

The Determination of the Standard Enthalpy of Formation of Tungsten Thiotetrafluoride *via* Hydrolysis in Alkaline Media

7.1 INTRODUCTION

It is generally impossible to measure enthalpies of formation of ternary compounds by direct combination of the elements. However, it is possible to make determinations via enthalpies of hydrolysis. This has been successfully demonstrated by the hydrolysis of WOF_4,[138] $MoOF_4$[138] and MoO_2F_2[139] in alkaline media, e.g.,

$$WOF_{4(s)} + 6[OH]^-_{(aq)} \longrightarrow [WO_4]^{2-}_{(aq)} + 4F^-_{(aq)} + 3H_2O_{(liq)}.$$

Thus by measuring the enthalpy of hydrolysis of the reaction and using the standard enthalpies of formation of $[OH]^-_{(aq)}$, $[WO_4]^{2-}_{(aq)}$, $F^-_{(aq)}$ and $H_2O_{(liq)}$, the standard enthalpy of formation of $WOF_{4(s)}$ can be estimated.

Mass spectrometry and gas transport measurements allow a more indirect method for estimation of enthalpies of formation, but these have been shown to yield results which are inconsistent with the more direct method of determination via alkaline hydrolysis.

7.2 PRESENT STUDY

Although the standard enthalpy of formation of $WSF_{4(s)}$ has been determined by mass spectrometric methods,[140] a value obtained via alkaline hydrolysis has not been reported.

In this study, the alkaline hydrolysis of WSF_4 has been investigated and a value for the enthalpy of hydrolysis obtained. From this result the standard enthalpy of formation of $WSF_{4(s)}$ has been determined.

$\Delta H_f^\ominus WSF_{4(s)}$ -1150.56 ± 5.39 kJ mol^{-1}.

7.3 DETERMINATION OF THE ENTHALPY OF HYDROLYSIS OF WSF_4 IN ALKALINE MEDIA

The enthalpy of hydrolysis of WSF_4 in alkaline media was determined using an L.K.B 8700 calorimeter equipped with a Wheatstone bridge circuit

which incorporated a Kipp Zonen BD5 recorder. Full experimental details are given in Appendix 1.

7.3.1 Preparation of WSF_4

Tungsten thiotetrafluoride, WSF_4, was prepared by the reaction of WF_6 with ZnS in an equimolar stoichiometry.[35] In a typical preparation 'Puratronic' ZnS (3.5 mmole) was introduced into a preseasoned stainless steel reactor in the dry box. The reactor and contents were then subject to dynamic vacuum ($<4 \times 10^{-5}$ mmHg) for at least four hours, after which a 10% excess of WF_6 was added by distillation into the reactor at -196°C. The reactor was heated to ca. 300°C for 10 hours. After opening in the dry box, long yellow needle crystals of WSF_4 were collected from the top of the reactor. Because of the light sensitive nature of WSF_4,[27] the crystals were stored in a foil-wrapped preseasoned Teflon FEP tube.

The purity of WSF_4 was monitored by X-ray powder diffraction, ^{19}F nmr and infra-red spectroscopy. These showed the purity of the sulphide to be in excess of 99%.

7.3.2 Enthalpy of hydrolysis measurements

The enthalpy of hydrolysis of WSF_4 has been measured using the procedure described in Appendix 1. The calorific measurements were carried out on 11 samples of WSF_4, from 4 separate preparations, each being hydrolysed in an excess of sodium hydroxide solution (0.1-0.5 M). The results are recorded in Table 34.

The mean value of the enthalpy of hydrolysis was calculated as -528.23 ± 5.39 kJ mol^{-1}; the error limits cited represent the 90% confidence limits of this mean.[141]

TABLE 34

Enthalpy of hydrolysis of tungsten thiotetrafluoride

Set Number	Sample Number	Mass of Sample [$\times 10^{-3}$ g]	Hydrolysing Agent [$NaOH_{(aq)}$]	Enthalpy of Hydrolysis [-kJ mol^{-1}]
1	1	49.2	90 ml. 0.1 M	539.87
	2	73.8	" "	519.16
2	3	46.8	" "	521.67
	4	42.0	" "	529.29
	5	31.0	" "	533.80
3	6	57.4	90 ml. 0.2 M	520.04
	7	28.2	" "	547.88
	8	42.2	" "	539.07
4	9	122.5	90 ml. 0.5 M	520.01
	10	73.7	" "	518.04
	11	43.1	90 ml. 0.1 M	521.78

Enthalpy of hydrolysis of WSF_4 *(solid)* $= -528.23 \pm 5.39$ *kJ* mol^{-1}.

7.4 CALCULATION OF THE STANDARD ENTHALPY OF FORMATION OF $WSF_{4(s)}$

The standard enthalpy of formation of $WSF_{4(s)}$ has been determined by assuming the reaction of hydrolysis of WSF_4 in an excess of sodium hydroxide solution proceeds according to Scheme 23 (cf. WOF_4).

$$WSF_{4(s)} + 7[OH]^-_{(aq)} \longrightarrow [WO_4]^{2-}_{(aq)} + 4F^-_{(aq)} + 3H_2O_{(liq)} + [HS]^-_{(aq)}$$

SCHEME 23

The presence of the tungstate anion, $[WO_4]^{2-}_{(aq)}$ in the alkaline media was determined by ultraviolet spectroscopic investigations of solutions immediately after the addition of WSF_4. Absorptions in the ultraviolet spectra particular to the thiotungstate species, $[WO_{4-x}S_x]^{2-}$,[142,143] x = 1-4, were absent.

This Scheme also assumes that the sulphur present in the alkaline media is in the form of $[HS]^-_{(aq)}$. Significant concentrations of $S^{2-}_{(aq)}$ are not anticipated due to the low second dissociation constant of H_2S[144] [Scheme 24].

$$[HS]^-_{(aq)} \rightleftharpoons H^+_{(aq)} + S^{2-}_{(aq)} \quad . \quad pKa,\ 14.15 \pm 0.05$$

SCHEME 24

Thus, knowing the enthalpy of hydrolysis derived assuming Scheme 23 and the standard enthalpies of formation of $[WO_4]^{2-}_{(aq)}$, $F^-_{(aq)}$, $H_2O_{(liq)}$, $[HS]^-_{(aq)}$ and $[OH]^-_{(aq)}$ (Table 35), the value of the standard enthalpy of formation of $WSF_{4(s)}$ can be calculated as -1150.56 ± 5.39 kJ mol^{-1}.

Comparison of the values of the enthalpy of formation of $WSF_{4(s)}$ obtained in this study with that obtained from mass spectroscopic investigations[140] (Table 36), shows the two to differ by ca. 65 kJ mol^{-1}. This difference is not unusual since similar discrepancies in results determined via hydrolysis and mass spectrometric methods have been shown

TABLE 35

The standard enthalpies of formation of $[WO_4]^{2-}(aq)$, $F^-(aq)$, $H_2O(liq)$, $[HS]^-(aq)$ and $[OH]^-(aq)$

Species	Standard enthalpy of formation/-kJ mol^{-1}	Reference
$[WO_4]^{2-}(aq)$	1072.20	145
$F^-(aq)$	335.40	146
$H_2O(liq)$	285.80	147
$[HS]^-(aq)$	17.55	148
$[OH]^-(aq)$	230.00	147

TABLE 36

The standard enthalpies of formation of oxide-fluoride and thio-fluoride compounds of molybdenum(VI) and tungsten(VI)

Compound	Standard enthalpy of formation [-kJ mol^{-1}]	
	Method of Determination	
	Hydrolysis	Mass. spec.
MoO_2F_2	1089[139]	1200[149]
WOF_4	1500[138]	1391[149]
WSF_4	1150[a]	1215[140]

[a] *This work.*

TABLE 37

Standard enthalpies of formation of gaseous W and atomic F and S

Species	Standard enthalpy of formation/kJ mol^{-1}	Reference
W (gas)	845.54	150
F (gas)	78.91	148
S (gas)	278.72	151

to exist for the oxide fluorides WOF_4[138,149] and MoO_2F_2[139,149] (Table 36).

7.5 DISCUSSION

7.5.1 The determination of the tungsten sulphur bond energy in gaseous WSF_4

Comparison of the standard enthalpy of $WOF_{4(s)}$[138] to that of $WSF_{4(s)}$ obtained in this study (Table 36) shows the value for the oxide to be ca. 350 kJ mol^{-1} more negative than that of the sulphide. As the following discussion demonstrates, this difference is a probable consequence of the weaker tungsten-sulphur bond.

Since WSF_4 vapourises to yield a monomeric gas,[38,39] the enthalpy of formation of gaseous WSF_4 (ΔHa) from its respective atoms can be calculated [Scheme 25]. Thus, using the known values of the standard enthalpies of formation of $W_{(g)}$, $S_{(g)}$ and $F_{(g)}$ (Table 37), the enthalpy of sublimation of $WSF_{4(s)}$ (79.8 kJ mol^{-1}[140]) and the standard enthalpy of formation of $WSF_{4(s)}$ (Table 36) a value of -2510.7 kJ mol^{-1} for ΔHa has been determined. If the average tungsten-fluorine bond energy, $\bar{D}(W-F)$, is assumed to be the same as in gaseous WF_6, then a tungsten-sulphur bond energy, $\bar{D}(W-S)$, of 478.7 kJ mol^{-1} in $WSF_{4(g)}$ may be assumed (Table 38). This compares with a value of 440 kJ mol^{-1} in $WS_2F_{2(g)}$.[25] It is interesting to note that the value of $\bar{D}(W-S)$ in $WSF_{4(g)}$ is some 336 kJ mol^{-1} lower in energy than $\bar{D}(W-O)$ in $WOF_{4(g)}$. It is thought that this decrease in tungsten-chalcogen bond energy is the determining factor in the observed difference in the standard enthalpies of formation of $WOF_{4(s)}$ and $WSF_{4(s)}$.

7.5.2 The estimation of the enthalpy of formation of gaseous WS_3

Tungsten trisulphide, WS_3, is a brown, air-sensitive, amorphous solid.[152] It can be conveniently prepared by the thermal decomposition

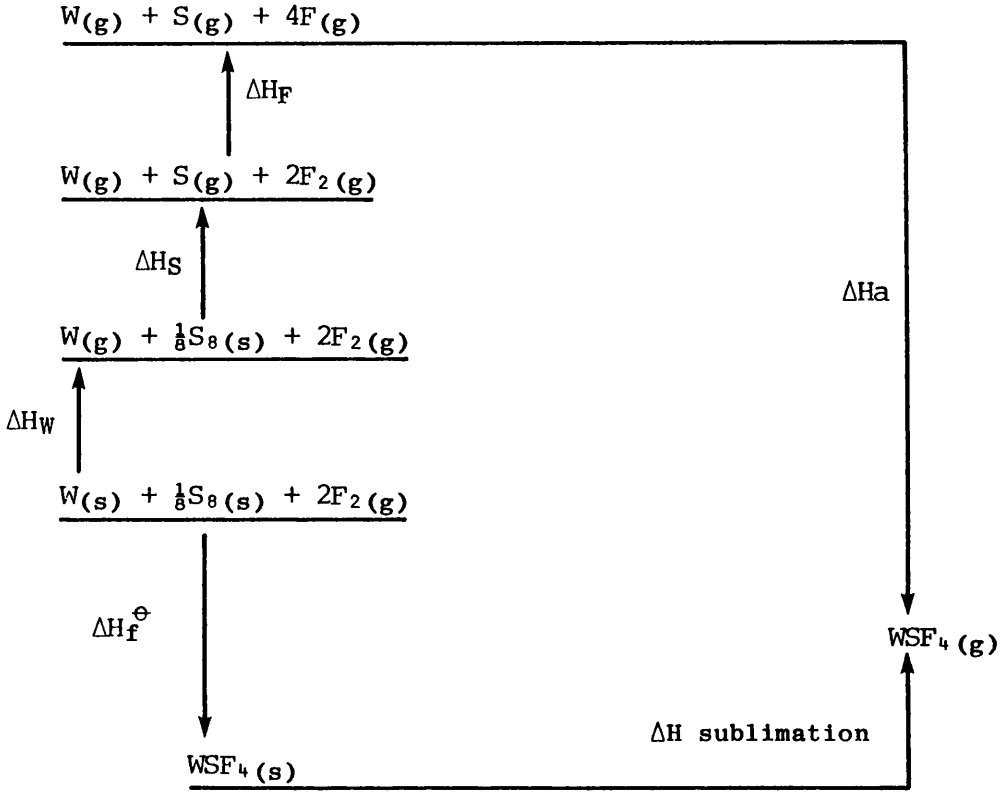

$$\Delta Ha = \Delta H_f^{\ominus} WSF_{4(s)} - \Delta H_W - \Delta H_S - 4\Delta H_F + \Delta H_{sublimation}$$

ΔH_W = Enthalpy of formation of gaseous tungsten;
ΔH_S = Enthalpy of formation of monomeric gaseous sulphur;
ΔH_F = Enthalpy of formation of a fluorine atom.

SCHEME 25

The thermodynamic cycle used to calculate the enthalpy of formation of gaseous WSF_4 from its respective atoms (ΔHa).

TABLE 38

Enthalpies of formation of some tungsten fluoride species from the respective atoms (ΔHa) and average bond dissociation energies ($\bar{D}$) in these molecules

Compound	$-\Delta Ha/kJ\ mol^{-1}$	$\bar{D}(W-F)/kJ\ mol^{-1}$	$\bar{D}(W-X^{b})/kJ\ mol^{-1}$	Reference
WF_6 (gas)	3048.0	508	-	138
WSF_4 (gas)	2510.7[a]	508	478.7	This work
WS_2F_2 (gas)	-	-	440.0	25
WOF_4 (gas)	2846.0	508	815.0	138

[a] *Enthalpy of sublimation = 79.8 kJ mol^{-1}, Reference 140;*
[b] *X = respective chalcogen.*

of $(NH_4)_2WS_4$ at ca. 200°C.[152-154] It has also been reported as a disproportionation product from the reaction of WSF_4 with CH_3CN,[27] but this has not been confirmed. Recent investigations using XPS,[156] IR[155] and EXAFS[154] have shown that WS_3 is structurally similar to MoS_3, and consists of chains that are based on the repeating $W_2(S^{2-})_4(S_2^{2-})$ unit.

Since there is a total absence of reported thermodynamic data concerning WS_3, the values of the enthalpies of formation of $WF_{6(g)}$, $WSF_{4(g)}$ and $WS_2F_{2(g)}$ [Table 39] have been used to predict an approximate value of the standard enthalpy of formation of $WS_{3(g)}$.

Shchukarev et al.[157] have predicted the existence of oxide-halides with enthalpies of formation intermediate between those of the corresponding binary oxide and halide. This is known as the 'substitution principle'. Assuming a similar principle exists for $WF_{6(g)}$, $WSF_{4(g)}$ and $WS_2F_{2(g)}$, an approximate value for the standard enthalpy of formation of $WS_{3(g)}$ can be estimated. Thus, by correlation of the standard enthalpies of formation of $WF_{6(g)}$, $WSF_{4(g)}$ and $WS_2F_{2(g)}$ [Table 39] as a function of the number of sulphur atoms in each compound [Figure 25] an approximate value for the standard enthalpy of formation of $WS_{3(g)}$ has been predicted: $\Delta H_f^{\ominus} WS_{3(g)} \sim 380$ kJ mol^{-1}. It should be noted that the values of $WSF_{4(g)}$ and $WS_2F_{2(g)}$ have been positioned below the assumed line joining $WS_{3(g)}$ and $WF_{6(g)}$ in Figure 25, otherwise instability of the thio-fluorides is implied.

Comparing the standard enthalpies of formation of $WS_{3(g)}$ and $WO_{3(g)}$ [Table 39] shows the value for the oxide to be ~672 kJ mol^{-1} more negative than that of the sulphide. It is interesting to note that if, like WO_3,[151] the enthalpy for the process $WS_{3(s)} \longrightarrow WS_{3(g)}$ is large and positive, then it is reasonable to assume that the standard enthalpy

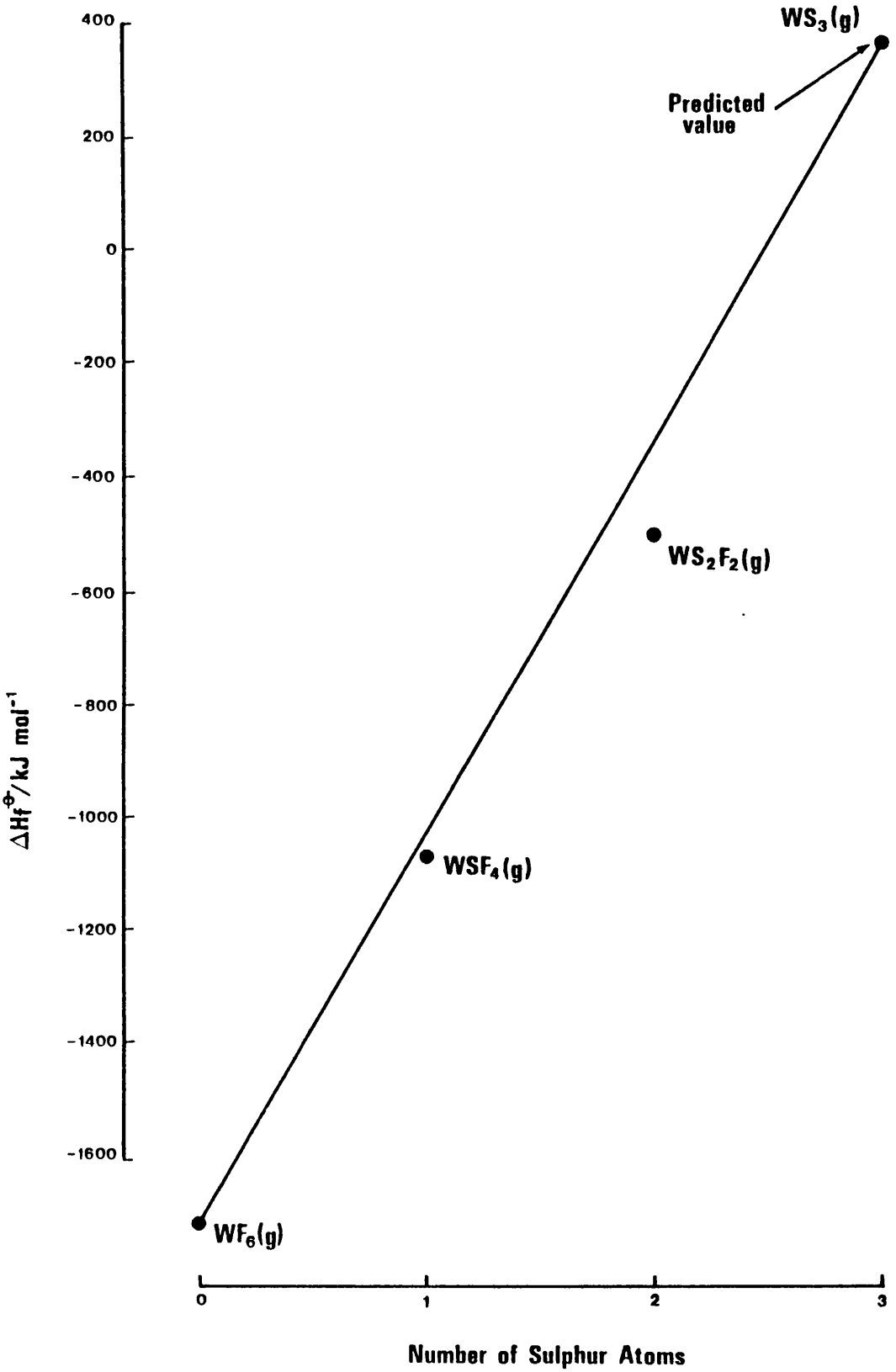

FIGURE 25

The correlation between the standard enthalpies of formation of $WF_{6(g)}$, $WSF_{4(g)}$ and $WS_2F_{2(g)}$ and their composition used to predict the standard enthalpy of formation of $WS_{3(g)}$.

TABLE 39

The standard enthalpies of formation of the gaseous compounds WS_nF_{6-2n} and WO_3

Compound	Standard enthalpy of formation/kJ mol^{-1}	Reference
WF_6 (gas)	-1723	138
WSF_4 (gas)	-1071.7[a]	This work
WS_2F_2 (gas)	-496.8	25
WS_3 (gas)	~380	This work
WO_3 (gas)	-292.6	151

[a] *Enthalpy of sublimation = 79.8 kJ mol^{-1}, Ref. 140.*

of formation of $WS_{3(s)}$ will be negative. However, further thermodynamic studies of WS_3 are required to confirm this.

Using the estimated value of the standard enthalpy of formation of $WS_{3(g)}$, the stability of $WSF_{4(g)}$ with respect to decomposition to $WS_{3(g)}$ and $WF_{6(g)}$ can be demonstrated [Scheme 26].

$$WSF_{4(g)} \longrightarrow \tfrac{2}{3}\,WF_{6(g)} + \tfrac{1}{3}\,WS_{3(g)}$$

SCHEME 26

From the thermodynamic data in Table 39, reaction Scheme 26 can be predicted to have an enthalpy change of ~48 kJ mol^{-1}. Thus assuming small entropy changes for this process, the decomposition reaction of $WSF_{4(g)}$ set out in Scheme 26 is not thermodynamically favourable. This prediction is in line with the fact that $WSF_{4(s)}$ can be readily sublimed and vapourised at temperatures in the region of 150°C without significant decomposition.[27,38,39] However, it should be noted that in CH_3CN, WSF_4 slowly reacts to yield WF_6 and what is thought to be WS_3.[27]

It is interesting to compare the decomposition reaction of $WSF_{4(g)}$ in Scheme 26 to that of Scheme 27.

$$WSF_{4(g)} \longrightarrow \tfrac{1}{2}WS_2F_{2(g)} + \tfrac{1}{2}WF_{6(g)}$$

SCHEME 27

From the thermodynamic data in Table 39, the enthalpy change for this process can be determined as -38.2 kJ mol^{-1}. This suggests that $WSF_{4(g)}$ should decompose to $WS_2F_{2(g)}$ and $WF_{6(g)}$. However, in light of the fact that WSF_4 is prepared at temperatures in excess of 300°C, the Gibbs free energy for this process must be positive.

7.6 CONCLUSION

This study has produced the first example of the standard enthalpy of formation of a transition metal thiofluoride derived via the alkaline hydrolysis method. The value obtained for WSF_4 has been used in conjunction with previously known thermodynamic data to estimate the tungsten-sulphur bond energy in $WSF_{4(g)}$. This has been shown to be some 336 kJ mol^{-1} less than the tungsten oxide bond in $WOF_{4(g)}$.

This study has also produced the first estimate for the standard enthalpy of formation of $WS_{3(g)}$, but due to the method of determination this is likely to contain a large amount of uncertainty. Assuming that like WO_3, the enthalpy change for the process $WS_{3(s)} \longrightarrow WS_{3(g)}$ is large and positive, it has been suggested that the enthalpy of formation of $WS_{3(s)}$ is likely to be negative. Thus, an obvious route for further investigation would be the determination of the enthalpy of formation of $WS_{3(s)}$. This may be achieved via the method of alkaline hydrolysis discussed in this study.

It would be interesting to extend this investigation to include WS_2F_2, $WSeF_4$ and the thio-fluorides of rhenium, $ReSF_5$ and $ReSF_4$. It is anticipated that the alkaline media used to hydrolyse $ReSF_4$ may require the presence of an oxidising agent such as hypochlorite. This

would convert any $ReO_{2(aq)}$ formed during hydrolysis to ReO_4^-.

It may also be interesting to investigate the fluoride-ion affinity of WSF_4. Since the salts $M^+[WSF_5]^-$, M = Rb or Cs, are known [Chapter 3] the enthalpies of hydrolysis could be calculated. Unfortunately, lattice enthalpy calculations are required, and at present it is impossible to carry out such calculations for the mixed anions of the type $[WSF_5]^-$.

CHAPTER 8

Experimental Techniques

8.1 GENERAL PREPARATIVE TECHNIQUES

Many of the starting materials used and the majority of the compounds prepared and studied are sensitive to air or moisture and require handling either *in vacuo* or inert atmospheres to prevent decomposition. Metal, glass or fluoroplastic containers provide vessels for reactions and storage. Metal reactors were baked, pumped to 10^{-4} mmHg, hydrogenated, seasoned with fluorine and re-evacuated before use. All glass and fluoroplastic apparatus was pumped to 5×10^{-4} mmHg with heating, seasoned with fluorine or chlorine trifluoride, and pumped to high vacuum.

Volatile air sensitive materials were transferred in metal or glass vacuum systems using either static vacuum conditions with a suitable temperature gradient, or dynamic vacuum. Non-volatile materials were manipulated under a dry nitrogen atmosphere in an auto-recirculating positive pressure dry box [Vacuum Atmospheres Co., VAC NE 42-2 Dri-lab]. The atmosphere of the box is circulated through columns of manganese oxide and molecular sieve to remove oxygen and water. The impurity levels were monitored by a Hersch oxygen meter [Mk II/L] and Elliot moisture meter [model 112]. When transferring or weighing small quantities of powders, in the dry box, static electricity caused difficulties. This problem was alleviated by exposing samples and apparatus to a 4 mCi ^{210}Po α-emitter [type PDV 1, Radiochemical Centre, Amersham, Bucks.]. Weighings accurate to ±0.1 mg were performed in the dry box with a Sartorious balance [model 1601 MP8]. Powdered solids were weighed in small glass weighing boats prior to loading into the reaction vessels. Weighings for mass balance calculations were carried out on a laboratory balance [Stanton Unimatic CL 41].

Samples not required for immediate use were sealed under vacuum or

an argon atmosphere in glass ampoules or Teflon FEP tubes. Volatile samples were usually stored in glass ampoules fitted with break seals. Thermally unstable samples were stored at -196°C in a cryostat [British Oxygen Co. Ltd.] or at -78°C in solid carbon dioxide.

8.2 VACUUM SYSTEMS AND REACTION VESSELS

Vacuum line methods were used to prepare all the compounds studied. A metal manifold with high and low vacuum facilities formed the basic system [Figure 26]. This was constructed from ⅜" o.d., ⅛" i.d. nickel tubing [H. Wiggin & Co., Hereford] and argon welded nickel "U" traps (~25 cm^3 capacity). The manifold was completed with AE-30 series hard drawn stainless steel needle valves, crosses and "T"s [Autoclave Engineers Inc., Erie, Pennsylvania, USA].

The low vacuum system (10^{-2} mmHg) consisted of a single-stage rotary pump [model PSR/2, NGN Ltd., Accrington, Lancashire] with a large metal trap charged with soda lime granules (5-10 mesh) between the pump and the manifold. The function of this chemical trap was to remove fluorine and volatile fluorides exhausted from the manifold. The low vacuum system served to remove large quantities of gases before opening the manifold to the high vacuum system. The main system vacuum (10^{-4} mmHg) was maintained by a single or double stage rotary pump [Genevac type GRS2 or GRD2, General Engineering Co., Radcliffe, Lancashire], mercury diffusion pump and -196°C cold trap. Facilities for admission of argon and hydrogen, directly into the manifold from cylinders, were provided and fluorine for seasoning apparatus was introduced to the lines from welded nickel cans (1 dm^3 capacity) fitted with AE-30 stainless steel needle valves.

Manifold pressures of plus or minus one atmosphere (0-1500 mmHg ± 5 mmHg) were measured using a stainless steel Bourdon-tube gauge [Type

C - Stainless steel cross
G - Bourdon tube gauge
N - Nickel "U" trap
T - Stainless steel "T"
V - Stainless steel needle valve

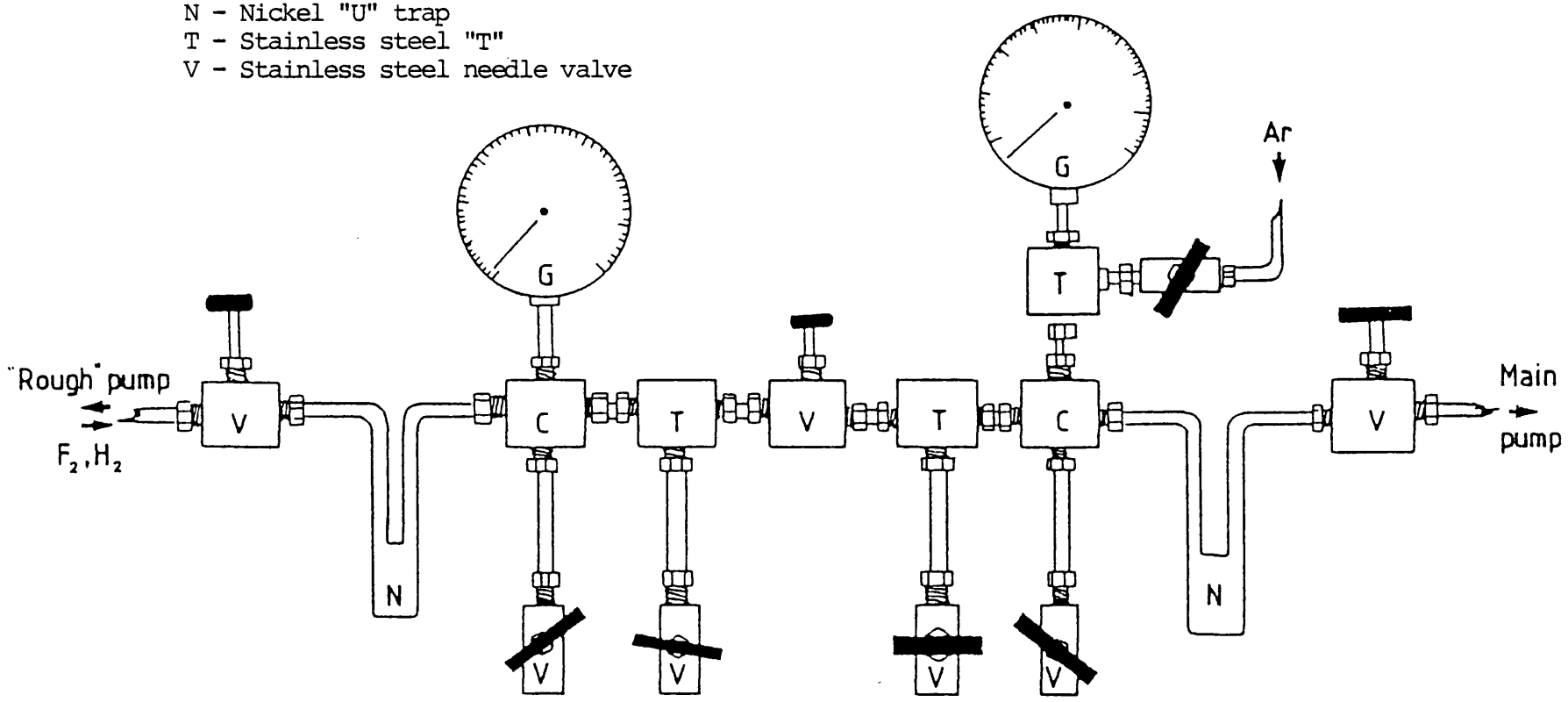

FIGURE 26

The Basic High Vacuum Manifold.

1F/66Z, Budenberg Gauge Co. Ltd., Broadheath, Greater Manchester]. The vacuum was monitored using a cold-cathode Penning ionisation gauge [Model 2A, Edwards High Vacuum Ltd., Crawley, West Sussex], capable of measuring pressures in the range 10^{-2} to 10^{-6} mmHg.

Leaks in the vacuum manifold and in the constructed reaction systems were located with a helium leak detector [Edwards High Vacuum Ltd., mass spectrometer Model LT 104].

A variety of metal, fluoroplastic, Pyrex or silica reaction vessels could be attached to the vacuum line. Glass reaction systems were designed and fabricated as required and were attached to the manifold by precision ¼" o.d. glass connected to ¼" o.d. stainless steel tubing (manifold outlet) with ChemCon Teflon connectors [Type STD/4 E1P, Production Techniques Ltd., Fleet, Hampshire] using Teflon compression unions. Greaseless glass valves [Quickfit 'Rotaflo' type TF2/13 and TF6/13 or J. Young, Scientific Glassware Ltd., Acton, London] fitted with Teflon stems were used where glass systems were employed or, alternatively, glass reaction vessels were fitted with ChemCon Teflon needle valves [Type STD/VC 4/P].

Small fluoroplastic reactors were fabricated by heating and moulding either 6 mm o.d. Kel-F tubing [Voltalef Paris] or ¼" o.d. Teflon FEP tubing [Trimflex Corporation, USA]. These reactors were fitted with ChemCon Teflon needle valves by ¼" o.d. compression unions [Plate 1C or E]. Larger reactors of ¾" o.d. Kel-F with approximately 30 cm^3 volume [obtained from Argonne National Laboratory] were fitted with ChemCon Teflon needle valves <u>via</u> a stem fabricated from a Teflon FEP block [Trimflex Corporation, USA], [Plate 1D].

Stainless steel reactors of approximately 30 cm^3 volume, employed in thermal reactions, were fitted with gold seals and closed with an

AE-30 series stainless steel needle valve [Figure 27].

8.3 APPARATUS FOR THE MANIPULATION OF ANHYDROUS HF AND NOF

Reactions involving the use of anhydrous HF or NOF were conducted using an all fluoroplastic 'parasite' vacuum line [Plate 1 and 2]. This was constructed from short lengths of ¼" o.d. Teflon FEP tubing, flared at one end, which were fitted to a Kel-F "Y" piece [Plate 2]. The line was completed by ChemCon Teflon needle valves D, (which was fitted to a ¾" Kel-F storage tube), E, (which was fitted to either a ¼" o.d. Teflon FEP reactor tube or a 4 mm o.d. Kel-F n.m.r. tube) and B. The line was attached to the main vacuum manifold, (stainless steel needle valve A), via ⅜" o.d., ⅛" i.d. nickel tubing, a stainless steel elbow and 'T' and ¼" o.d. tubing. Evacuation of the line was achieved by the coordinated use of the ChemCon Teflon needle valve B and the stainless steel needle valve A. Volatile material exhausted from the line during reaction procedures was collected in the ¼" o.d. Teflon FEP tube fitted to the ChemCon Teflon needle valve C.

8.4 CHARACTERISATION OF PRODUCTS

8.4.1 X-ray powder diffraction

Samples were ground to a fine powder in a dry box and loaded into seasoned glass capillaries. These were sealed temporarily in the dry box using modelling wax [AD International Ltd., Weybridge] and immediately on removal from the dry box sealed using a micro-torch [Model H164/1, Jencons, Hemel Hempstead, Hertfordshire]. Photographs were taken in a Phillips 11.64 cm diameter camera, on a Koldirex KD59T film [Kodak Ltd.]. Nickel filtered Cu-$K\alpha$ radiation (28 Kv, 18 Amps) was used with exposure times of two to five hours.

Plate 1

Fluoroplastic 'Parasite' Vacuum Line

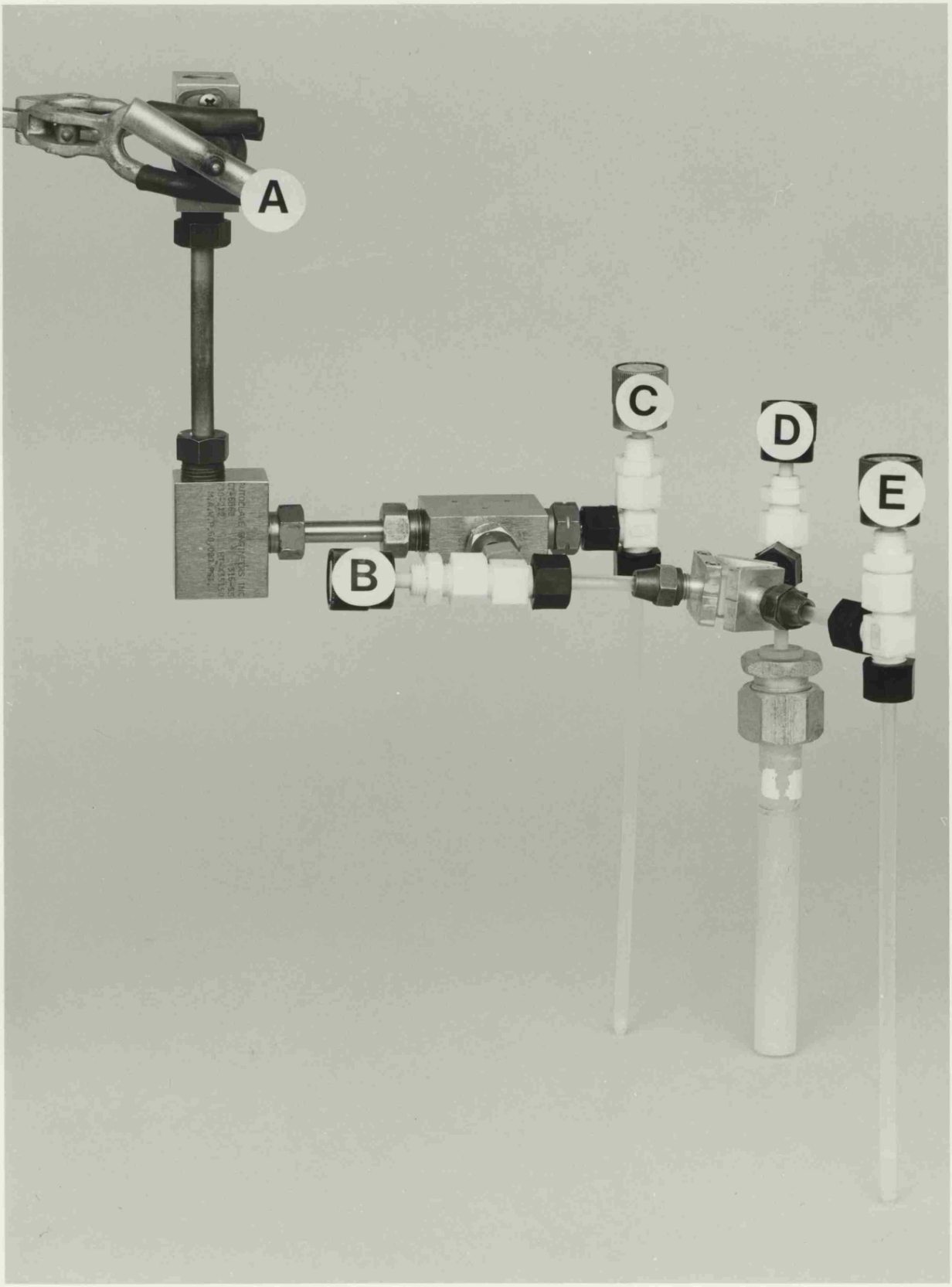
A
B
C
D
E

Plate 2

Plan View of Fluoroplastic 'Parasite' Vacuum Line

D
E
C
B

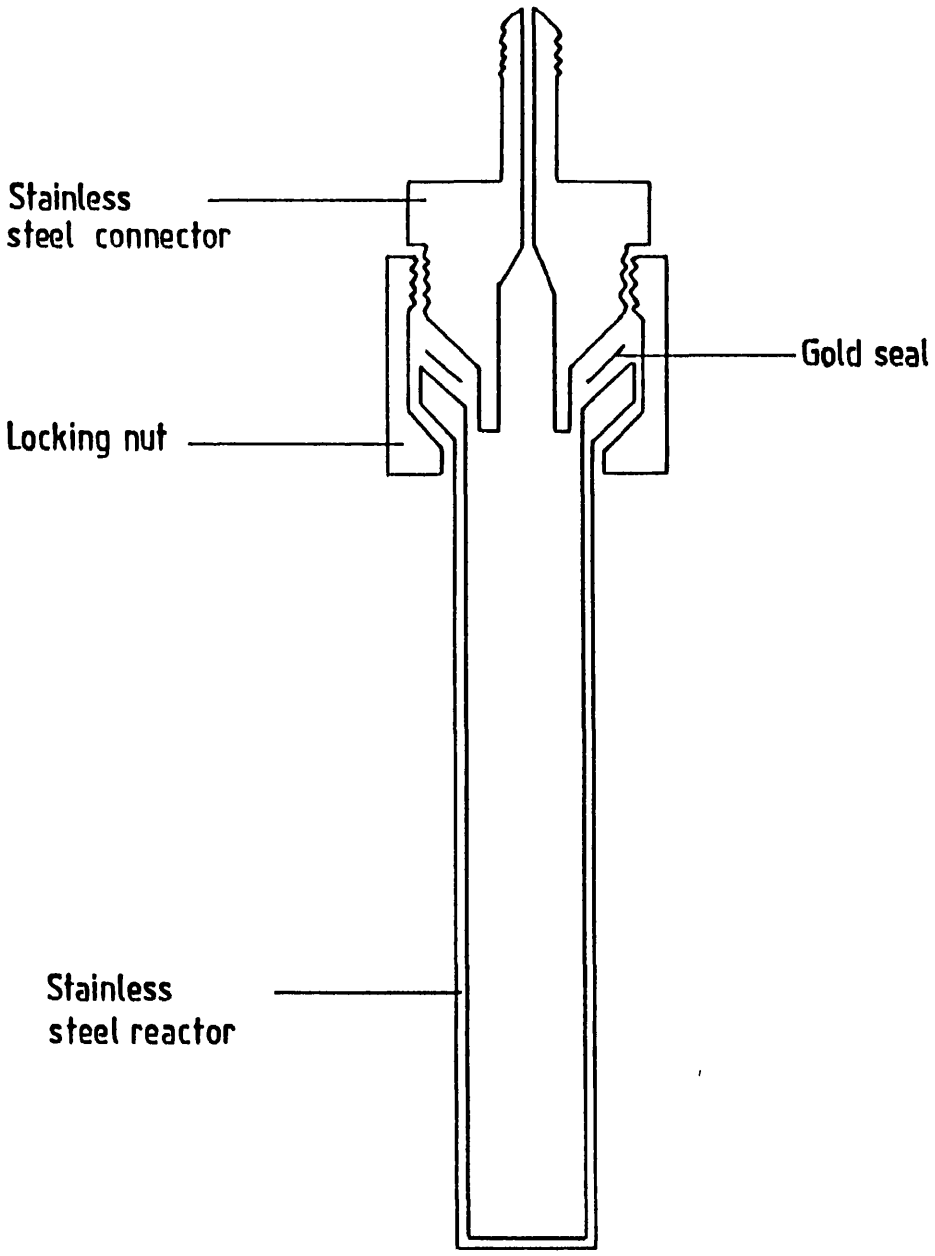

FIGURE 27

Cross-sectional view of a stainless steel reactor.

8.4.2 Infra-red spectroscopy

A Perkin Elmer 580 spectrometer was used to obtain infra-red spectra. Solid samples were run as dry, finely ground powders pressed between discs of KBr (4000-350 cm^{-1}). Gas-phase spectra were obtained using a 10 cm path-length copper cell, closed with AgCl windows (4000-400 cm^{-1}), which could be attached directly to the main vacuum manifold. Teflon gaskets provided an air-tight seal between the windows and the cell body.

8.4.3 Raman spectroscopy

Raman spectra were recorded with a Coderg T800 spectrometer, with either a 250 mW Ar^+ laser [Model 52, Coherent Radiation Laboratories] or a 500 mW Kr^+ laser [Model 164, Spectra Physics Inc.]. The Ar^+ laser provided 5145 Å (green) and 4880 Å (blue) radiation, and the Kr^+ laser gave 6471 Å (red) radiation. Solid samples were contained in Pyrex capillaries. Samples likely to be decomposed by the beam were cooled in a stream of cold nitrogen gas. The capillaries were secured in an evacuated double-walled Pyrex jacket [Figure 28]. Temperatures in the range 0 to -120°C could be maintained by the nitrogen stream generated from a 25 litre Dewar vessel of liquid nitrogen fitted with a controlled heat source. A copper-constantan thermocouple [Model 1623, Comark Electronics Ltd., Littlehampton, Sussex] recorded the temperature.

8.4.4 Nuclear magnetic resonance spectroscopy

^{19}F nmr spectra were recorded on a Jeol JNM-PS-100 instrument [Leicester University] operating at 94.08 MHz. All samples were prepared in preseasoned 4 mm o.d. Kel-F nmr tubes [Voltalef-Paris] which were fitted to ChemCon needle valves by $^3/_{16}$" o.d. compression unions. This was achieved by fitting the Kel-F nmr tubes with short collars of $^3/_{16}$" o.d. Teflon FEP tubing [Plate 3, sequence A to C]. Heat

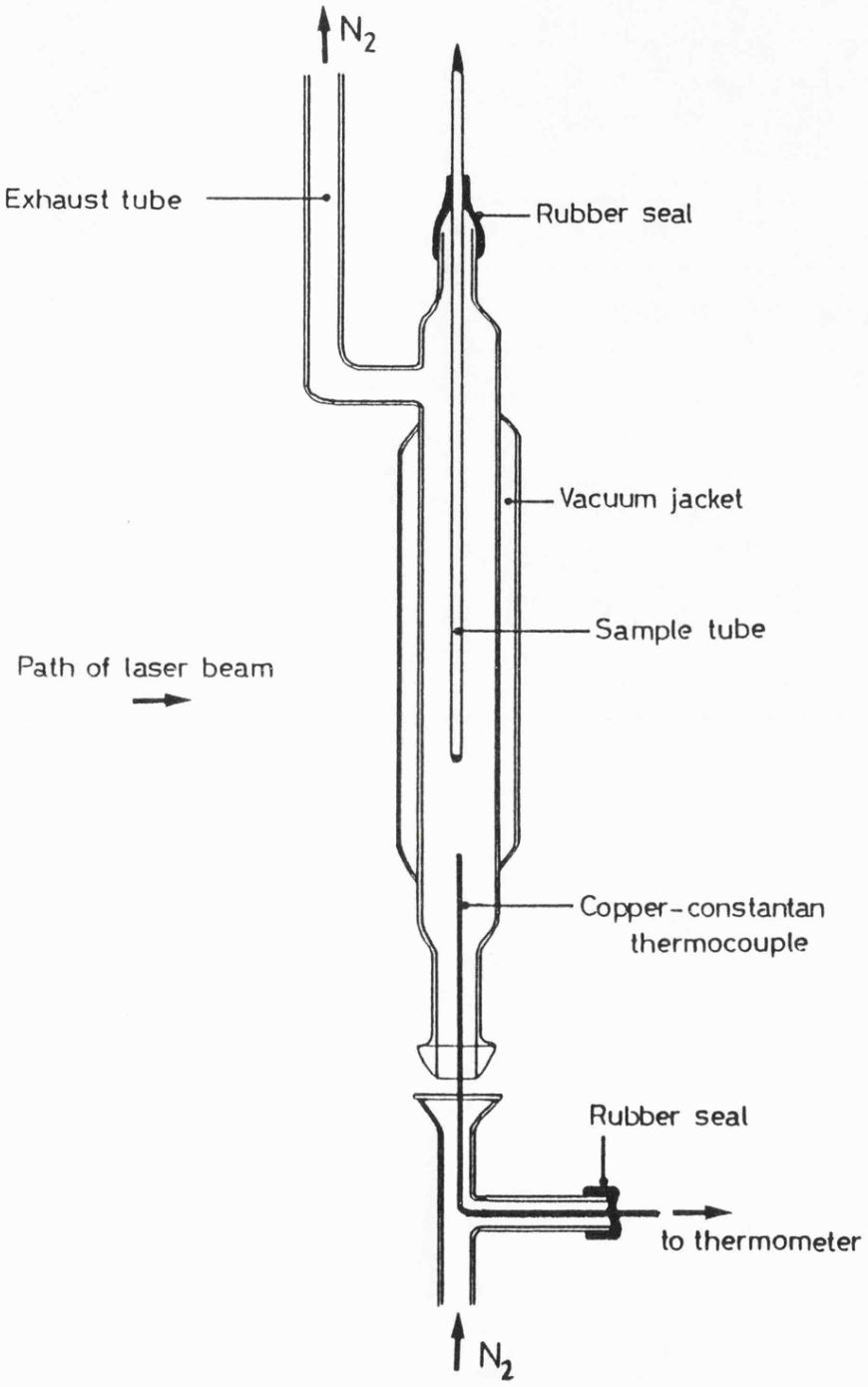

FIGURE 28

Low-Temperature Raman Apparatus.

Plate 3

4 mm o.d. Kel-F NMR Tube connected to
a $^{3}/_{16}$" Compression Union

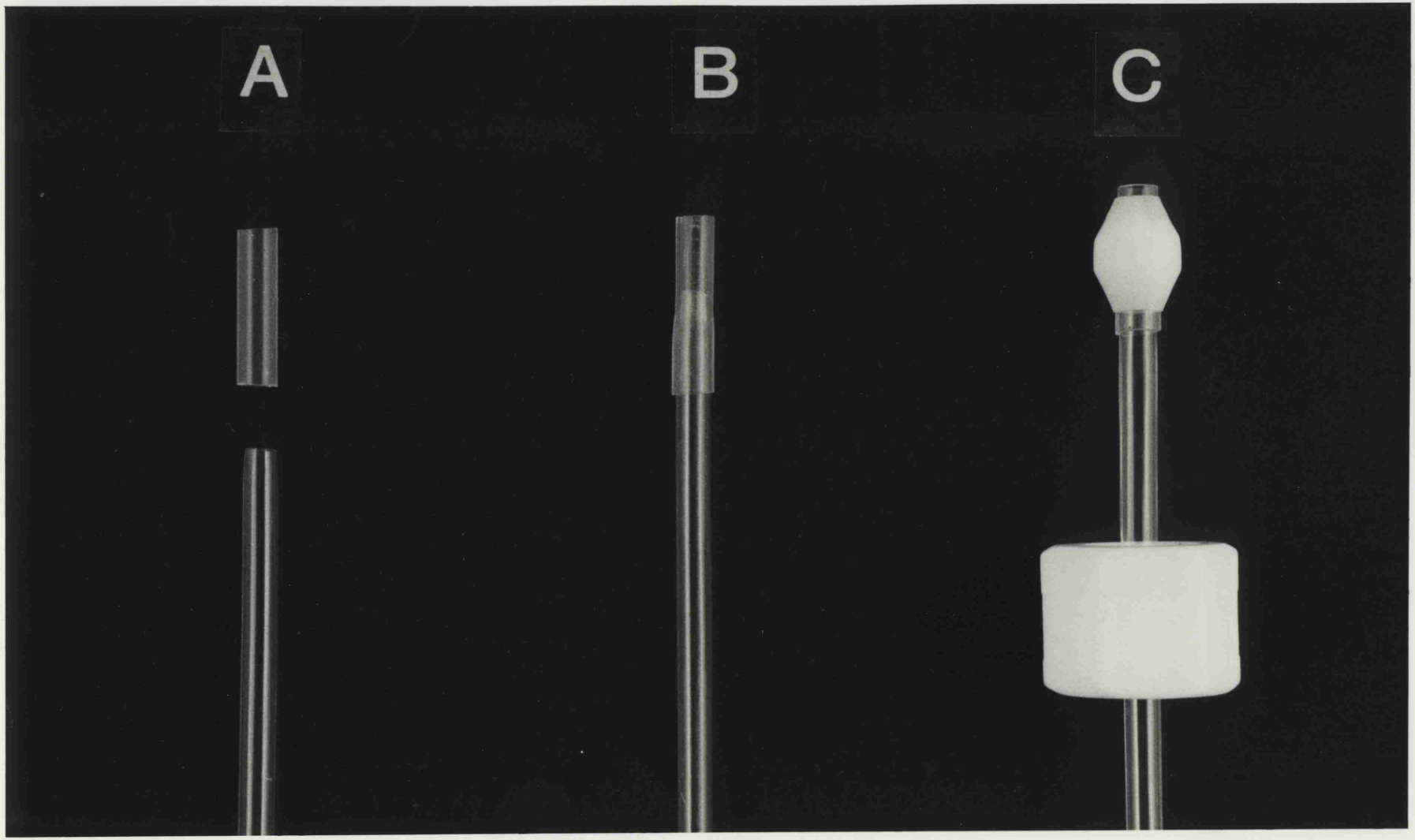
A
B
C

sealed tubes containing the samples were inserted into a 5 mm o.d. precision glass nmr tube [Aldrich Chemical Co. Ltd.] which, in turn, was inserted into a spinning turbine. Low-temperatures (probe temperature 0 to -130°C) were obtained by cooling the spinning sample with a stream of cold, dry nitrogen from a 5 litre Dewar vessel of liquid nitrogen. The temperature was recorded with an electric thermometer [model 1623, Comark]. Spectra were calibrated using $CFCl_3$ as an external standard.

Spectra were also recorded on a Bruker AM 300 Fourier Transform nmr spectrometer, operating at 282.4 MHz [Leicester University] and a Bruker WP80 Fourier Transform nmr spectrometer, operating at 74.8 MHz [Edinburgh University]. Samples were 'locked' internally using CD_3CN or a mixture of $(CD_3)C{=}O$ and $(C_2D_5)_2O$ which was contained in the capillary space between the Kel-F nmr tube and precision glass nmr tube.

Simulated nmr spectra were obtained by the computer programme PANIC.

8.4.5 Electron spin resonance

Electron spin resonance spectra were recorded on a Varian E-109 spectrometer calibrated with a Hewlett-Packard 5246L frequency counter and a Bruker B-H12 field probe, which were standardised with a sample of diphenylpicrylhydrazyl (dpph). The samples were contained in a heat sealed 4 mm o.d. Kel F nmr tube.

8.4.6 Mass spectrometry

Mass spectra were recorded on a V.G. Micromass 16B instrument, the sample being introduced directly into the ionising chamber. In order to minimise decomposition of the sample during passage through the mass spectrometer, the entire system was pre-seasoned by flushing with small amounts of fluorine.

8.4.7 Elemental analysis

All elemental microanalyses were performed by C.H.N. Analysis Ltd., South Wigston, Leicester. The analytical samples were loaded into seasoned glass or Teflon FEP tubes in the dry box. The sample tubes were then evacuated on the manifold and sealed under vacuum.

8.5 CHEMICALS, SOURCES AND PURIFICATION PROCEDURES

8.5.1 Starting materials

Fluorine [Matheson Gas Products]; for reactions on the manifold was used without purification from a cylinder (½ lb., 99.8%). For safety and convenience the gas was transferred to welded nickel cans (~1 dm^3 capacity).

Chlorine trifluoride [Fluorochem Ltd.] for seasoning was used without purification from a cylinder.

Tantalum [BDH Ltd.], osmium and iridium [Johnson Matthey Spec. Pure Grade]; the powdered metals were reduced at red heat in a stream of hydrogen before use.

Xenon [British Oxygen Company Ltd.] was used without purification from a cylinder.

Zinc sulphide, ZnS, [Johnson Matthey, Puratronic], antimony sulphide, Sb_2S_3, [BDH Ltd., Technical Grade], boron sulphide, B_2S_3, [Ventron GmbH] and boron oxide, B_2O_3, [Aldrich Chemical Co. Ltd.] were stored in a dry box and degassed before use.

Lithium fluoride [BDH Ltd., Extra-Pure], sodium fluoride [Hopkins and Williams Ltd.], potassium fluoride [BDH Ltd., 'Anhydrous'], rubidium fluoride [Aldrich Chemical Co. Ltd., Gold Label 99.9%+] and caesium fluoride [Aldrich Chemical Co. Ltd., 99%] were heated to 400°C in a

stainless steel reactor under dynamic vacuum (~10^{-4} mmHg) for 12 hours to remove traces of water and hydrogen fluoride. The fluorides were transferred to a dry box and stored in ¼" Teflon FEP tubes fitted with Teflon stoppers.

Tungsten hexafluoride [Allied Chemicals Ltd.] was vacuum distilled from a cylinder and stored over sodium fluoride in a ¾" o.d. Kel-F tube.

Hydrogen sulphide [ARGO International Ltd., Essex] and sulphur tetrafluoride [PCR Inc., Gainsville, Florida, USA] were used without purification from a cylinder.

Nitric oxide [British Oxygen Company Ltd.] was vacuum distilled, from a cylinder, through a Kel-F "U" trap maintained at -160°C and stored in a ¾" o.d. Kel-F tube. This process is discussed in Chapter 4.

8.5.2 Solvents

Anhydrous acetonitrile [BDH Ltd., special for spectroscopy] was repeatedly distilled onto, and over, phosphorous pentoxide. It was then distilled into glass ampoules containing a molecular sieve [type 3A] which had been dried at 350°C for 12 hours under dynamic vacuum (<10^{-4} mmHg).

Anhydrous hydrogen fluoride [BDH Ltd., 99.8%] was vacuum distilled from a cylinder into a ¾" o.d. Kel-F reactor tube. To remove traces of moisture, approximately one atmosphere of gaseous fluorine was introduced and the tube judiciously agitated periodically over several days.

Sulphuryl chloride fluoride [Aldrich Chemical Co. Ltd.] was purified by distillation onto mercury at -196°C and allowed to warm slowly to

room temperature with vigorous agitation. The reaction was moderated by cooling in liquid nitrogen. The solvent was then distilled onto antimony pentafluoride and thoroughly mixed at room temperature before distilling onto pre-dried sodium fluoride. After standing over the sodium fluoride for several hours with frequent shaking, the sulphuryl chloride was distilled into a storage vessel.

Sulphur dioxide [Aldrich Chemical Co.] was vacuum distilled from a cylinder into a glass ampoule containing phosphorous pentoxide. This was left standing for several days and was used without further purification.

8.5.3 Synthesised reactants

Tantalum pentafluoride, osmium hexafluoride and iridium hexafluoride were prepared by direct high pressure fluorination of the respective hydrogenated metal in a stainless steel reactor at ca. 300°C. The pentafluoride was purified by vacuum sublimation whereas the hexafluorides were purified by trap-to-trap distillation.

Xenon difluoride was prepared by exposing a xenon/fluorine mixture (~1:1), contained in a spherical, Pyrex reactor (~1 dm^3 capacity), to sunlight for several days. The crystalline solid was purified by vacuum sublimation.

Tungsten thiotetrafluoride was prepared by the thermal reaction of tungsten hexafluoride with zinc sulphide (1:1) in a stainless steel reactor as described in Chapter 7. The yellow crystalline solid was used without further purification.

Tungsten oxidetetrafluoride was prepared by the reaction of tungsten hexafluoride with boron oxide (~5:1 molar ratio) in a stainless steel reactor at 50°C.

Nitrosyl fluoride was prepared according to the method of Faloon and Kenna[80] in which liquid nitric oxide at -160°C is fluorinated with gaseous fluorine. Owing to the refractory nature of the reagents and synthesised product, the preparation is discussed fully in Chapter 4.

APPENDIX

The L.K.B 8700 Calorimeter

i) The L.K.B. 8700 Calorimeter

The L.K.B. 8700 is an example of an isoperibol calorimeter, in which there is a deliberate heat loss which is small and measurable so that it may be accurately accounted for.

The calorimeter itself [Figure 29] consists of a thin walled Pyrex glass reaction vessel of ca. 90 cm^3 volume. This is fitted with a 1000 Ohm resistor (giving good temperature sensitivity over the range 290 to 313 K), a calibration heater (a coil of constantan resistance wire), a sharpened glass rod fused to the bottom of the reaction vessel, a stainless steel stirrer, which also serves as a holder for the cylindrical glass ampoules. The glass vessel is contained in a chromium-plated stainless steel (water tight) case and this is totally submerged in an insulated tank of water maintained at 298.20 K $\pm$ 0.001 K. The wells in which the heater and thermistor are inserted are filled with paraffin oil to give good thermal contact with the contents of the calorimeter. The thermistor [Figure 30] forms one arm of a d.c. wheatstone bridge and any change in its resistance due to change in temperature results in an imbalance in the bridge which is detected by the Kipp-Zonen Micrograph BD5 chart recorder. The sensitivity of the system was such that a temperature change of about 5×10^{-5} K can be detected.

ii) Experimental

The samples of WSF_4 were weighed out into thin-walled ampoules of approximately 1 cm^3 capacity. Prior to use, these had been seasoned with chlorine trifluoride (to remove any traces of moisture on the surface of the glass) and stored in the dry box. Sealing the ampoules was accomplished by using Araldite Rapid glue.

In all these hydrolyses it was necessary to use a large excess of

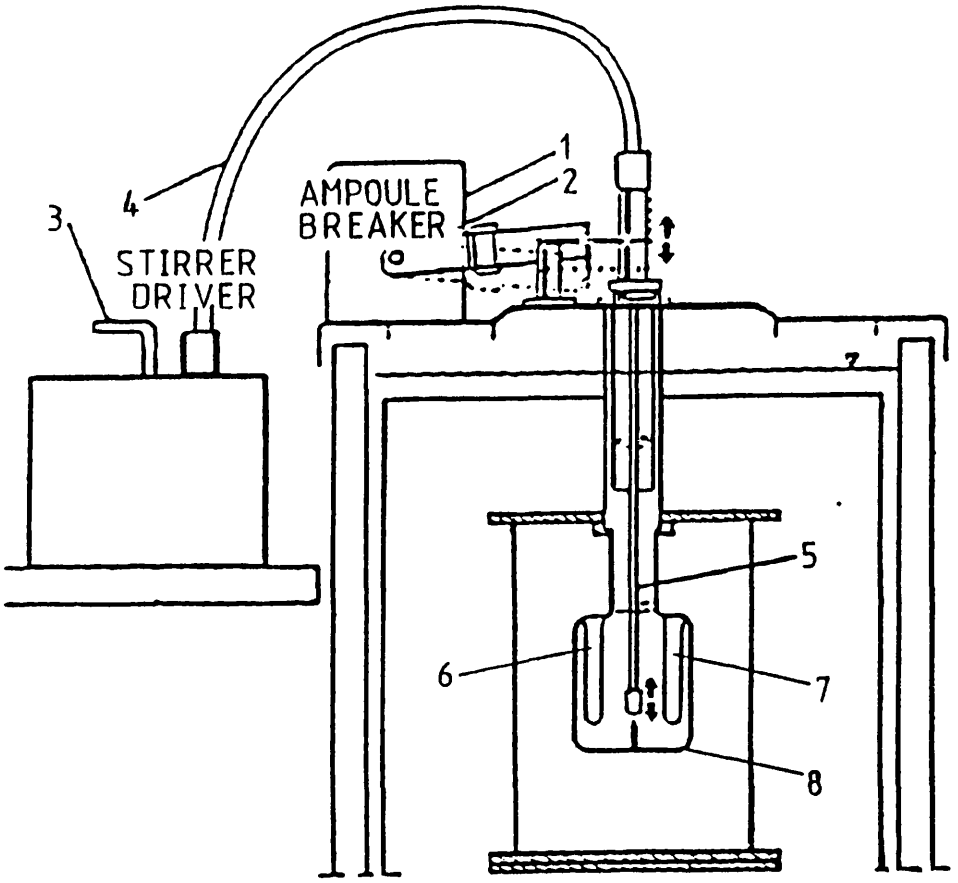

FIGURE 29

The L.K.B 8700 Calorimeter.

1. Motor for the Ampoule Breaker
2. Moving Arm
3. Grip
4. Flexible Coupling Wire
5. Stirrer/Ampoule Holder
6. Thermistor
7. Heater
8. Thin-Walled Pyrex Reaction Vessel

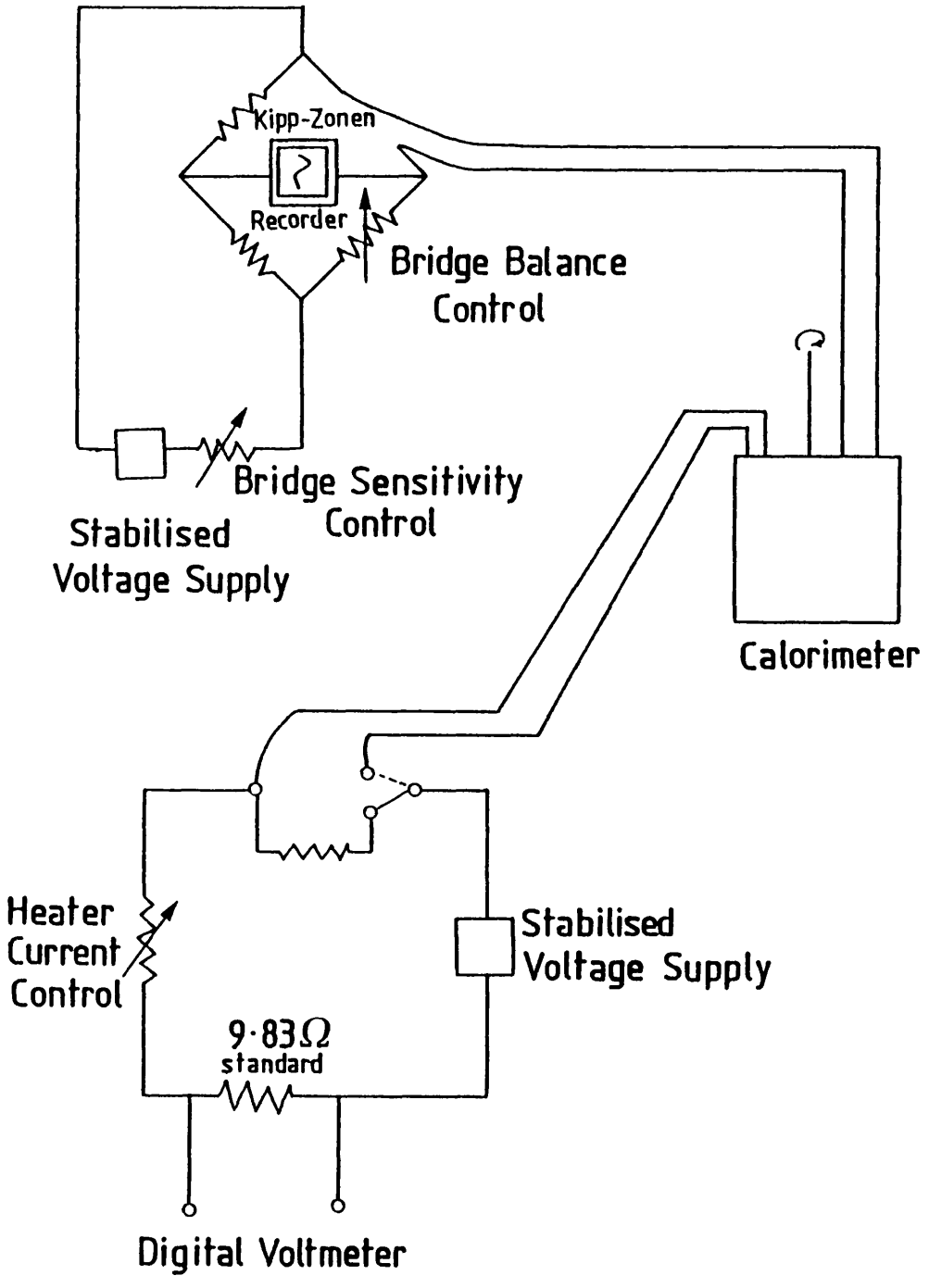

FIGURE 30

Basic Electrical Circuits for the L.K.B 8700 Calorimeter.

aqueous sodium hydroxide hydrolysing agent so that the change in dilution of this reagent was minimised. It was then possible to use a constant enthalpy of formation for $[OH]^-_{(aq)}$ without introducing errors due to enthalpy of dilution effects. Enthalpies of formation of $[OH]^-_{(aq)}$, $F^-_{(aq)}$, $[WO_4]^{2-}_{(aq)}$ and $[HS]^-$ were those measured at infinite dilution in aqueous media [Table 35].

A sealed ampoule was placed carefully inside the stirrer and the calorimeter bottle (containing the aqueous sodium hydroxide at a temperature just below 298.2 K) was carefully guided over it and screwed onto the top of the case. The case was then submerged in the water tank maintained at 298.2 K ± 0.001 K. This was left for about four hours so as to reach thermal equilibrium. Half an hour before the start of the reaction, stirring was commenced. Just before the initiation of the reaction the chart recorder was started and a base line traced by the pen for at least four minutes. Reaction was initiated by pushing the stirrer down, thereby breaking the ampoule against the spike. The onset of the reaction was accompanied by a deflection of the pen. Once the reaction was complete the pen started to trace a post-reaction line. This line was traced for about five minutes.

The pre-reaction and post-reaction lines were extrapolated to the exact time at which the reaction commenced. The true deflection was the distance between those lines at that time. The calorimeter system was calibrated several times by introducing a known quantity of heat into the calorimeter by means of a heater of known resistance [Figure 30]. Both the time of heating and deflection were noted. Figure 31 shows typical reaction and calibration curves and the way in which deflections were measured to take account of heat of transfer between the calorimeter and environment.

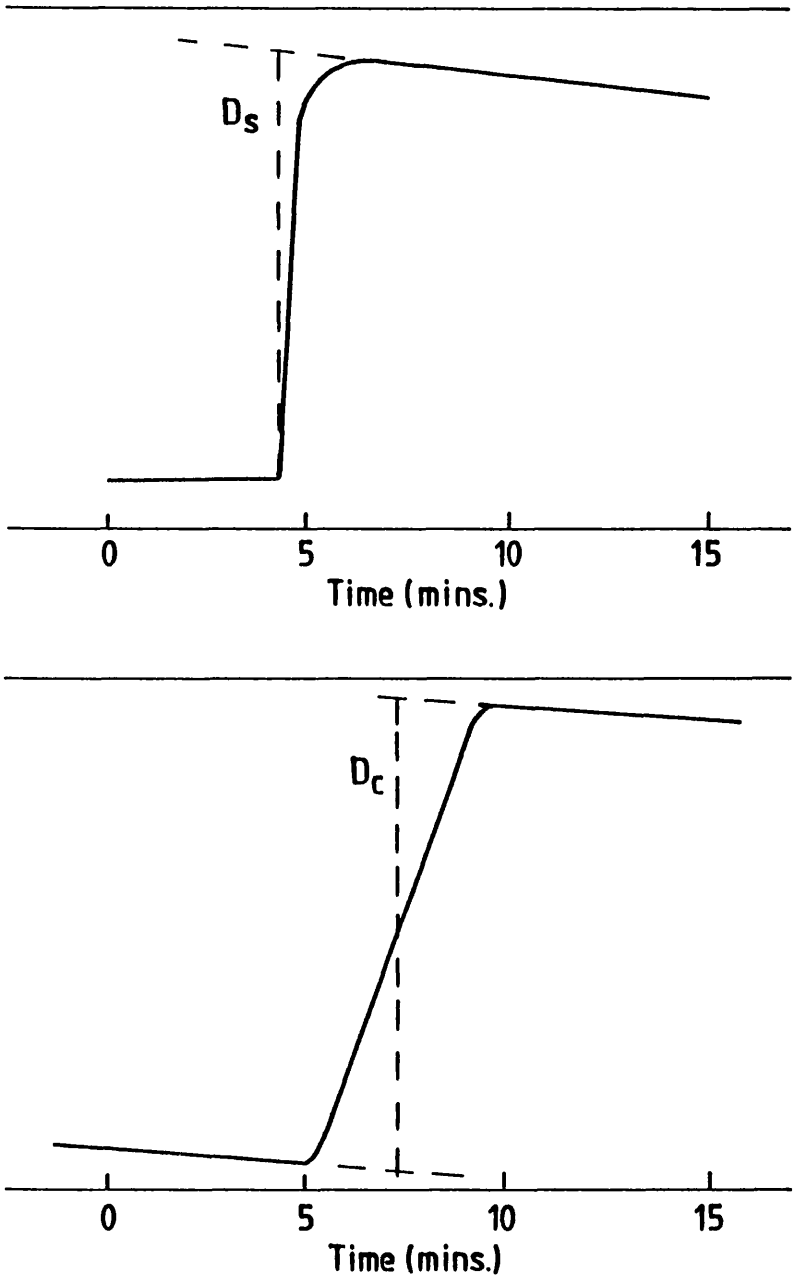

FIGURE 31

Typical temperature-time profiles for the sample and calibration runs.

The change in enthalpy for the reaction of WSF_4 with aqueous sodium hydroxide is given by the equation,

$$\Delta H = \frac{V^2RT}{r \times 10^3} \times \frac{Ds}{Dc} \times \frac{M}{W} \quad \text{kJ mol}^{-1}$$

where,

V is the average voltage (in volts) measured midway through the calibration;

R is the heater resistance (on Ohms). In this case it was 9.5 Ω;

r is 9.83 Ω for the particular L.K.B. 8700 used at Leicester University;

T is the time (in seconds) during which the heater current was supplied;

Ds is the deflection observed for the reaction of the sample;

Dc is the deflection observed for the calibration;

M is the molecular weight of WSF_4;

W is the mass of the sample.

The reliability of the calorimeter was checked periodically by the measurement of the enthalpy of solution of potassium chloride. Typical runs gave enthalpies of +17.39, +17.68 and +17.46 kJ mol^{-1}. These compare well with the value of +17.56 kJ mol^{-1} obtained by Sumner and Wadsö.

iii) Experimental accuracy

The low heat capacity of the thermistor was particularly suitable for this work and any errors produced by this section of equipment are likely to be minimal. The circuit incorporating the thermistor, however, has been estimated to produce an error of 1% in the monitored deflection. The measurements of the deflections have involved the extensions of monitored cooling curves. Since WSF_4 hydrolyses rapidly, the error is negligible (<¼%). Moreover, the mass of WSF_4 hydrolysed, and the heat dissipated in the calibration were chosen to give a maximum

deflection on the chart, and thus minimise the error in the physical measurement.

Another expected source of error might be the enthalpy associated with breaking the ampoule. However, the experimental average enthalpy of breaking an ampoule was estimated as only 2.5×10^{-2} J. [Heat generated through friction when the stirrer is pushed down onto the spike is normally negligible.]

A significant error can arise from ineffective stirring or a continually varying speed of stirring since both affect the rate of heat exchange. Such errors were minimised by using a bladed stirrer and by oiling the stirrer guide regularly. Nevertheless, a contribution to the overall error of perhaps 1% might be expected from this phenomenon.

REFERENCES

REFERENCES

1. See, for example, J. H. Holloway and D. Laycock, Adv. in Inorg. Chem. and Radiochem., 27, 157 (1983).
2. C. Dagron and F. Thevet, Ann. Chim. (Paris), 6, 67 (1971).
3. L. Y. Markovskii, V. M. Lantratov and E. Y. Pesina, Orkrytiya Izobret, Prom. Obraztsy Tovarnye Znaki, 52, 51 (1975) (Russ.).
4. L. Brixner and G. Hyatt, Mater. Res. Bull., 19, 745 (1984).
5. C. Dagron and F. Thevet, C.R. Hebd. Seances Acad. Sci., Ser. C, 268, 1867 (1969) (French).
6. N. Raysenek and O. Loye, Acta Cryst. Sect. B, B29, 1567 (1973).
7. C. Dagron, C.R. Hebd. Seances Acad. Sci., Ser. C, 275, 811 (1972).
8. C. Dagron, C.R. Hebd. Seances Acad. Sci., Ser. C, 283, 743 (1976).
9. N. H. Dung, Acta Cryst. Sect. B, B29, 2095 (1973).
10. N. H. Dung, C. Dagron and P. Laruelle, Acta Cryst. Sect. B, B31, 519 (1975).
11. D. Van Dyck, J. Van Landuyt, S. Amelinckx, N. H. Dung and C. Dagron, J. Solid State Chem., 19, 179 (1976).
12. S. S. Batasonov, V. S. Filatkina and G. N. Kustova, Izvest. Akad. Nauk SSSR, Ser. Khim., 1190 (1971) (Russ.).
13. H. Hahn and R. Schmid, Naturwiss., 52, 475 (1965).
14. H. N. Verkovets, A. A. Kamarazin and V. V. Sokolov, Izvest. Akad. Nauk SSSR, Ser. Khim., 125 (1973).
15. R. Schmid and H. Hahn, Z. Anorg. Allg. Chem., 373, 168 (1970).
16. C. Dagron, C.R. Hebd. Seances Acad. Sci., Ser. C, 273, 352 (1971).
17. N. M. Dung, Bull. Soc. France Mineral Crystallogra., 96, 41 (1973).
18. V. S. Pervov, V. D. Butskii and L. G. Podzolko, Russ. J. Inorg. Chem., 23, 819 (1978).
19. I. P. Malkerova, A. S. Alikhanyan, V. S. Pervov, V. D. Butskii and V. I. Gorgoraki, Russ. J. Inorg. Chem., 25, 1145 (1980).
20. I. P. Malkerova, A. S. Alikhanyan and V. I. Gorgoraki, Russ. J. Inorg. Chem., 25, 1742 (1980).
21. S. A. Ryabov, V. D. Butskii, A. S. Alikhanyan, V. S. Pervov, O. G. Ellert and Y. A. Buslaev, Dokl. Akad. Nauk SSSR, 273, 1992 (1983).
22. J. H. Holloway and D. C. Puddick, Inorg. Nucl. Chem. Lett., 15, 85 (1978).
23. M. J. Atherton and J. H. Holloway, Inorg. Nucl. Chem. Lett., 14, 121 (1978).
24. D. C. Puddick, Ph.D. Thesis, Leicester University (1982).
25. D. L. Hildenbrand, U.S. Navy Tech. Inf. Serv. AD Rep. No. 757231 (1972) and J. Chem. Phys., 62, 3074 (1975).

26. Y. A. Buslaev, Y. V. Kokunov and Y. D. Chubar, Dokl. Akad. Nauk SSSR, 213, 912 (1973).

27. M. J. Atherton and J. H. Holloway, J. Chem. Soc. Chem. Comm., 424 (1977).

28. Y. V. Kokunov, Y. D. Chubar, V. A. Bochkareva and Y. A. Buslaev, Koord. Khim., 1, 1100 (1975).

29. Y. V. Kokunov, Y. D. Chubar, A. V. Kopytin and Y. A. Buslaev, Koord. Chim., 2, 196 (1976).

30. G. M. Staunton, Ph.D. Thesis, Leicester University (1983).

31. J. H. Holloway, V. Kaučič and D. R. Russell, J. Chem. Soc. Chem. Comm., 1079 (1983).

32. Y. A. Buslaev, Y. V. Kokunov, M. P. Gustyakova and Y. D. Chubar, Dokl. Akad. Nauk SSSR, 233, 357 (1977).

33. Y. V. Kokunov, Y. D. Chubar and Y. A. Buslaev, Koord. Khim., 5, 866 (1979).

34. Y. V. Kokunov, Y. D. Chubar and Y. A. Buslaev, Koord. Khim., 2, 1227 (1976).

35. J. H. Holloway and J. Rook, in preparation.

36. V. D. Butskii and V. S. Pervov, Russ. J. Inorg. Chem., 22, 6 (1977).

37. I. P. Malkerova, A. S. Alikhanyan, V. D. Butskii, V. S. Pervov and V. I. Gorkoraki, Russ. J. Inorg. Chem., 26, 1055 (1981).

38. P. J. Jones, W. Levason, J. S. Ogden, J. W. Turff, E. M. Page and D. A. Rice, J. Chem. Soc. Dalton, 2625 (1983).

39. D. A. Rice, K. Hagen, L. Hedberg, K. Hedberg, G. M. Staunton and J. H. Holloway, Inorg. Chem., 23, 1826 (1984).

40. J. Fawcett, J. H. Holloway and D. R. Russell, J. Chem. Soc. Dalton, 1212 (1981).

41. K. Hagen, D. A. Rice, J. H. Holloway and V. Kaučič, J. Chem. Soc. Dalton, 1821 (1986).

42. Y. V. Kokunov, Y. D. Chubar and Y. A. Buslaev, Dokl. Akad. Nauk SSSR, 239, 1361 (1978).

43. J. H. Holloway, D. C. Puddick, G. M. Staunton and D. Brown, Inorg. Chim. Acta, 64, L209 (1982).

44. I. R. Beattie, K. M. S. Livingstone, D. J. Reynolds and G. A. Ozin, J. Chem. Soc. (A), 1210 (1970).

45. M. G. B. Drew, D. A. Rice and D. M. Williams, J. Chem. Soc. Dalton, 845 (1984).

46. See, for example, D. H. Williams and I. Flemming, Spectroscopic Methods in Organic Chemistry, pp.51-52, 3rd. Edition (McGraw-Hill Book Company).

47. O. L. Keller and A. Chetham-Strode, Inorg. Chem., 5, 367 (1966).

48. Yu. V. Mironov, V. P. Fedin, P. P. Semyannikov and V. E. Fedorov, Russ. J. Inorg. Chem., 4, 617 (1986).

49. B. Frlec and J. H. Holloway, J. Chem. Soc. Dalton, 535 (1975).

50. K. O. Christe, Inorg. Chem., 14, 2230 (1975).

51. N. K. Jha, Ph.D. Thesis, University of British Columbia (1965).

52. P. L. Robinson and G. J. Westland, J. Chem. Soc., 4481 (1956).

53. R. E. Dodd, L. A. Woodward and H. L. Roberts, Trans. Faraday Soc., 52, 1052 (1952).

54. K. O. Christe, W. Sawodny and P. Pulay, J. Molecular Struct., 21, 158 (1974).

55. J. Gaunt, Trans. Faraday Soc., 49, 1122 (1953).

56. D. Eclelsen, J. Am. Chem. Soc., 74, 262 (1952).

57. J. K. Wilmhurst and H. J. Bernstein, Can. J. Chem., 35, 191 (1975).

58. C. W. Brown and J. Overend, Spectrochim. Acta, 25A, 1533 (1969).

59. N. Bartlett, S. P. Beaton and N. K. Jha, J. Chem. Soc. Chem. Comm., 168 (1966).

60. R. C. Burns and T. A. O'Donnell, J. Inorg. Nucl. Chem., 42, 1285 (1980) and references cited therein.

61. N. Bartlett and P. L. Robinson, J. Chem. Soc., 3417 (1961).

62. M. Azeem, M. Brownstein and R. J. Gillespie, Can. J. Chem., 47, 4159 (1969).

63. R. D. Peacock and D. W. A. Sharp, J. Chem. Soc., 2762 (1959); J. L. Bolton and D. W. A. Sharp, J. Chem. Soc., 907 (1960).

64. A. J. Edwards and G. R. Jones, J. Chem. Soc. (A), 1491 (1970) and ibid., 1891.

65. D. D. Gibler, C. J. Adams, M. Fischer, A. Zalkin and N. Bartlett, Inorg. Chem., 11, 2325 (1972).

66. T. E. Mallouk, G. L. Rosenthal, G. Müller, R. Brusasco and N. Bartlett, Inorg. Chem., 23, 3167 (1984).

67. W. W. Wilson and K. O. Christe, Inorg. Chem., 20, 4139 (1981).

68. R. Bougon, T. Bui Huy and P. Charpin, Inorg. Chem., 14, 1822 (1975).

69. K. O. Christe, W. W. Wilson and R. Bougon, Inorg. Chem., 25, 2163 (1986).

70. E. G. Hope, P. J. Jones, W. Levason, J. S. Ogden, M. Tajik and J. W. Turff, J. Chem. Soc. Dalton, 529 (1985).

71. R. D. W. Kemmitt, D. R. Russell and D. W. A. Sharp, J. Chem. Soc., 4408 (1963).

72. W. McFarlane, A. M. Noble and J. M. Winfield, J. Chem. Soc. (A), 948 (1971).

73. R. L. Reddington and T. E. Reddington, J. Phys., 72, 2456 (1968) and references cited therein.

74. M. F. A. Dove, J. Chem. Soc. (A), 3722 (1959) and references cited therein.

75. E. B. R. Prideaux and K. R. Webb, J. Chem. Soc., 1346 (1936).

76. V. A. Shipachev, S. V. Zemsokov, B. I. Peshchevitskii, V. I. Belerantsev, K. A. Grigorova and L. Y. Al't, Tezisy Dokl.-vses. Soveshch. Khim., Anal. Teknol. Blagorod n-Met., 10th. (1976), 1, 43.

77. I. I. Tychinskagov and N. S. Nikolaev, Zh. Neorg. Khim., 8, 734 (1963).

78. A. Beurer and W. Sawodny, Z. Anorg. Allg. Chem., 427, 37 (1978).

79. O. Ruff, W. Menzel and W. Neumann, Z. Anorg. Allg. Chem., 208, 293 (1932).

80. A. V. Faloon and W. B. Kenna, J. Amer. Chem. Soc., 73, 2937 (1951).

81. R. Schmutzler, Angew. Chem. Int. Ed., 440 (1968).

82. J. H. Holloway, private communication.

83. N. Bartlett, S. Yeh, K. Kourtakis and T. Mallouk, J. Fluorine Chem., 26, 97 (1984).

84. O. Ruff and K. Stäuber, Z. Anorg. Allg. Chem., 47, 190 (1905).

85. G. Balz and E. Mailänder, Z. Anorg. Allg. Chem., 217, 161 (1934).

86. G. A. Sokol'skii and I. K. Knunyants, Izvest. Akad. Nauk SSSR, Otdel. Chim. Nauk, 779 (1960).

87. P. J. Green and G. L. Gard, Inorg. Nucl. Chem. Lett., 14, 179 (1978).

88. J. H. Holloway and H. Selig, J. Inorg. Nucl. Chem., 30, 473 (1968).

89. O. Ruff, K. Stäuber and H. Graf, Z. Anorg. Allg. Chem., 58, 325 (1908).

90. G. J. Moody and H. Selig, Inorg. Nucl. Chem. Lett., 2, 319 (1966).

91. S. W. Peterson, J. H. Holloway, B. A. Coyle and J. M. Williams, Science, 173, 1238 (1971).

92. J. R. Geichman, E. A. Smith and P. R. Ogle, Inorg. Chem., 2, 1012 (1968).

93. W. A. Guillory and C. E. Hunter, J. Chem. Phys., 55, 3404 (1971).

94. R. A. Frey, R. L. Reddington and A. L. K. Aljbury, J. Chem. Phys., 54, 344 (1971).

95. P. J. H. Woltz, E. A. Jones and A. H. Nielson, J. Chem. Phys., 20, 378 (1952).

96. J. R. Holmes, B. B. Stewart and J. S. Mackenzie, J. Chem. Phys., 37, 2728 (1962).

97. E. L. Muetterties and W. D. Phillips, J. Amer. Chem. Soc., 81, 1084 (1959).

98. R. J. Gillespie and E. A. Robinson, Can. J. Chem., 29, 2171 (1961).

99. J. R. Geichman, L. R. Swaney and P. R. Ogle, U.S. Atomic Energy Commission, Rep. GAT-T-971 (1962).

100. H. L. Roberts, Quarterly Reviews, 15, 30 (1961).

101. C. W. Tullock, F. S. Fawcett, W. C. Smith and D. D. Coffman, J. Amer. Chem. Soc., 82, 539 (1960).

102. R. Tunder and B. Siegel, J. Inorg. Nucl. Chem., 25, 1097 (1963).

103. K. O. Christe, E. C. Curtis, C. J. Schack and D. Pilipovich, Inorg. Chem., 11, 1679 (1972).

104. W. C. Smith, C. W. Tullock, R. D. Smith and V. A. Engelhardt, J. Amer. Chem. Soc., 82, 551 (1960).

105. Ibid., 82, 551 (1960).

106. W. C. Smith, Angew. Chem. Int. Ed., 1, 467 (1962).

107. A. L. Oppegard, W. C. Smith, E. L. Muetterties and V. A. Engelhardt, J. Amer. Chem. Soc., 82, 3835 (1960).

108. W. C. Smith, U.S. 2,904,398, Sept. 15, (1959), (Chem. Abs., 54, 3883i).

109. N. Bartlett and P. L. Robinson, Chem. Ind. London, 1351 (1956); J. Chem. Soc., 3417 (1961).

110. J. H. Holloway, G. M. Staunton, K. Rediess, R. Bougon and D. Brown, J. Chem. Soc. Dalton, 2163 (1984).

111. J. Berkowitz, W. A. Chupka, P. M. Guyon, J. H. Holloway and R. Spohr, J. Phys. Chem., 75, 1461 (1971).

112. H. Meinert, L. Friedrich and W. Kohl, Z. Chem., 15, 492 (1975).

113. J. H. Holloway, G. J. Schrobilgen and P. Taylor, J. Chem. Soc. Chem. Comm., 40 (1975).

114. J. H. Holloway and G. J. Schrobilgen, Inorg. Chem., 19, 2632 (1980).

115. Ibid., Inorg. Chem., 20, 3363 (1981).

116. P. A. Taylor, P. A. Tucker, J. H. Holloway and D. R. Russell, Acta Crystallogr., Sect. B, 31, 906 (1975).

117. See, for example, K. Nakamoto, Infra-red and Raman Spectra of Inorganic and Coordination Compounds, 3rd. Edition, Wiley-Inter-Science, 1977.

118. R. Filler, Isr. J. Chem., 17, 71 (1978).

119. K. Seppelt and D. Lentz, Novel Developments in Noble Gas Chemistry.

120. R. C. Burns, I. D. Macleod, T. A. O'Donnell, T. E. Peel, K. A. Phillips and A. B. Waugh, J. Inorg. Nucl. Chem., 39, 1737 (1977).

121. D. M. Bruce, A. J. Hewitt, J. H. Holloway, R. D. Peacock and I. L. Wilson, J. Chem. Soc. Dalton, 2230 (1976).

122. R. J. Gillespie and B. Landa, Inorg. Chem., 12, 1383 (1973).

123. A. J. Edwards, J. H. Holloway and R. D. Peacock, Proc. Chem. Soc., 275 (1963).

124. B. Cohen and R. D. Peacock, J. Inorg. Nucl. Chem., 68, 3056 (1966).

125. V. M. McRae, R. D. Peacock and D. R. Russell, J. Chem. Soc. Chem. Comm., 62 (1969).

126. F. O. Sladky, P. A. Bulliner and N. Bartlett, J. Chem. Soc. A, 2199 (1969).

127. O. D. Maslov, V. A. Legasov, V. N. Prusakov and B. B. Chaivanov, Zh. Fiz. Khim., 41, 1832 (1967).

128. J. Binenboym, H. Selig and J. Shamin, J. Inorg. Nucl. Chem., 30, 2863 (1968).

129. J. H. Holloway and J. G. Knowles, J. Chem. Soc. (A), 756 (1969).

130. B. Frlec and J. H. Holloway, J. Chem. Soc. Dalton, 535 (1975).

131. N. Bartlett, M. Gennis, D. D. Gibler, B. K. Morrell and A. Zalkin, J. Chem. Soc. (A), 12, 1717 (1973).

132. R. J. Gillespie and P. K. Ummar, Inorg. Chem., 11, 1674 (1972).

133. W. E. Giggenbach, J. Chem. Soc. Chem. Comm., 852 (1970).

134. R. C. Burns, R. J. Gillespie and J. F. Sawyer, Inorg. Chem., 19, 1423 (1980).

135. H. Chandra, D. N. R. Rao and M. C. R. Symons, J. Chem. Soc. Dalton, 729 (1987).

136. R. S. Eachus and M. C. R. Symons, J. Chem. Soc. (A), 304 (1971).

137. M. C. R. Symons and R. Janes, private communication.

138. J. Burgess, I. Haigh and R. D. Peacock, J. Chem. Soc. Dalton, 1062 (1974).

139. M. J. Atherton, J. Burgess, J. H. Holloway and N. Morton, J. Fluorine Chem., 11, 215 (1978).

140. I. P. Malkerova, A. S. Alikhanyan, V. D. Butskii, V. S. Pervov and V. I. Gorkoraki, Russ. J. Inorg. Chem., 26, 1055 (1981).

141. See, for example, E. S. Swinbourne, 'Analysis of Kinetic Data', Nelson, London, 1971, pp.7-9.

142. P. J. Aymonino, A. C. Rande, E. Dieman and A. Müller, Z. Anorg. Allg. Chem., 372, 295 (1969).

143. Ibid., 372, 300 (1969).

144. M. Widmer and A. Schwarzenback, Helv. Chim. Acta, 47, 266 (1964).

145. I. Dellien, F. M. Hull and L. G. Hepler, Chem. Rev., 76, 283 (1976).

146. G. K. Johnson, P. N. Smith and W. N. Hubbard, J. Chem. Thermodynamics, 5, 793 (1973).

147. J. Chem. Thermodynamics, 7, 1 (1975); 8, 603 (1976).

148. N.B.S. Selected Values of Chemical Thermodynamic Properties. Technical Note 270-3. D. D. Wagman, W. H. Evans, V. B. Parker, D. Halow, S. M. Bailey and R. H. Schum (1968).

149. K. F. Zmbov, O. M. Uy and J. L. Margrave, J. Phys. Chem., 73, 3008 (1969).

150. N.B.S. Technical Note 270-4 (1969) (see Reference 148).

151. J.A.N.A.F. Thermochemical Tables, D. R. Stull et al., Dow Chemical Co., Midland, Michigan (1971), NSRDS, NB537.

152. J. C. Widervanck and F. Jellinek, Z. Anorg. Allg. Chem., 328, 309 (1964) and references cited therein.

153. O. Glemser, H. Sauer and P. König, Z. Anorg. Allg. Chem., 257, 241 (1948).

154. S. P. Cramer, K. S. Laing, A. J. Jacobson, C. H. Chang and R. R. Chianelli, Inorg. Chem., 23, 1215 (1984).

155. K. S. Laing, S. P. Cramer, D. C. Johnson, C. H. Chang, A. J. Jacobson, J. P. de Neufville and R. R. Chianelli, J. Non-Cryst. Solids, 42, 345 (1980).

156. K. S. Laing, J. P. de Neufville, A. J. Jacobson, R. R. Chianelli and F. Betts, J. Non-Cryst. Solids, 35-36, 1249 (1980).

157. S. A. Shchukarev, I. V. Vasil'kova, V. M. Drozdova and N. S. Martynova, Russ. J. Inorg. Chem., 4, 13 (1959).